(2)

STUDIES ON ELECTRONIC AND MAGNETIC PROPERTIES IN SOLID STATE CHEMISTRY

KAZUNARI YOSHIZAWA

PREFACE

Solid state chemistry is largely concerned with molecular design and construction of functional materials at the electronic, atomic, and molecular levels. Thus the study of the electronic and magnetic structures and the intramolecular and intermolecular interactions is important. The study of solid state chemistry began in the 1960s following the discovery of molecular semiconductors and the publication of a series of calculations of the electronic state based on the molecular orbital theory and successful predictions of the properties of molecular assemblies. The first organic conductor, reported in 1954, was a perylene-bromine complex with electrical conductivity of 1 $S \cdot cm^{-1}$. Such materials with conjugated π-electron backbone display characteristic electronic properties compared with conventional organic materials. These properties are due to low-energy optical transitions, low ionization potentials, and high electron affinities, which comes from delocatization of π electrons. In the early 1960s, on the other hand, several theoreticians predicted the existence of bond alternation defects in the conjugated chains, called "misfits" in those days, using the Hückel molecular orbital theory. Surprisingly, their predictions are basically consistent with a lot of detailed experimental results of these days concerning electrical transport and magnetic properties.

In recent years, remarkable success has been achieved in this field, due to the extensive use of sophisticated experimental apparatus and the great advance in molecular theory based on quantum mechanics and statistical mechanics. Another main factor is in the rapid progress of data-processing ability. Moreover, an increasingly important facet of research in this field is the growing interest in practical applications to novel conducting, superconducting, magnetic, and optical materials. The author hopes that the studies made in this thesis will contribute to the realization of these long-range programs.

ACKNOWLEDGMENTS

The present thesis is a summary of the author's studies from 1981 to 1984 at the Department of Hydrocarbon Chemistry and from 1988 to 1991 at the Division of Molecular Engineering, Faculty of Engineering, Kyoto University.

The author cordially thanks Professor Tokio Yamabe for his valuable suggestions, stimulating discussion, and constant encouragement. He is deeply grateful to Associate Professor Kazuyoshi Tanaka for his many important suggestions, stimulating and informative discussion, and constant encouragement. Acknowledgement is also made to Associate Professor Jun Yamauchi and Professor Yasuo Deguchi for their kind advice in ESR measurements and valuable discussion. The author is grateful to Professor Hideki Shirakawa of University of Tsukuba for his kind advice in the synthesis and the doping techniques for polyacetylene and stimulating discussion. He also wishes to thank Professor Katsumi Yoshino of Osaka University for his kind advice and valuable discussion. The author wishes to express his gratitude to Professor Keisaku Kimura of Himeji Institute of Technology and Dr. Shunji Bandow of the Institute for Molecular Science for their kind help in ESCA, ESR, and magnetic measurements and stimulating discussion. He is grateful to Dr. Akitomo Tachibana and Dr. Yohji Misaki for their valuable comments and discussion on his study. The author would record his warmest acknowledgments to Mr. Katsuhisa Ohzeki, Dr. Tsuneaki Koike, Dr. Tokushige Shichiri, Dr. Shozo Yamanaka, Mr. Hiromi Kobayashi, Mr. Michio Toriumi, Mr. Satoru Nishio, Mr. Tomonari Takeuchi, Mr. Akira Takata, Mr. Akihiro Ito, Mr. Yukihito Matsuura, Mr. Akihisa Chano for their collaborations in the Associate Professor Tanaka's research group. Thanks are also due to Dr. Shizukuni Yata, Dr. Shu Hotta, and Mr. Wataru Shimotsuma for their collaborations in the author's early study. He would like to thank other members of Professor Yamabe's laboratory for stimulating discussion in various seminars. He also expresses his appreciation to Miss Hideko Yamada, Professor Yamabe's secretary, for her official work. Numerical calculations were carried out at the Data Processing Center of Kyoto University, of which staffs he would like to thank. Thanks are also due to the Instrument Center, the Institute for Molecular Science in obtaining ESCA, ESR, and magnetic data.

The author counts himself fortunate to have had the experience of working in Professor Fukui's laboratory in the early University education. It is a great pleasure to thank Professor Kenichi Fukui for his kind guidance and constant encouragement. The author is also indebted to Associate Professor Kazuo Akagi, Mr. Tooru Matsui, Dr. Yukitoshi Tanabe for their kind advice and encouragement.

It is a pleasure of the author to thank Professor Masayoshi Hyodo and Mrs. Hiroe Hyodo for their understanding and encouragement. Finally, the author would like to express his sincere gratitude to his parents Seijiro Yoshizawa and Sumie Yoshizawa, and his wife Mika Yoshizawa for their support, understanding, and encouragement.

Kyoto, November 1991

Kazunari Yoshizawa

LIST OF PUBLICATIONS

(1) *Cis-trans* isomerization of iodine-doped polyacetylene
K. Tanaka, K. Yoshizawa, K. Ohzeki, and T. Yamabe, *Solid State Commun.*, **45**, 391(1983). (Not included in this thesis)

(2) Photoisomerization of *cis*-polyacetylene
K. Tanaka, T. Koike, K. Ohzeki, K. Yoshizawa, and T. Yamabe, *Solid State Commun.*, **47**, 127(1983). (Not included in this thesis)

(3) Structural change in the photoexcited *cis*-polyacetylene
K. Tanaka, T. Koike, K. Yoshizawa, K. Ohzeki, and T. Yamabe, *Solid State Commun.*, **49**, 165(1984). (Not included in this thesis)

(4) ESR studies of electrochemically prepared poly(3-methylthienylene) films
K. Tanaka, T. Shichiri, K. Yoshizawa, T. Yamabe, S. Hotta, W. Shimotsuma, J. Yamauchi, and Y. Deguchi, *Solid State Commun.*, **51**, 565(1984). (Not included in this thesis)

(5) ESR studies of polyacenic semiconductive material
K. Tanaka, K. Yoshizawa, T. Koike, T. Yamabe, J. Yamauchi, Y. Deguchi, and S. Yata, *Solid State Commun.*, **52**, 343(1984). (Not included in this thesis)

(6) A stability condition for the Hartree-Fock solution of the infinite one-dimensional system
K. Tanaka, H. Kobayashi, S. Yamanaka, K. Yoshizawa, and T. Yamabe, *J. Chem. Phys.*, **91**, 3724(1989).

(7) Interaction of two solitons on two *trans*-polyacetylene chains
K. Yoshizawa, K. Tanaka, and T. Yamabe, *Synth. Met.*, **36**, 75(1990).

(8) Midgap levels of photoexcited conductive polymers. I. A simple description of the midgap levels based on molecular orbital interaction
K. Tanaka, K. Yoshizawa, and T. Yamabe, *Int. J. Quantum Chem.*, **40**, 305(1991).

(9) Midgap levels of photoexcited conductive polymers. II. Detailed analysis of *trans*-polyacetylene
K. Tanaka, K. Yoshizawa, T. Takeuchi, and T. Yamabe, *Int. J. Quantum. Chem.*, **40**, 315(1991).

(10) Theoretical study on ferromagnetic interaction in stacked diphenylcarbene polymer
K. Tanaka, T. Takeuchi, K. Yoshizawa, M. Toriumi, and T. Yamabe, *Synth. Met.*, **44**, 1(1991).

(11) Crystal orbital study of ferromagnetic state of poly(*m*-aniline)
K. Yoshizawa, A. Takata, K. Tanaka, and T. Yamabe, *Polym. J.*, submitted.

(12) Unrestricted Hartree-Fock method for infinite systems with antiferromagnetic array: Antiferromagnetic state of *trans*-polyacetylene
K. Yoshizawa, A. Ito, K. Tanaka, and T. Yamabe, *J. Chem. Phys.*, submitted.

(13) Magnetic property measurement of simple alkylene-aromatic polymers
K. Tanaka, K. Yoshizawa, A. Takata, T. Yamabe, and J. Yamauchi, *Synth. Met.*, **39**, 103(1990).

(14) Magnetic properties of simple alkylene-aromatic polymers
K. Tanaka, K. Yoshizawa, A. Takata, T. Yamabe, and J. Yamauchi, *J. Chem. Phys.*, **94**, 6868(1991).

(15) Synthesis of poly(*m*-aniline) by dehydrohalogenation of *m*-chloroaniline

K. Yoshizawa, K. Tanaka, and T. Yamabe, *Chem. Lett.*, **1990**, 1311.

(16) Synthesis and ESR measurements of polymeric product of *m*-chloroaniline as an approach to magnetic polymers
K. Tanaka, K. Yoshizawa, A. Takata, T. Yamabe, and J. Yamauchi, *Synth. Met.*, **43**, 3297(1991).

(17) Polymerization of *m*-bromoaniline to poly(*m*-aniline) by the use of Ullmann reaction
K. Yoshizawa, K. Tanaka, T. Yamabe, and J. Yamauchi, *Chem. Mater.*, submitted.

(18) Ferromagnetic interaction in poly(*m*-aniline): Electron spin resonance and magnetic susceptibility
K. Yoshizawa, K. Tanaka, T. Yamabe, and J. Yamauchi, *J. Chem. Phys.*, submitted.

(19) Plasma polymerization of thiophene and 3-methylthiophene
K. Tanaka, K. Yoshizawa, T. Takeuchi, T. Yamabe, and J. Yamauchi, *Synth. Met.*, **38**, 107(1990). (Not included in this thesis)

(20) Plasma polymerization of 1-benzothiophene
K. Tanaka, T. Takeuchi, K. Yoshizawa, S. Nishio, and T. Yamabe, *J. Appl. Phys.*, in press. (Not included in this thesis)

(21) Electrical conductivity measurements of the plasma-polymerized 1-benzothiophene thin film
S. Nishio, T. Takeuchi, Y. Matsuura, K. Yoshizawa, K. Tanaka, and T. Yamabe, *Synth. Met.*, in press. (Not included in this thesis)

(22) Crystal structure and characterization of 1,3,5-tris(diphenylamino)-benzene

K. Yoshizawa, A. Chano, K. Tanaka, and T. Yamabe, *Chem. Lett.*, submitted. (Not included in this thesis)

(23) Electron spin resonance of the quartet state of 1,3,5-tris(diphenylamino)-benzene
K. Yoshizawa, A. Chano, A. Ito, K. Tanaka, T. Yamabe, H. Fujita, and J. Yamauchi, *Chem. Lett.*, submitted. (Not included in this thesis)

(24) Synthesis of polyaniline by the use of Ullmann reaction
K. Tanaka, A. Ito, K. Yoshizawa, and T. Yamabe, to be published. (Not included in this thesis)

CONTENTS

GENERAL INTRODUCTION

Materials that exhibit electrical conductivity, superconductivity, ferromagnetism, and nonlinear optical process have been considered to be inorganic solids with bonding in three dimensions. In particular, the former three properties belong to the typical properties of naturally occurring elemental metals and their combinations which produce alloys. Although most organic materials are insulators, a class of organic materials known as "organic metals" or "synthetic metals" exhibit metallic properties.

It was pointed out in 1954 by Akamatsu, Inokuchi, and Matsunaga,[1] that complex formation between electron acceptors and electron donors, based on π-conjugated systems, increases the electrical conductivity by several orders of magnitude. The electrons in the conjugated systems are delocalized in a way very similar to that in benzene. Delocalization of electrons is a typical metallic property. Keeping step with a series of experiments, Longuet-Higgins and Salem[2] in 1959 and Pople and Walmsley[3] in 1962 investigated the electronic structure of the simplest π-conjugated chain, namely, polyene or polyacetylene by the use of the Hückel molecular orbital theory, and suggested the importance of bond alternation defects associated with electrical transport and magnetic properties.

In the course of the study on high-temperature superconductivity, Little[4] in 1964 proposed a model of chain conductors very similar to polyacetylene in a polarizable medium. In view of Little's work, one can think of an organic conductivity along the organic chain together with a superconductivity not mediated by phonon, that is, polarization-mediated. Although Little had underestimated the importance of the Peierls distortion on actual one-dimensional conductors, his proposal has clearly activated the study toward organic conductors and superconductors. On the basis of the theoretical investigations by Peierls, Overhauser, Landau, Mott, Anderson, and others, a one-dimensional electron system differs from a three-dimensional one in several more fundamental aspects[5]:

(1) In the presence of interactions the ground state is unstable against the

formation of charge- and spin-density waves.

(2) In a one-dimensional system with short-range interactions thermal fluctuations destroy long-range order at any non-zero temperature.

(3) An arbitrarily small amount of disorder localizes all the electrons and therefore transforms a one-dimensional metal into an insulator.

Interest in "conducting polymers" as a novel class of electronic materials began in 1971 with the preparation of polyacetylene, $(CH)_x$ in the form of shiny silvery films by Shirakawa,[6] with the discovery in 1977 that $(CH)_x$ could be doped by charge-transfer reactions with electron acceptors or electron donors, and with the discovery that the doped polymer exhibits a dramatic increase in conductivity with values in the metallic regime.[7] Recently by modifying the Shirakawa's polymerization conditions, a defect-free and therefore highly stretchable $(CH)_x$ was polymerized by Naarmann and Theophilou.[8] As a result of a highly oriented and defect-free film, very high electrical conductivity more than 10^5 S•cm^{-1}, which compares with that of copper, was materialized.

On the other hand, following the theoretical work of Su, Scrieffer, and Heeger (SSH)[9] on the role of bond alternation defects or "solitons" in $(CH)_x$, significant progress has been made concerning the concept of transport and dynamical properties of $(CH)_x$ in the presence of solitons. Much experimental support for the presence of solitons in $(CH)_x$ has also accrued. It must be noted that basically identical work to the SSH model was presented in the early 1960s as mentioned above.[2,3]

Associated with the potential application for a novel class of polymers in the field of conductors, organic batteries, and display devices, the most intensively studied polymers are polyphenylene, polypyrrole, polythiophene, polyaniline, and their derivatives. In particular, polyaniline[10] is being studied more and more, and in recent years has become one of the centers of considerable scientific interest in the application field. More recent systematic studies have been undertaken by numerous groups on the actual use of polyaniline as a storage cell materials.

Details of the measurements of the metallic properties of inorganic polysulfur nitride, $(SN)_x$ crystals and films were published in 1974.[11] Measurements of specific heat, optical reflectivity, and magnetic susceptibility confirmed the essentially metallic nature of this polymer down to 1.2 K. The activity on $(SN)_x$ was further stimulated by the exciting observation of superconductivity in $(SN)_x$ at 0.26 K. The first "organic superconductor", quasi-one-dimensional bis(tetramethyltetraselenafulvalenium) hexafluoro-phosphate $(TMTSF)_2PF_6$ (T_c = 0.9 K at P = 12 kbar), was discovered in 1979.[12] Organic superconductors have various electronic and magnetic properties and crystal structures that are similar to those of the inorganic copper oxide high T_c superconductors[13]; these similarities include highly anisotropic conductivities, critical fields, and short coherence lengths. The years after the discovery of the first organic superconductor, they now total almost 40, and T_c values have increased an order of magnitude to just below 13 K.[14]

Furthermore, following the breakthrough by Krätschmer et al.[15] in synthesis of buckminsterfullerene, the 60-carbon atom molecule with the geometry of a soccer ball, studies of solid-state properties of the single crystal have shown peculiarities of this molecule, for example, the molecule rotates in *fcc* lattice sites at temperature well below 300 K.[16] Surprisingly, Hebard et al.[17] provided unambiguous evidence for superconductivity in solids composed of C_{60} molecules doped with potassium (K_xC_{60}) with an onset near T_c = 18 K. A Rb_xC_{60} sample prepared and analyzed in an analogous way subsequently exhibited evidence for superconductivity with T_c = 28 K.[18] Furthermore, $Cs_xRb_yC_{60}$ was reported to show superconductivity at 33 K.[19] The onset of superconductivity at 33 K marks the highest transition temperature yet observed for a molecular superconductor.

One of the most challenging themes in the field of solid state chemistry is design and synthesis of organic ferromagnets based on molecular crystals or polymers.[20,21] Since the discovery of the loadstone (FeO-Fe_2O_3), many different magnetic materials have been developed, almost all based on

transition metals and/or rare-earth elements. Technological application of magnetism also has a long history, from the compass to today's sophisticated magnetic memory systems. Upon application of a magnetic field all substances exhibit a magnetic moment. Paramagnetic compounds have their induced moment aligned parallel to the field, and in the simplest case the susceptibility, χ may be modeled by the Curie expression. If the spins align parallel (ferromagnet) to each other, then a macroscopic spontaneous magnetization is present with a characteristic saturation moment. If antiparallel spin (antiferromagnet) alignment occurs, there is not net moment. Ferrimagnetism occurs when antiferromagnetically aligned spins have different local moments and the incomplete cancellation of the spins results in a reduced, but finite moment. The materials that exhibit these cooperative phenomena are inorganic solids with bonding in three dimension. Moreover, the known cases of ferromagnetism always involve spins of either *d* or *f* electrons, which is considered to presumably play an essential role in the mechanism of this interaction.

In recent years, several groups have started a long-range difficult program to prepare ferromagnetic materials based on organic molecules and/or polymers. Such quantitative spin control seems really a challenging theme in this field. One can imagine that such materials would have fundamentally new properties that would provide valuable insight into the nature of magnetism. Although no such substance exhibiting clear ferromagnetism has been so far found, several fundamental strategies and theoretical models have been described for designing this type of materials by McConnell,[22] Mataga,[23] Ovchinnikov,[24] and others. The recent success includes demonstration both of a strong ferromagnetic interaction between the eight neighboring spins on a phenylcarbene oligomer[25,26] and of a ferromagnetic intermolecular interaction in a mixed crystal of garvinoxyl and hydrogarvinoxyl.[27] However, note the distinction between ferromagnetism, a solid-state phenomenon, and ferromagnetic interaction, an indication of a local high-spin interaction between a few of magnetic moments. Very recently the γ-phase of some nitronyl nitroxide was reported to become a

ferromagnet at very low temperature of 0.65 K from the measurements of magnetization, magnetic susceptibility, and heat capacity.[28] Furthermore, C_{60} doped with tetrakis(dimethylamino) ethylene was reported to show soft ferromagnetism with a Curie temperature of 16.1 K, although it shows no hysteresis loop.[29]

In this thesis, the author is engaged in the study of the electronic structure of conducting polymers, particularly polyacetylene, and the design and construction of organic ferromagnets.

In Part I, first, the midgap levels associated with the photogeneration of soliton-antisoliton pair in a prototype conducting polymer, *trans*-$(CH)_x$ are treated using the idea of the interaction of the highest occupied molecular orbital (HOMO) and the lowest unoccupied molecular orbital (LUMO). It is important to note that such levels result in a large charge-separation of π-conjugated chains. Moreover, it is essential to consider this type of excitation in order to properly evaluate the nonlinear optical process in π-conjugated systems.

Second, the instability problems of one-dimensional electron systems especially of *trans*-$(CH)_x$, that is, CDW and SDW states are dealt with. Both in the CDW and in the SDW states, a modulation of wavevector $2k_F$, where k_F is the radius of the Fermi sphere, plays an essential role in the appearance of the insulating phases of one-dimensional solids. It is important to stress that these phenomena are deeply related to the electron-hole correlation, in other words, the HOMO-LUMO interaction.

In Part II, molecular design of organic ferromagnets based on the crystal orbital method is attempted. First the interplane interaction between stacked diphenylcarbene is analyzed by the crystal orbital method and the McConnell's rule. It is found that intermolecular magnetic interaction can be analyzed on the basis of the crystal orbital method. Second the magnetic structure of a novel ferromagnetic model-polymer, poly(*m*-aniline) is calculated using the crystal orbital method. It can be expected that the ferromagnetic state is energetically more stable than the non-magnetic state in

the cationic and the dehydrogenated forms of poly(*m*-aniline). The crystal orbital method is found to be useful to design and analyze the magnetic structure of organic ferromagnets.

In Part III, a series of studies on the synthesis and characterization of what are called organic ferromagnets are described. As a basic skeleton of ferromagnetic polymers, alkylene-aromatic (AA) polymer and poly(*m*-aniline) are treated. In particular, radical spins in poly(*m*-aniline) are expected to be stable and therefore to have very high spin concentration, which is indispensable for magnetic interaction in this type of polymers. Ferromagnetic interaction in spin clusters is observed by electron spin resonance and magnetic susceptibility measurements at low temperatures in the AA polymers and poly(*m*-aniline) although bulk ferromagnetism such as a magnetic hysteresis loop has not so far been found. These studies on AA polymer and poly(*m*-aniline) are of interest as an approach to ferromagnetic polymers.

References

1. H. Akamatsu, H. Inokuchi, and Y. Matsunaga, *Nature*, **173**, 168(1954).
2. H. C. Longuet-Higgins and L. Salem, *Proc. Roy. Soc.*, A **251**, 172(1959).
3. J. A. Pople and S. H. Walmsley, *Mol. Phys*, **5**, 15(1962).
4. W. A. Little, *Phys. Rev.*, A**134**, 1416(1964).
5. D. Jérome and H. J. Schulz, *Adv. Phys.*, **31**, 299(1982).
6. H. Shirakawa and S. Ikeda, *Polym. J.*, **2**, 231(1971).
7. H. Shirakawa, E. J. Louis, A. G. MacDiarmid, C. K. Chiang, and A. J. Heeger, *J. Chem. Soc., Chem. Commun.*, **1977**, 578.
8. H. Naarmann and N. Theophilou, *Synth. Met.*, **22**, 1(1987).
9. W. P. Su, J. R. Scrieffer, and A. J. Heeger, *Phys. Rev.*, B**22**, 2099(1980).
10. E. M. Geniès, A. Boyle, M. Lapkowski, and C. Tsintavis, *Synth. Met.*, **36**, 139(1990).
11. See, M. M. Labes, P. Love, and L. F. Nichols, *Chem. Rev.*, **79**, 1(1979).
12. D. Jérome, A. Mazaud, M. Ribault, K. Bechgaard, *J. Phys. (Paris) Lett.*, **41**, L95(1980).
13. J. G. Bednorz and K. A. Müller, *Z. Phys.*, B**64**, 189(1986).
14. J. M. Williams, A. J. Schultz, U. Geiser, K. D. Carlson, A. M. Kini, H. H. Wang, W.-K. Kwok, M.-H. Whangbo, and J. E. Schirber, *Science*, **252**, 1501(1991).
15. W. Krätschmer, L. D. Lamb, K. Fostiropoulos, D. R. Huffman, *Nature*, **347**, 354(1990).
16. P. J. Benning, J. L. Martins, J. H. Weaver, L. P. F. Chibante, and R. E. Smalley, *Science*, **252**, 1417(1991).
17. A. F. Hebard, M. J. Rossinsky, R. C. Haddon, D. M. Murphy, S. H. Glarum, T. T. M. Palstra, A. P. Ramirez, and A. R. Kortan, *Nature*, **350**, 600(1991).
18. M. J. Rosseinsky, A. P. Ramirenz, S. H. Glarum, D. M. Murphy, R. C.

Haddon, A. F. Hebard, T. T. M. Palstra, A. R. Kortan, S. M. Zahurak, and A. V. Makhija, *Phys. Rev. Lett.*, **66**, 2830(1991).
19. K. Tanigaki, T. W. Ebbesen, S. Saito, J. Mizuki, J. S. Tsai, Y. Kubo, and S. Kuroshima, *Nature*, **352**, 222(1991).
20. J. S. Miller, A. J. Epstein, and W. M. Reiff, *Chem. Rev.*, **88**, 201(1988).
21. D. A. Dougherty, *Acc. Chem. Res.*, **24**, 88(1991).
22. H. M. McConnell, *J. Chem. Phys.*, **39**, 1910(1963).
23. N. Mataga, *Theor. Chim. Acta* (*Berl.*), **10**, 372(1968).
24. A. A. Ovchinnikov, *Theor. Chim. Acta* (*Berl.*), **47**, 297(1978).
25. T. Sugawara, S. Bandow, K. Kimura, H. Iwamura, and K. Itoh, *J. Am. Chem. Soc.*, **108**, 368(1986).
26. Y. Teki, T. Takui, K. Itoh, H. Iwamura, and K. Kobayashi, *J. Am. Chem. Soc.*, **108**, 2147(1986).
27. K. Awaga, T. Sugano, and M. Kinoshita, *J. Chem. Phys.*, **85**, 2211(1986).
28. M. Kinoshita, P. Turek, M. Tamura, K. Nozawa, D. Shiomi, Y. Nogami, M. Ishikawa, M. Takahashi, K. Awaga, T. Inabe, and Y. Maruyama, *Technical Report of ISSP*, Ser. A, No. 2408(1991).
29. P.-M. Allemand, K. C. Khemani, A. Koch, F. Wudl, K. Holzer, S. Donovan, G. Grüner, and J. D. Thompson, *Science*, **253**, 301(1991).

PART I

THEORETICAL APPROACH TO ELECTRONIC STRUCTURE AND PHOTOEXCITED STATE OF POLYACETYLENE

INTRODUCTION

Usually, polyacetylene, $(CH)_x$ is regarded as a prototype conducting polymer. Perhaps *trans*-$(CH)_x$ is an ideal substance by which we can realize our dream of one-dimensional metal. $(CH)_x$ is synthesized using the Ziegler-Natta catalyst of $Ti(OC_4H_9)_4$-$Al(C_2H_5)_3$ with an Al/Ti ratio of 2-4.[1] The *cis* form can be prepared at low temperature as silvery flexible films which can be made either free-standing or on a substrate.[2] The *trans* isomer is the thermodynamically stable form. Any *cis-trans* ratio can be maintained at low temperature, but complete isomerization from *cis*- to *trans*-$(CH)_x$ can be accomplished after synthesis by heating the film to temperature above 150 °C from a few minutes to more extended time periods. $(CH)_x$ is doped with various electron acceptors such as AsF_5, I_2, Br_2, BF_3, HF, and $HClSO_3$ as well as by electron donors such as Li, Na, and K.[2] The electrical conductivity of $(CH)_x$ can be varied in a controlled manner over 15 orders of magnitude through chemical or electrochemical doping. It is suggested that small amount of AsF_5 or I_2 induces *cis* to *trans* isomerization[3] and that consequently heavily doped samples would be *trans* form. Moreover, we have observed the occurrence of *cis* to *trans* isomerization accompanied by photoexcitation[4] as well as by doping[5].

In conducting polymers, the linear structure leads to strong coupling of the electronic states to conformational excitations such as solitons, polarons, and bipolarons peculiar to one-dimensional electron systems.[2] The attraction of the soliton model of Su, Schrieffer, and Heeger (SSH)[6] shown below is both theoretical simplicity and its apparent ability to interpret magnetic, electrical, and optical properties of *trans*-$(CH)_x$.

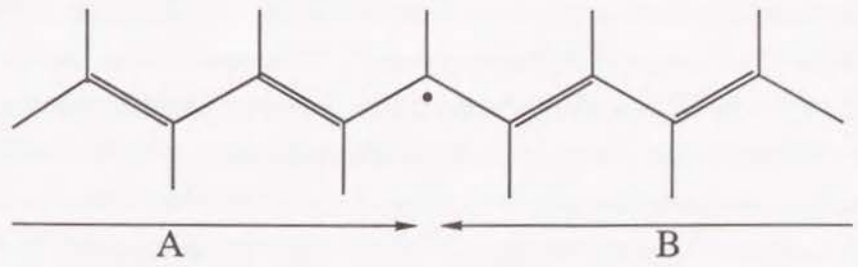

The proposed soliton in *trans*-$(CH)_x$ illustrated above is a topological kink in the electron-lattice system: a bond alternation domain wall A and B phase with opposite bond alternation. The width of the soliton is approximately 14 lattice spacing for $(CH)_x$ and its mass is remarkably small, roughly six times of an electron mass.[6] Since there is complete degeneracy between A and B phase and since the mass is small, the kink is expected to be mobile. There is clear and extensive evidence that charged solitons are produced both by charge transfer doping and by photoexcitation. The positively charged soliton, S^+ and the negatively charged one, S^- have spin zero in contrast with holes and electrons having spin 1/2. Also, the neutral soliton, S^0 has spin 1/2.[6]

Photoexcitation studies of conjugated conducting polymers were stimulated by the calculations of Su and Schrieffer, which demonstrated that in *trans*-$(CH)_x$ an electron-hole (*e-h*) pair should evolve into a pair of solitons within about 10^{-13} s.[7] The visible spectrum of *trans*-$(CH)_x$ film shows a strong absorption band at 1.9 eV and a band gap of about 1.4 eV. The *cis* isomer has a similar spectrum with slightly higher energies. In the *trans* isomer there is also additional absorption at lower energy which is observed to appear at 0.5 eV.[8] From the asymmetric shape of this absorption, it is believed that this peak is due to an electronic transition from a state in the gap to the nearest band of continuum levels.[9] The photoconductivity in *trans*-$(CH)_x$ has a threshold at 1.0 eV, well below the interband absorption edge at 1.4 eV, implying the presence of states deep inside the gap.[10] The observations of luminescence in *cis*-$(CH)_x$, but not in *trans*-$(CH)_x$, and of photoconductivity in *trans*-$(CH)_x$, but not in *cis*-$(CH)_x$ give confirmation of the proposal that solitons are the photogenerated carriers. In *trans*-$(CH)_x$, the degenerate ground state leads to free soliton excitations, absence of band-edge luminescence, and photoconductivity.[10] In *cis*-$(CH)_x$, on the other hand, the nondegenerate ground state leads to confinement of the photogenerated carriers, absence of photoconductivity, and to the observed recombination luminescence.

A number of investigators have suggested charged soliton to be the

transport species in the spinless conductivity regions, up to 5 %-doping level.[11] It is well established that interchain transport must be facile for efficient carrier migration. In fact, interchain conduction is probably rate limiting in all conducting polymer systems. A few of theoretical models on the interchain soliton-hopping have been presented by Kivelson[12] and Yamabe et al.[13] Associated with this interchain interaction, the study of photoinduced electron spin resonance (ESR) is important. A decrease in the ESR signal upon photoexcitation has been observed in a rather poor sample containing a high density of defects and short conjugation length, and not in a high-quality sample.[14] This is an indication of the occurrence of interchain soliton-hopping.

Recent studies in the field of conducting polymers are concerned with nonlinear optical process with characteristic time scale in the picosecond range or faster. The major shifts in oscillator strength due to photoexcitation of solitons, polarons, and bipolarons lead to relatively large third-order nonlinear optical process ($\chi^{(3)}$).[7] These nonlinear phenomena are intrinsic and originate from the instability of these conjugated polymers toward structural distortion.

One of the most important problems in the theoretical aspect of one-dimensional electron system is the prediction and understanding of charge density wave (CDW) and spin density wave (SDW) states. Peierls and Overhauser have shown that a one-dimensional electron system is unstable against a modulation of wavevector $2k_F$, where k_F is the radius of the Fermi sphere.[15] The CDW and SDW states are insulating phases which are induced by a modulation of the mixture of periodic lattice with charge and that of only the electron spin polarization, respectively. In the CDW structure, the charge densities for the two spin states are modulated in phase; consequently the spin density is zero everywhere. The SDW structure differs from the CDW case in two important aspects. The SDW structure has spatially inhomogeneous charge densities for both spin states, but 180° out of phase. Therefore, the total charge density of the SDW is a constant,

independent of position.[16]

The Hartree-Fock equations are based on the variation principle that the first variation of the functional $E(\Phi) = \langle\Phi|H|\Phi\rangle/\langle\Phi|\Phi\rangle$ be zero for the Slater determinant. Strictly speaking, the second variation has to be examined in order to check whether the stationary points correspond to the minimum, the maximum, or a more complicated state. Until the prediction of Overhauser in 1960, such instability problems associated with the Hartree-Fock solutions were not treated at all. Following the general derivation for the stability by Thouless,[17] Čížek and Paldus[18] presented using the method of quantum chemistry the stability condition which ensures that the Hartree-Fock determinant minimizes the energy expectation value. The main correction to the Hartree-Fock solutions must arise from the correlation of antiparallel-spin electrons, because parallel-spin electrons are kept apart by the effect of the antisymmetrization operator. The most important concepts to correct the Hartree-Fock theory are the configuration interaction and the alternant molecular orbital (AMO) method proposed by Löwdin.[19] In particular, since the AMO method preserves the simplicity of the one-electron picture, it schematically shows us the correlation effect.

Interestingly, these theoretical concepts were found to be deeply related to the actual electronic structure of one-dimensional solids such as $(CH)_x$, $(SN)_x$, and a series of molecular crystals. Hartree-Fock crystal orbital studies on a hydrogen chain, a carbon chain, $(SN)_x$, and $(CH)_x$ have been performed by Kertész et al.[20] and André et al.[21] in a numerical manner.

In Chapter 1 (*Int. J. Quantum. Chem.*, **40**, 305(1991)), the midgap levels generated in photoexcited conducting polymers such as *trans*- and *cis*-$(CH)_x$, poly(*p*-phenylene), polypyrrole, and polyacene are described on the basis of the interaction between the highest occupied molecular orbital and the lowest unoccupied molecular orbital using the Pariser-Parr-Pople approximation. As a result of the wavefunctions associated with these midgap levels, large polarization is induced between adjacent carbon atoms.

In Chapter 2 (*Int. J. Quantum. Chem.*, **40**, 315(1991)), the problem of a photogenerated soliton pair is treated using the formulation obtained above. In particular, chain deformation accompanied by the creation of the soliton pair is explicitly taken into account in this study. The soliton pair, S^+-S^-, is bound owing to the Coulomb attraction; consequently, the intersoliton distance is estimated to be 10 Å. It is found that the energy gap between the midgap levels is estimated to be 0.45 eV, signifying the relation to the additional photoinduced absorption of *trans*-$(CH)_x$.

In Chapter 3 (*Synth. Met.*, **36**, 75(1990)), the idea described in Chapters 1 and 2 is expanded to the interchain problem within the same level of approximation. The interaction of two solitons on two *trans*-$(CH)_x$ chains is studied within the framework of the restricted Hartree-Fock and unrestricted Hartree-Fock methodologies. Energetical stability for a singlet pair of neutral solitons and a pair of oppositely charged solitons, each existing and interacting on the two chains, is discussed. On the basis of this model, the decrease in the ESR signal of *trans*-$(CH)_x$ upon photoexcitation is discussed.

In Chapter 4 (*J. Chem. Phys.*, **91**, 3724(1989)), a simplified stability condition for the Hartree-Fock solution of the infinite one-dimensional system is formulated. Since the present formulation, particularly for the systems having nearly or entirely degenerate highest occupied and lowest unoccupied crystal orbitals, contains only two physical parameters, that is, the density of states and the Coulomb repulsion integrals both at the Fermi level. Along the present criterion, the energetical stability of the bond-alternating structure, which is related to the off-diagonal CDW, for *trans*-$(CH)_x$ is treated.

In Chapter 5 (*J. Chem. Phys.*, submitted), an intrinsic unrestricted Hartree-Fock (UHF) crystal orbital (CO) scheme for polymers and crystals having antiferromagnetic spin array is presented. The procedure of this method is composed of two steps of self-consistent-field (SCF) equations; the second SCF equation is solved using the canonical transformation between the crystal orbitals near the Fermi level of the first SCF solution. This scheme is based on the concept of the $2k_F$-instability in one-dimensional solids. Our calculations clearly show that the bond-alternating structure of

trans-$(CH)_x$ is more stable than the antiferromagnetic state.

References

1. H. Shirakawa, Y.-X. Zhang, K. Mochizuki, K. Akagi, H. Kyotani, and Y. Tanabe, *Synth. Met.*, **41**, 13(1991).
2. A. O. Patil, A. J. Heeger, and F. Wudl, *Chem. Rev.*, 88, 183(1988).
3. S. Roth and H. Bleier, *Adv. Phys.*, **36**, 385(1987).
4. K. Tanaka, T. Koike, K. Ohzeki, K. Yoshizawa, and T. Yamabe, *Solid State Commun.*, **47**, 127(1983); K. Tanaka, T. Koike, K. Yoshizawa, K. Ohzeki, and T. Yamabe, *ibid*, **49**, 165(1984).
5. K. Tanaka, K. Yoshizawa, K. Ohzeki, and T. Yamabe, *Solid State Commun.*, **45**, 391(1983).
6. W. P. Su, J. R. Schrieffer, and A. J. Heeger, *Phys. Rev.*, B**22**, 2099(1980), and W. P. Su and J. R. Schrieffer, *Proc. Nat. Acad. Sci. U.S.A.*, **77**, 5626(1980).
7. A. J. Heeger, D. Moses, and M. Sinclair, *Synth. Met.*, **15**, 95(1986).
8. J. Orenstein and G. L. Baker, *Phys. Rev. Lett.*, **49**, 1043(1982).
9. Z. Vardeny, J. Orenstein, and G. L. Baker, *Phys. Rev. Lett.*, **50**, 2032(1983).
10. L. Lauchlan, S. Etemad, T.-C. Chung, A. J. Heeger, and A. G. MacDiarmid, *Phys. Rev.*, B**24**, 3701(1981).
11. R. R. Chance, D. S. Boudreaux, J. -L. Brédas, and R. Silbey, *Solitons, Polarons, and Bipolarons in Conjugated Polymers*, T. A. Skotheim Ed., *Handbook of Conducting Polymers*, Marcel Dekker, New York, 1986.
12. S. Kivelson, *Phys. Rev.*, B**26**, 4173(1982).
13. T. Yamabe, K. Tanaka, S. Yamanaka, T. Koike, and K. Fukui, *J. Chem. Phys.*, **82**, 5737(1985).
14. F. Moraes, Y. W. Park, and A. J. Heeger, *Synth. Met.*, **13**, 113(1986).
15. See, for instance, D. Jérome and H. J. Schulz, *Adv. Phys.*, **31**, 299(1982).
16. A. W. Overhauser, *Adv. Phys.*, **27**, 343(1978).
17. D. J. Thouless, *The Quantum Mechanics of Many Body Systems*, Academic, New York, 1961.

18. J. Čížek and J. Paldus, *J. Chem. Phys.*, **47**, 3976(1967).
19. P. O. Löwdin, *Phys. Rev.*, **97**, 1509(1955).
20. M. Kertész, J. Koller, and A. Azman, *Phys. Rev.*, B**19**, 2034(1979) and references therein.
21. J.-M. André, J.-L. Brédas, J. Delhalle, Y. Kalenov, and L. Piela, *Int. J. Quantum. Chem.: Quantum Chem. Symp.*, **14**, 419(1980).

Chapter 1

Midgap Levels of Photoexcited Conductive Polymers. I. A Simple Description of the Midgap Levels Based on Molecular Orbital Interaction

Introduction

The concept of the charged soliton in *trans*-polyacetylene, or *trans*-$(CH)_x$, has been widely accepted concomitant with the idea of the neutral soliton proposed by Su, Schrieffer and Heeger (SSH).[1] For example, it is well known that the origin of several characteristic infrared (IR) absorption peaks newly appearing in the doped $(CH)_x$[2] and the electrical conduction carriers therein at a certain doping range have been ascribed to the function of the charged solitons generated in the $(CH)_x$ chain interacting with the dopant species.[3] Furthermore, Su and Schrieffer have shown that an electron-hole (*e-h*) pair generated in the photoexcited *trans*-$(CH)_x$ is unstable and evolves into a *soliton-antisoliton* namely, positively charged soliton-negatively charged soliton (S^+-S^-) pair within 10^{-13} seconds in the course of the simulation of dynamical processes of solitons.[4] The S^+-S^- pair thus generated is considered to be responsible for the photoconductivity observed in *trans*-$(CH)_x$ with the threshold value 1.0 eV[5] being smaller than the optical band gap 1.4 eV.[6] These suggest that the energy level of the S^+-S^- pair lies in the midgap between the valence and the conduction bands (VB and CB).

As shown in Fig. 1(a), there is no difference in the energetical levels of the S^+ and S^- within the framework of the original SSH model.[1] Actually, however, these levels are split off the gap center when an explicit Coulomb

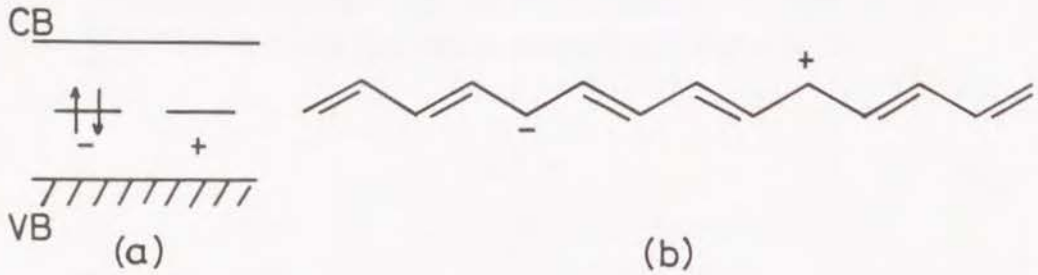

Fig. 1. Schematic representation of (a) the energetical and (b) the chemical structure of the photoexcited *trans*-$(CH)_x$. VB and CB signify the valence and the conduction bands, respectively.

interaction is included,[7] and hence, the picture in Fig. 1(a) has to be modified. The idea of breather formed after the injection of an *e-h* pair has been proposed and applied to elucidate the observation of the photoinduced absorption spectra of *trans*-$(CH)_x$.[8-10] In recent years, on the other hand, preparation of $(CH)_x$ with highly oriented polymer chains have been developed.[11,12] Such $(CH)_x$ sample has shown the electrical conductivity more than 10^5 $S \cdot cm^{-1}$ upon doping.[13] The development of these high-quality $(CH)_x$ samples may further accelerate the basic understanding on this material by virtue of more minute experiment on its solid state properties.

Considering these situations, we feel that it would be worth while reexamining the occurrence of the photoinduced charged solitons and visualizing it, using a molecular orbital (MO) method. In the present article, we afford a simple description of the midgap levels appearing in photoexcited $(CH)_x$ as well as other several conductive polymers such as poly(*p*-phenylene), polypyrrole and polyacene based on the orbital interaction around the Fermi level. The midgap levels in the photoexcited states of these polymers have not yet been studied theoretically. Basic calculations are carried out using the MO method for π electrons including the explicit Coulomb interactions (Pariser-Parr-Pople approximation).[14,15] The energy gap between the two midgap levels generated under the photoexcitation is to be estimated for all these polymers.

Formulation

The explicit Hamiltonian for π electrons in the framework of the Pariser-Parr-Pople approximation[14,15] can be written as follows:

$$H = \sum_{rs\sigma} t_{rs} c_{r\sigma}^{\dagger} c_{s\sigma} + \frac{1}{2} \sum_{rs\sigma\sigma'}{}' R_{rs} c_{r\sigma}^{\dagger} c_{r\sigma} c_{s\sigma'}^{\dagger} c_{s\sigma'} , \tag{1}$$

where $c_{r\sigma}^{\dagger}$ and $c_{r\sigma}$ are the fermion creation and annihilation operators,

respectively, for an electron with spin σ at the rth site, t_{rs} the core integral between the atomic π orbitals χ_r and χ_s, and R_{rs} the Coulomb repulsion integral between the electrons in χ_r and χ_s. The prime in Σ' of the second term means that it excludes all the terms, $r = s$ and at the same time $\sigma = \sigma'$. For the core integrals, we consider the on-site and the nearest neighboring site interactions in a semi-empirical manner,

$$t_{rr} = -I_r - \sum_{s \neq r} n_r R_{rs} \tag{2}$$

and

$$t_{rs} = -0.4314\, S_{rs}(I_r + I_s) \qquad (s = r \pm 1) \tag{3}$$

where I_r and I_s are the ionization potentials for χ_r and χ_s, n_r the effective nuclear charge of the atom r (= +1 for a carbon), and S_{rs} the overlap integral between χ_r and χ_s. For the estimation of the Coulomb repulsion integrals, we use the following formula,

$$R_{rr} = I_r - A_r \tag{4}$$

and

$$R_{rs} = 7.1975[\ 1/\{d^2 + 5.2831(1/Z_r - 1/Z_s)^2\}^{1/2} + 1/\{d^2 + 5.2831(1/Z_r + 1/Z_s)^2\}^{1/2}] \qquad (\text{for } d \geq 2.8\text{Å})$$

$$R_{rs} = (R_{rr} + R_{ss}) + ad + bd^2 \qquad (\text{for } d < 2.8\text{Å}) \tag{5}$$

where A_r is the electron affinity for χ_r, d the distance between the rth and the sth sites, Z_r and Z_s Slater's effective nuclear charges (= 3.25 for a carbon), and a and b constants.[14] We solve the Schrödinger equation of π electrons based on the Hamiltonian in Eq. (1) by the self-consistent-field (SCF) method.

The S^+-S^- pair eventually generated in photoexcited $(CH)_x$ is illustrated in Fig. 1(b), which is a kind of intramolecular charge transfer complex or zwitterionic state. This zwitterionic state or S^+-S^- levels should lie in the midgap of the VB and the CB, and the wave functions accompanied by are considered to be somewhat localized at least to represent the identified soliton pictures. Zwitterionic states of small molecules such as ethylene has been extensively discussed by Salem and Rowland.[16]

In order to represent the midgap levels we employ the picture of the two orthonormal MOs constructed from the transformation of the highest occupied molecular orbital (HOMO) φ_{HO} and the lowest unoccupied molecular orbital (LUMO) φ_{LU} defined by

$$\psi_R = \cos\theta\varphi_{HO} + \sin\theta\varphi_{LU}$$
$$\psi_{R'} = -\sin\theta\varphi_{HO} + \cos\theta\varphi_{LU} \tag{6}$$

Here θ is the mixing parameter to be chosen between 0 and $\pi/2$. These ψ_R and $\psi_{R'}$ are doubly occupied and vacant, respectively, and they can be regarded as a kind of localized MO analogous to alternant MO developed by Löwdin and coworkers[17,18] when $\theta = \pi/4$ as is employed in later. We confine ourselves to the finite chain of each polymer including ca. 100 carbon atoms for the sake of simplicity.

An orthonormal orbital set $(\psi_1 \ldots \psi_n)$ can be defined with a transformation of the SCF orbital set $(\varphi_1 \ldots \varphi_n)$ as follows:

$$\psi_i = \sum_j U_{ij}\ \varphi_j\ , \tag{7}$$

$$U = \begin{pmatrix} 1 & & & & & & & \\ & \ddots & & & & & & \\ & & 1 & & & & & \\ & & & \cos\theta & \sin\theta & & & \\ & & & -\sin\theta & \cos\theta & & & \\ & & & & & 1 & & \\ & & & & & & \ddots & \\ & & & & & & & 1 \end{pmatrix} .$$

In particular, we are interested in the limited case of $\theta = \pi/4$ because the HOMO and the LUMO are mixed completely, and the maximum ionic character can be issued. Detailed discussion on θ will be given in later. Although the obtained orthonormal orbitals are not the exact eigenvectors of the Fock operator, yet the orbital energies can be approximately estimated from the diagonal elements of quadratic form, ε_{ij},

$$\varepsilon_{ii} = \sum_{rs} c_{ir}\, c_{is}\, F_{rs} \ , \tag{8}$$

$$\varepsilon_{ij} = \sum_{rs} c_{ir}\, c_{js}\, F_{rs} \approx 0, \tag{9}$$

$$\varepsilon_{RR'} \neq 0 \tag{10}$$

where c_{ir} is the coefficient of the π atomic orbital on the rth site in the ith MO, and F_{rs} is the element of the Fock operator newly composed of the transformed orbital set ($\psi_1 \ldots \psi_n$) in Eq.(7).

Results and discussion

We apply the representation of the midgap levels to some conductive polymers.

Application to trans-$(CH)_x$

We calculate a *trans*-$(CH)_x$ chain with finite length having 100 CH units. For the order of this size, the occupied and the unoccupied orbitals practically form two bands, namely, the VB and the CB, respectively. Figure 2 shows the HOMO, the LUMO, and two localized orbitals ψ_R and $\psi_{R'}$ for *trans*-$(CH)_x$ when $\theta = \pi/4$. Due to the symmetries of the HOMO and the LUMO patterns, ψ_R and $\psi_{R'}$ are localized on alternate carbon sites.

The overall AO coefficients of ψ_R are shown in Fig. 3. These decay in the both ends of $(CH)_x$ chain. In the Hückel-type approximation including no Coulomb interactions, however, the AO coefficients become larger in the ends of the polyene.[19] Accordingly, the charges are diffused all over the polyene chain when we utilize the Hückel approximation.

As the result of the localization of ψ_R, positive and negative charges are alternately induced in the $(CH)_x$ chain as illustrated in Fig. 4. This result suggests that the photoinduced charges spatially correlate owing to the Coulomb interaction and polarize the $(CH)_x$ chain. The polarization is also found in the doped $(CH)_x$ based on the MO calculations of finite polyenes losing one or two electrons.[20] Thus, photoexcited $(CH)_x$ and doped $(CH)_x$ are in a sense analogous to one-dimensional ionic polymers such as organosilane polymers[21] and $(SN)_x$,[22] wherein silicon and sulfur atoms are positively charged and, on the other hand, carbon and nitrogen atoms negatively charged. The polarization has a strong influence on enhanced IR bands appearing in the doped and in photoexcited $(CH)_x$ which are usually called soliton bands.

Figure 5 illustrates the orbital energies of ψ_R and $\psi_{R'}$ plotted as a function of θ and the corresponding electronic configurations. The point *a* in the figure indicates the band structure of the ground state, where no midgap

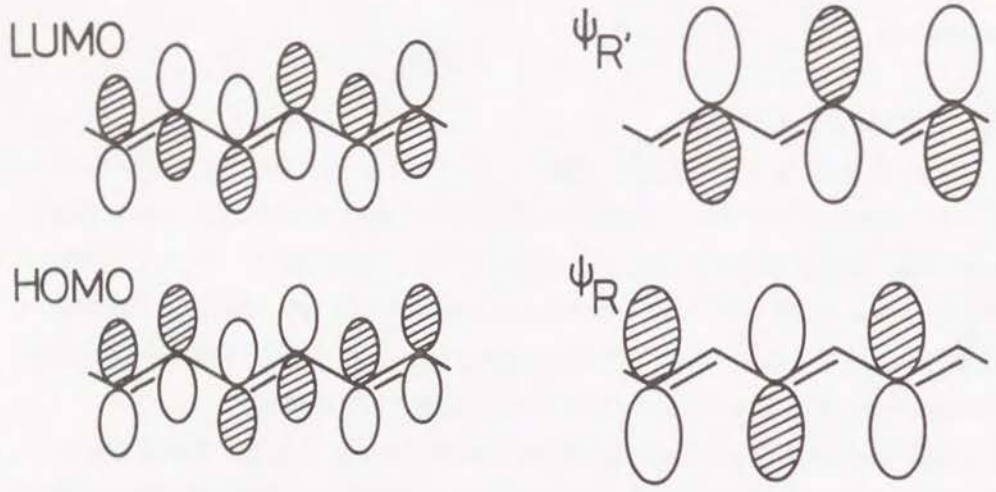

Fig. 2. Orbital patterns of the HOMO, the LUMO and the wavefunctions associated with the midgap levels of *trans*-$(CH)_x$.

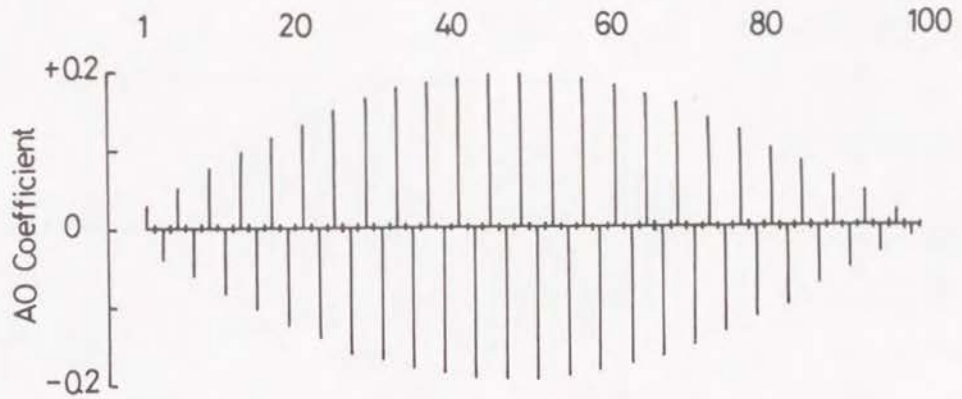

Fig. 3. Shape of ψ_R of the photoexcited trans-$(CH)_x$, in case n (the number of carbon atoms) = 100 and $\theta = \pi/4$.

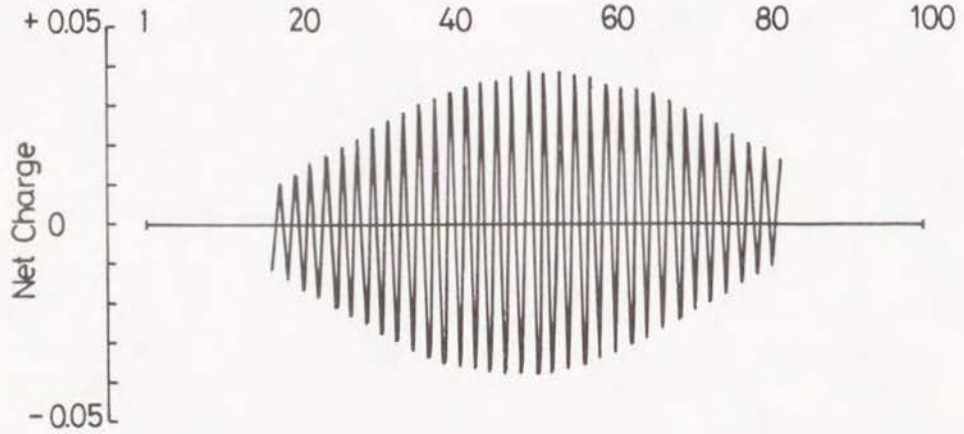

Fig. 4. π-charge distribution of the photoexcited *trans*-$(CH)_x$, in case n = 100 and $\theta = \pi/4$. Note the polarization is induced between adjacent carbon atoms.

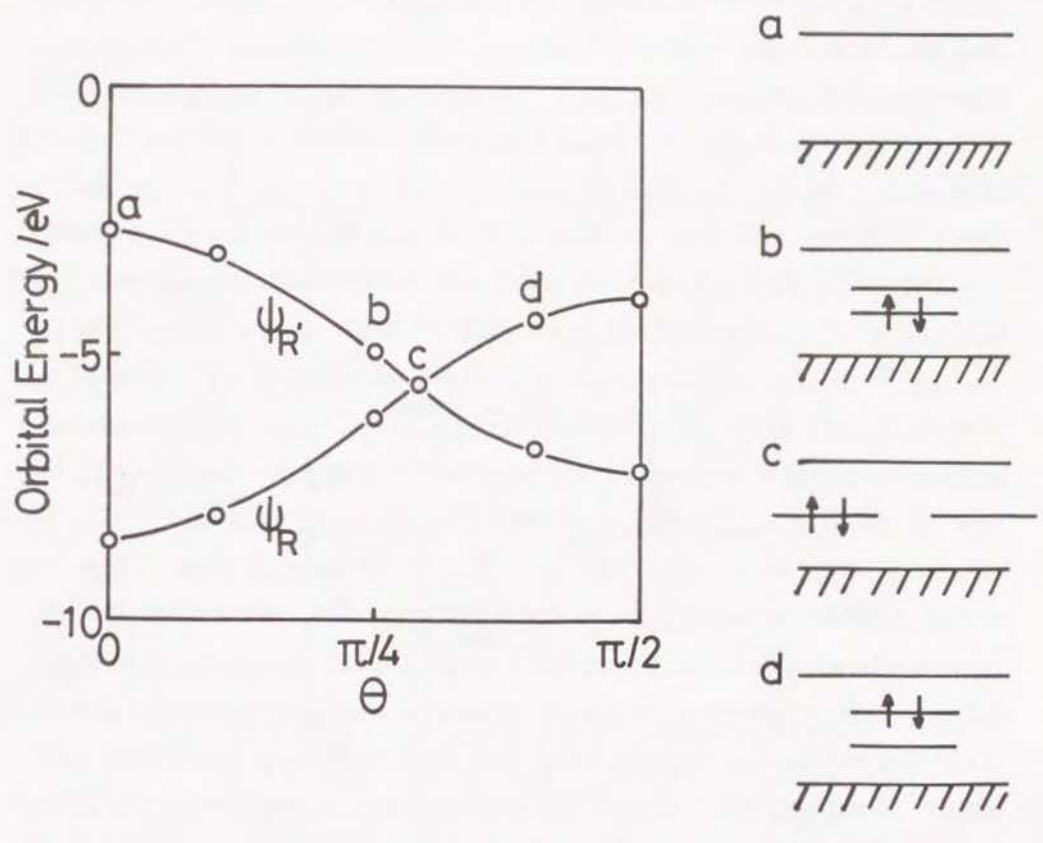

Fig. 5. θ-dependency of the midgap levels and the electronic configurations associated for *trans*-$(CH)_x$ in case n = 100.

levels exist. The MOs under the next HOMO and over the next LUMO are insensible to the transformation in Eq.(7) and they form the VB and the CB, respectively, at any θ. When $\theta = \pi/4$ (the point b in the figure), the HOMO and the LUMO are mixed completely, yielding two equivalent orbitals. However, a small energy gap exists between the two midgap levels, due to inclusion of the explicit Coulomb interaction, when ψ_R is filled with two electrons. Within the Hückel approximation, as a matter of course, the energy difference between the midgap levels is zero when $\theta = \pi/4$. When θ becomes more than $\pi/4$, one can anticipate that the system is unstable. In general, since the SCF method has a tendency to overestimate the band gap energy,[23] the above energy gap is scaled down to 0.29 eV utilizing the observed band gap value 1.4 eV of *trans*-$(CH)_x$.[6] Figure 6 schematically represents the band structure of photoexcited *trans*-$(CH)_x$. In this figure one can see the appearance of the two midgap levels owing to the transformation of the HOMO and the LUMO of $(CH)_x$ in the ground state. The two wavefunctions ψ_R and $\psi_{R'}$ associated with these midgap levels are spatially correlated each other and, hence, the charged centers cannot move so freely. However, they can be rather easily separated and carry electrical charges under the application of the external electrical field when this correlation is small. The degree of this correlation is described by the energy gap values between the S^+ and the S^- levels at $\theta = \pi/4$ listed in Table I. *Cis*-$(CH)_x$ has a little larger gap 0.45 eV compared with *trans*-$(CH)_x$. As the result, the photoconductivity for the *cis*-form should be less remarkable compared with that for the *trans*-form. In fact, the observation of the photoconductivity has not been reported with respect to *cis*-$(CH)_x$.[5]

On the other hand, several authors[25-27] have observed an additional absorption peak around 0.5 eV in photoexcited *trans*-$(CH)_x$. Vardeny et al.[26] have concluded that this peak is due to an electronic transition from a midgap state to the nearest band of continuum levels. From the present analysis, another interpretation is possible. That is, this peak has the origin in the transition from the occupied localized level to the vacant one.

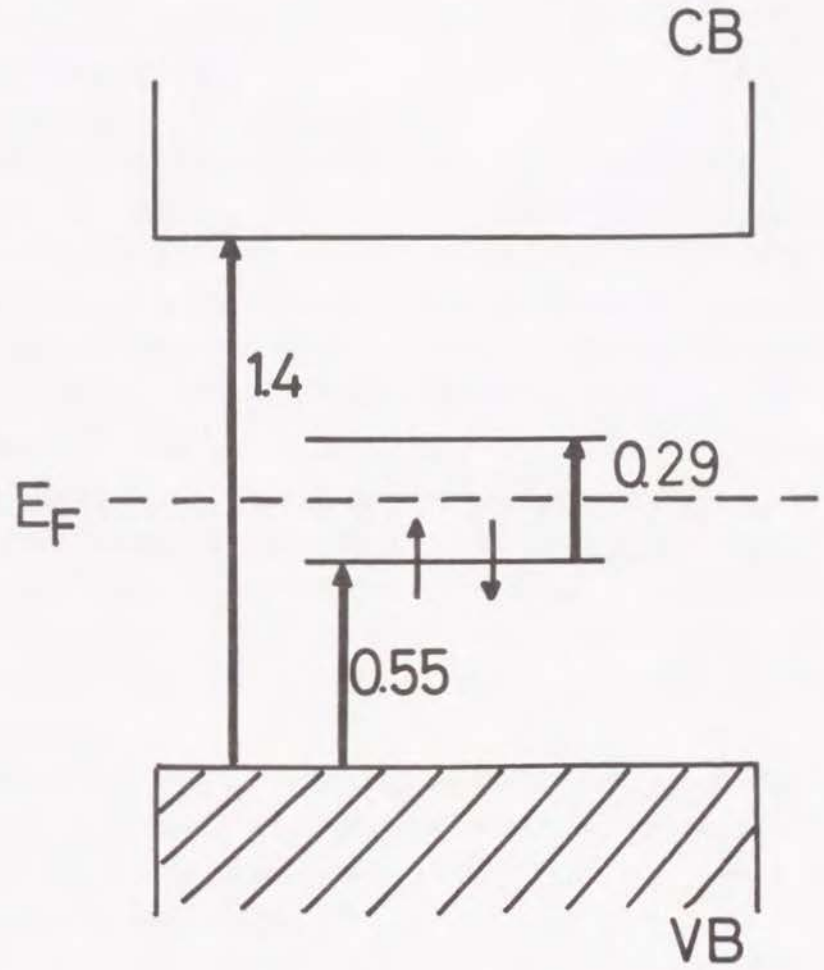

Fig. 6. Schematic representation of the energetical structure of photoexcited *trans*-$(CH)_x$ (in eV). E_F signifies the Fermi level.

Table I. Energy gaps between the midgap levels of the photoexcited states (in eV)[a] for some conductive polymers.

Polymer	Energy gap
trans-$(CH)_x$[b]	0.29
cis-$(CH)_x$[b]	0.45
PPP[b]	0.73
PPy[b]	0.73
PA[c]	0.15

[a] For $\theta = \pi/4$.

[b] Energy gap is scaled down using the observed band gap in each polymer.

[c] Energy gap is scaled down using the calculated band gap of PA. See Ref. 24.

Application to other polymers

We apply the above analysis to the model chains of poly(*p*-phenylene) (PPP), polypyrrole (PPy) and polyacene (PA) having 18, 20, and 22 units, respectively. Brédas et al.[28] have carried out the MO calculations on the bipolaron bands of the doped chains for PPP and PPy. Here we would like to examine the midgap levels of the photoexcited these polymers. Figure 7 illustrates the HOMOs, the LUMOs and the two localized orbitals, ψ_R and $\psi_{R'}$ of PPP, PPy and PA. PPP and PPy have no energetically degenerated ground states. In PPP, localization takes place on one of the *para* sites of the connected benzene rings. The patterns of ψ_R and $\psi_{R'}$ of PPy are analogous to those of PPP. On the other hand, ψ_R and $\psi_{R'}$ in PA are localized on the lower and the upper edges, respectively, of the polymer skeleton. The orbital pattern on each edge resembles that of *trans*-$(CH)_x$ and, hence, PA would be interpreted as two interacting *trans*-$(CH)_x$ chains from the viewpoint of the π electronic structure. When PA is photoexcited, the electrical current due to the positively charged or the negatively charged solitons would separately run along the upper or lower edge of the condensed benzene rings.

Charge distributions for PPP, PPy and PA are illustrated in Fig. 8. Large polarization is induced in each polymer. Consequently, strong enhanced IR bands would also be observed in the photoexcited states of these conductive polymers like in *trans*-$(CH)_x$.

PA has a small energy gap like *trans*-$(CH)_x$ compared with PPP and PPy as seen in Table I. Hence, the charged centers should be separated less easily in PPP and PPy. That photoconductivities have not yet been reported for PPP and PPy seems to be justified on the basis of the present analysis. Considerably clear photoconductivity phenomenon, on the other hand, would be observed in the perfect skeleton of PA.

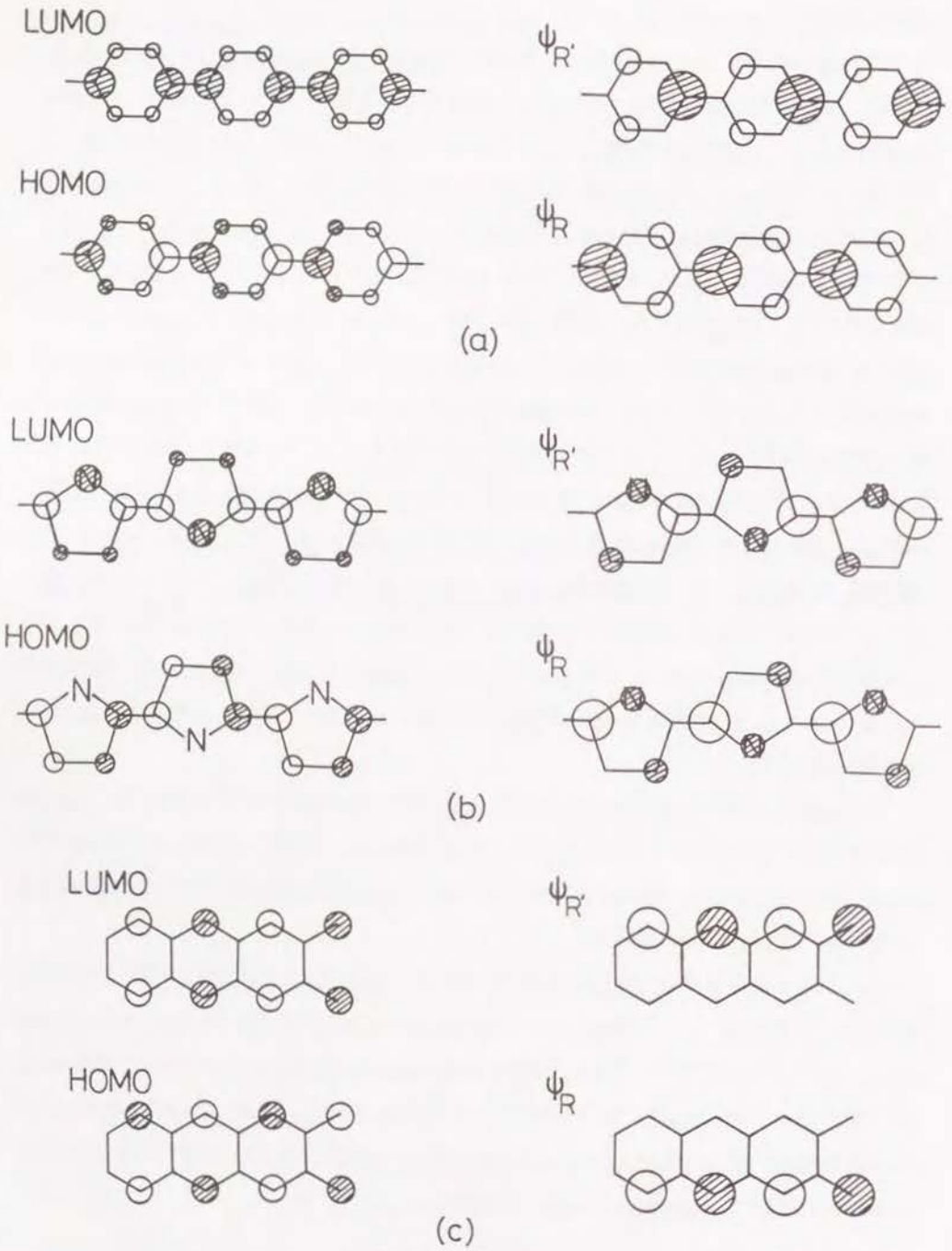

Fig. 7. Orbital patterns of the HOMOs, the LUMOs and the wavefunctions associated with the midgap levels of (a) PPP, (b) PPy and (c) PA.

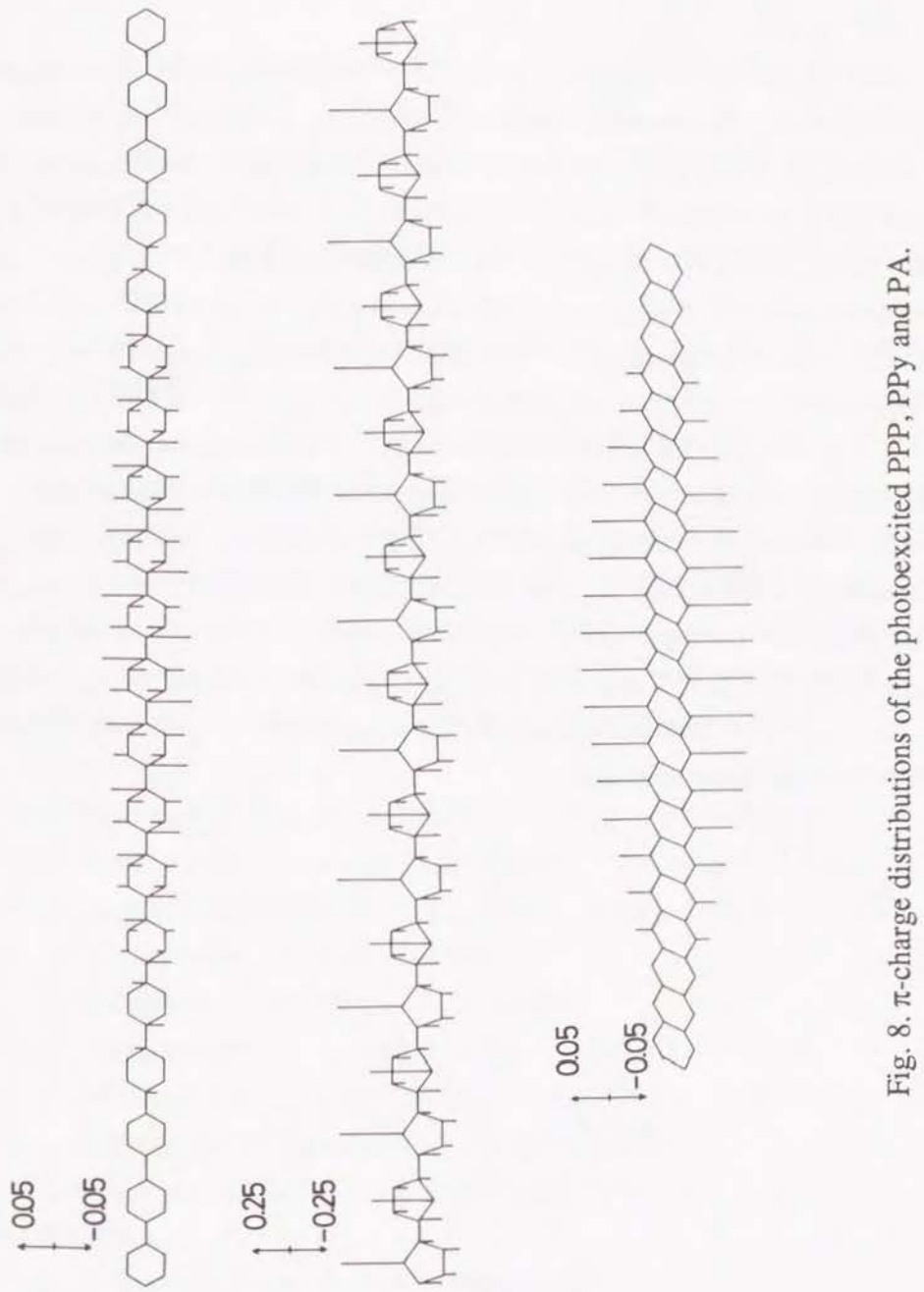

Fig. 8. π-charge distributions of the photoexcited PPP, PPy and PA.

Conclusion

A simple representation of the midgap levels appearing in the photoexcited conductive polymers has been presented. We have reexamined the occurring of the midgap levels in the photoexcited state of some conductive polymers in terms of the mixing of the HOMO and the LUMO of the ground state. We have visualized that these levels are associated with the S^+-S^- pair in the photoexcited conductive polymers, actually playing an important role in the photoconductivity especially in *trans*-$(CH)_x$. The energy gaps between the midgap levels have been estimated for *trans*- and *cis*-$(CH)_x$, PPP, PPy and PA. In particular, an additional peak at 0.5 eV observed in photoexcited *trans*-$(CH)_x$ would be ascribed to an electronic transition between two midgap levels. Because the energy gap is predicted to be small in PA, this polymer would show even a larger photoconductivity than *trans*-$(CH)_x$. As compared with polymers having degenerate ground states, non-degenerate polymers such as *cis*-$(CH)_x$, PPP and PPy have large gaps between the two localized levels, which should be responsible to no reports on photoconductive phenomena of these polymers.

References

1. W. P. Su, J. R. Schrieffer, and A. J. Heeger, *Phys. Rev. Lett.*, **42,** 1698(1979), and *Phys. Rev.*, B**22**, 2099(1980).
2. S. Etemad, A. Pron, A. J. Heeger, A. G. MacDiarmid, E. J. Mele, and M. J. Rice, *Phys. Rev.*, B**23**, 5137(1981).
3. See, for instance, K. Tanaka and T. Yamabe, *Adv. Quantum Chem.*, **17**, 251(1985).
4. W. P. Su and J. R. Schrieffer, *Proc. Natl. Acad. Sci. U.S.A.*, **77**, 5626(1980).
5. L. Lauchlan, S. Etemad, T. -C. Chung, A. J. Heeger, and A. G. MacDiarmid, *Phys. Rev.*, B**24**, 3701(1981).
6. C. R. Fincher, Jr., M. Ozaki, M. Tanaka, D. Peebles, L. Lauchlan, A. J. Heeger, and A. G. MacDiarmid, *Phys. Rev.*, B**20**, 1589(1979).
7. K. R. Subbaswamy and M. Grabowski, *Phys. Rev.*, B**24**, 2168(1981).
8. A. R. Bishop, D. K. Campbell, P. S. Lomdahl, B. Horovitz, and S. R. Phillpot, *Phys. Rev. Lett.* , **52**, 671(1984), and *Synth. Met.*,**9**, 223(1984).
9. M. Sasai and H. Fukutome, *Synth. Met.*, **9**, 295, 495(1984).
10. M. Sasai and H. Fukutome, *Prog. Theoret. Phys.*, **79**, 61(1988).
11. K. Akagi, S. Katayama, H. Shirakawa, K. Araya, A. Mukoh, and T. Narahara, *Synth. Met.*, **17**, 241(1987).
12. H. Naarmann, *Synth. Met.*, **17**, 223(1987).
13. H. Naarmann and N. Theophilou, *Synth. Met.*, **22**, 1(1987).
14. R. Pariser and R. G. Parr, *J. Chem. Phys.*, **21**, 466, 767(1953).
15. J. A. Pople, *Trans Faraday Soc.*, **49**, 1375(1953).
16. L. Salem and C. Rowland, *Angew. Chem. Intern. Ed. Engl.*, **11**, 92(1972).
17. P. O. Löwdin, *Phys. Rev.*, **97**, 1509(1955).
18. R. Pauncz, J. de Heer, and P. O. Löwdin, *J. Chem. Phys.*, **36**, 2247, 2257(1962).
19. See, for instance, A. Streitwieser, Jr., *Molecular Orbital Theory for*

Organic Chemists, John Wiley and Sons, New York, 1966.
20. T. Yamabe, K. Akagi, Y. Tanabe, K. Fukui, and H. Shirakawa, *J. Phys Chem.,* **86**, 2359(1982).
21. K. Tanaka, H. Kobayashi, T. Koike, T. Yamabe, Y. Osawa, S. Niwa, and N. Yasuda, *Synth. Met.*, **25**, 289(1988).
22. T. Yamabe, K. Tanaka, A. Imamura, H. Kato, and K. Fukui, *Bull. Chem Soc. Jpn.,* **50**, 798(1977).
23. See, for instance, M. Kertész, *Adv. Quantum Chem.,* **15**, 161(1982).
24. K. Tanaka, K. Ohzeki, S. Nankai, T. Yamabe, and H. Shirakawa, *J. Phys Chem. Solids*, **44**, 1069(1983).
25. J. Orenstein and G. L. Baker, *Phys. Rev. Lett.*, **49**, 1043(1982).
26. Z. Vardeny, J. Orenstein, and G. L. Baker, *Phys. Rev. Lett.*, **50**, 2032(1983).
27. G. B. Blanchet, C. R. Fincher, T. C. Chung, and A. J. Heeger, *Phys. Rev Lett.* **50**, 1938(1983).
28. J. L. Brédas, B. Thémans, J. G. Fripiat, J. M. André, and R. R. Chance, *Phys Rev.*, B**29**, 6761(1984).

Chapter 2

Midgap Levels of Photoexcited Conductive Polymers. II Detailed Analysis of *trans*-Polyacetylene

Introduction

Dynamical simulation[1] of photogenerated solitons in *trans*-polyacetylene, $(CH)_x$, has achieved a considerable success in terms of the photoconductive phenomena[2,3] within the framework of the Su-Schrieffer-Heeger (SSH) Hamiltonian.[4] When an electron-hole (*e-h*) pair is created in *trans*-$(CH)_x$ by photoexcitation, it has been shown that the *e-h* pair is unstable in the polyene and evolves into an oppositely charged soliton-antisoliton (S^+-S^-) pair, which lies between the valence and the conduction bands, within 10^{-13} seconds. Bishop et al.,[5] and Sasai and Fukutome[6] have further studied the breather oscillations left behind after the injection of an *e-h* pair.

On the other hand, spectroscopic studies and theoretical calculations including configuration interaction have shown that the lowest exited state is 2^1A_g state, which is strongly related to the neutral soliton pair.[7] However, the photoconductivity of *trans*-$(CH)_x$ is considered to be due to the S^+-S^- pair, and we are therefore interested in the the midgap levels associated with the S^+-S^- pair. Salem and coworkers[8] have shown that the singly-excited π-π^* state in ethylene leads through the molecular twisting to an occurrence of zwitterionic state which is an elementary representation of the S^+-S^- pair. Furthermore, it has been indicated that the ionic state significantly contributes to the 1^1B_u state of the zig-zag shaped polyene with the C_{2h} point group.[7] The 1^1B_u state is essentially represented by the one-electron excitation from

the highest occupied molecular orbital (HOMO) to the lowest unoccupied molecular orbital (LUMO) based on the one-electron picture, as shown by Yamabe et al.[9] for example.

In a previous paper,[10] we have studied the occurring of the midgap levels in the photoexcited state of some conductive polymers such as *trans*- and *cis*-$(CH)_x$, poly(*p*-phenylene), polypyrrole, and polyacene. The S^+-S^- pair in photoexcited *trans*-$(CH)_x$ is indeed associated with these localized midgap levels. In the present paper, we would like to reexamine a detailed structure of the midgap levels in terms of the formation of the charged soliton pair especially in *trans*-$(CH)_x$.

Method of calculation

In order to express a $(CH)_x$ model chain consisting of 100 carbons, we adopt the Pariser-Parr-Pople (PPP) Hamiltonian,[11,12]

$$H = \sum_{rs\sigma} t_{rs} c_{r\sigma}^{\dagger} c_{s\sigma} + \frac{1}{2}{\sum_{rs\sigma\sigma'}}' R_{rs} c_{r\sigma}^{\dagger} c_{r\sigma} c_{s\sigma'}^{\dagger} c_{s\sigma'} + \frac{1}{2}\sum_{r\neq s} U_{rs} \quad , \tag{1}$$

where $c_{r\sigma}^{\dagger}$ ($c_{r\sigma}$) creates (annihilates) an electron with spin σ on site r; t_{rs} is the core integral between the π atomic orbitals χ_r and χ_s; R_{rs} is the Coulomb repulsion between the electrons in χ_r and χ_s. For the core integrals, we consider the on-site and the nearest neighboring site. The prime in Σ' of the second term means that it excludes all terms, $r = s$ and at the same time $\sigma = \sigma'$. The detailed parametrization is given in the previous paper.[10] The last term in the Hamiltonian (1) represents effective nuclear repulsions which are simple Coulomb energy and contains a part of the energy of the σ-core.[12]

$$U_{rs} = n_1 n_2 e^2 / d_{rs}, \tag{2}$$

where n_1 and n_2 are effective nuclear charges (+1 for carbon), and d_{rs} is the

distance between sites r and s. We can obtain a set of canonical MOs (φ_i) by solving the Hartree-Fock equation under the π-electron approximation. As suggested by Orenstein and Baker,[13] the photogenerated levels in *trans*-$(CH)_x$ cannot be explained within the one-electron approximation. The concept of the orbital interaction around the Fermi level has played an important role in the theoretical studies on electronic structure of molecules and solids, and chemical reactions.[14,15] Here we therefore assume that the midgap levels associated with the S^+-S^- pair would be described by the mixing of the HOMO, φ_{HO}, and the LUMO, φ_{LU}, as

$$\begin{aligned} \psi_{S^-} &= \cos\theta\varphi_{HO} + \sin\theta\varphi_{LU}, \\ \psi_{S^+} &= -\sin\theta\varphi_{HO} + \cos\theta\varphi_{LU} \ . \end{aligned} \tag{3}$$

Here ψ_{S^-} and ψ_{S^+} are related to the doubly occupied S^- level and the vacant S^+ level, respectively.

Figure 1(a) and 1(b), both of which belong to the C_{2h} point group, illustrate model chains with perfect bond-alternation and with a pair of topological kinks, respectively. The location of the kinks is represented by wedges in the figure. N indicates the number of carbons inserted between a couple of kinks, and it takes 0, 2, 6, 10, 14, 18, and 22 so as to keep the structure of the model chain in the C_{2h} point group. The short bond length is fixed at 1.364 Å, the long one at 1.429 Å, and the bond angle at 120°. We thus calculate both the ground state and the zwitterionic state as a function of molecular geometry designated by N, from the formulation given above.

Now let us consider the mixing parameter, θ, which must be chosen between 0 and $\pi/2$. As mentioned above, the zwitterionic state is significantly related to the 1^1B_u state, that is, the HOMO to the LUMO one-electron excitation. On the basis of the singlet excitation energy from the HOMO to the LUMO, we can estimate θ at $43° \equiv \pi/4$, where the HOMO and the LUMO are completely mixed. We will discuss the limited case of $\theta = \pi/4$ throughout the present article.

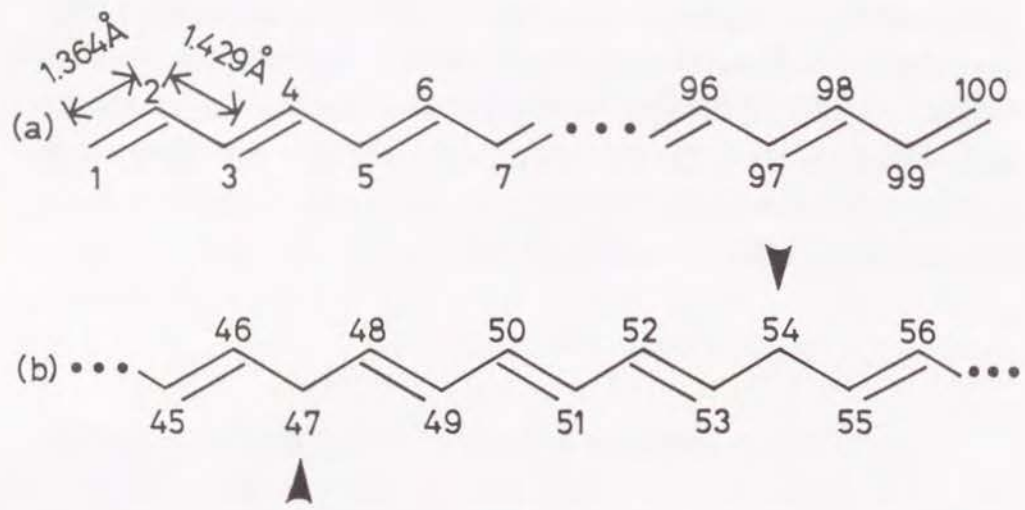

Fig. 1. Schematic representation of the model chains with (a) perfect bond-alternation and (b) a couple of topological kinks at a fixed intersoliton distance $N = 6$.

Results and discussion

Figure 2 shows the total energy for the ground state and the zwitterionic state as a function of N. The total energy for the ground state increases with an increase in N, whereas that for the zwitterionic state becomes the minimum at $N = 6$. Orbital patterns of the HOMO, the LUMO, ψ_{S^-}, and ψ_{S^+} for $N = 6$ are shown in Fig. 3, where the localization of the wave functions takes place around the kinks. Together with the result in Fig. 2, this clearly illustrates the creation of the S^+-S^- pair. In the PPP model, it is shown that the S^+-S^- pair cannot freely separate each other owing to the Coulomb attraction acting on a pair of the kinks.

For the molecular geometry, we restrict distortion of the model chain to the creation of the topological kinks constrained on the molecular plane to neglect the twisting of the chain; the extent of the decrease in the energy for the zwitterionic state would be larger if the twisting of the chain is taken into account. As a result, the energy difference between the zwitterionic state and the ground state will become smaller at a certain N because the zwitterionic state and the ground state are considered to be stabilized and unstabilized by introducing the twisting into the chain, respectively. One can suppose consequently that the photoexcited state in *trans*-$(CH)_x$ would relax radiationlessly via either the internal conversion to the 2^1A_g state or the recombination of the S^+-S^- pair, as shown by Orenstein et al.[16]

The charge distribution of the zwitterionic state in *trans*-$(CH)_x$ is displayed as a function of N in Fig. 4. Because of the symmetries of the HOMO and the LUMO patterns, ψ_{S^-} and ψ_{S^+} are localized on alternate carbon sites as illustrated in Fig. 3, and, accordingly, positive and negative charges are induced alternately around the kinks. The degree of the charge localization is the maximum at $N = 6$, where the zwitterionic state is the most stable, as seen in Fig. 2.

The energy gap between the S^+ and the S^- levels is shown as a function of N in Fig. 5. The above energy gap is obtained by scaling down the calculated value utilizing the observed optical band gap, 1.39 eV.[17] The gap

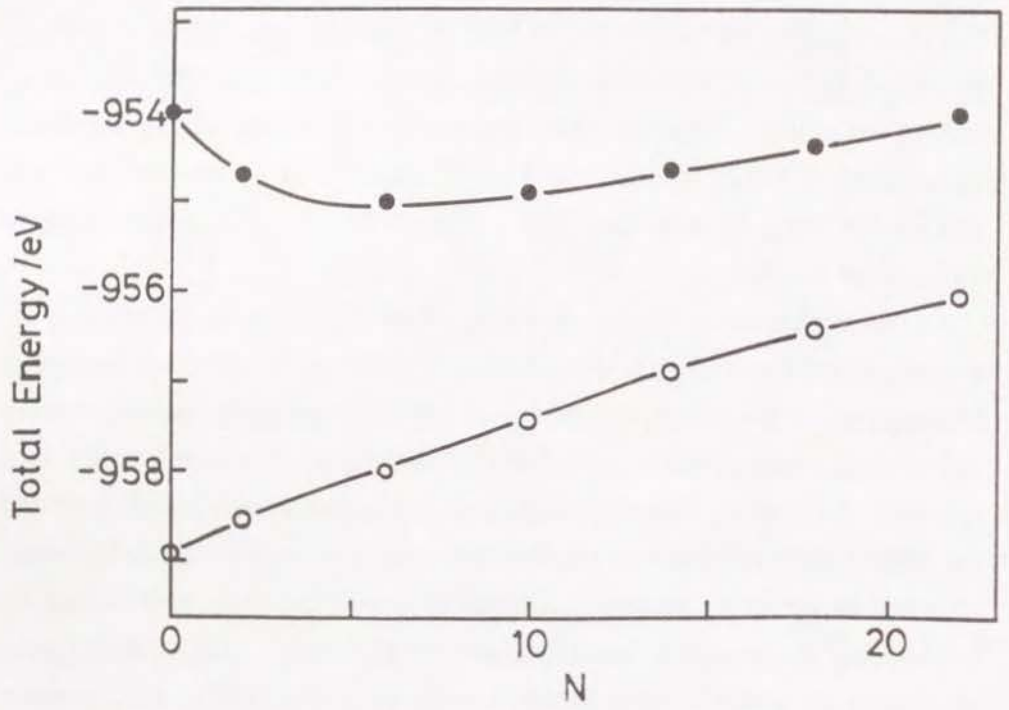

Fig. 2. Configurational-coordinate diagrams for (a) the ground state (open circle) and (b) the zwitterionic state (closed circle) vs. intersoliton distance N.

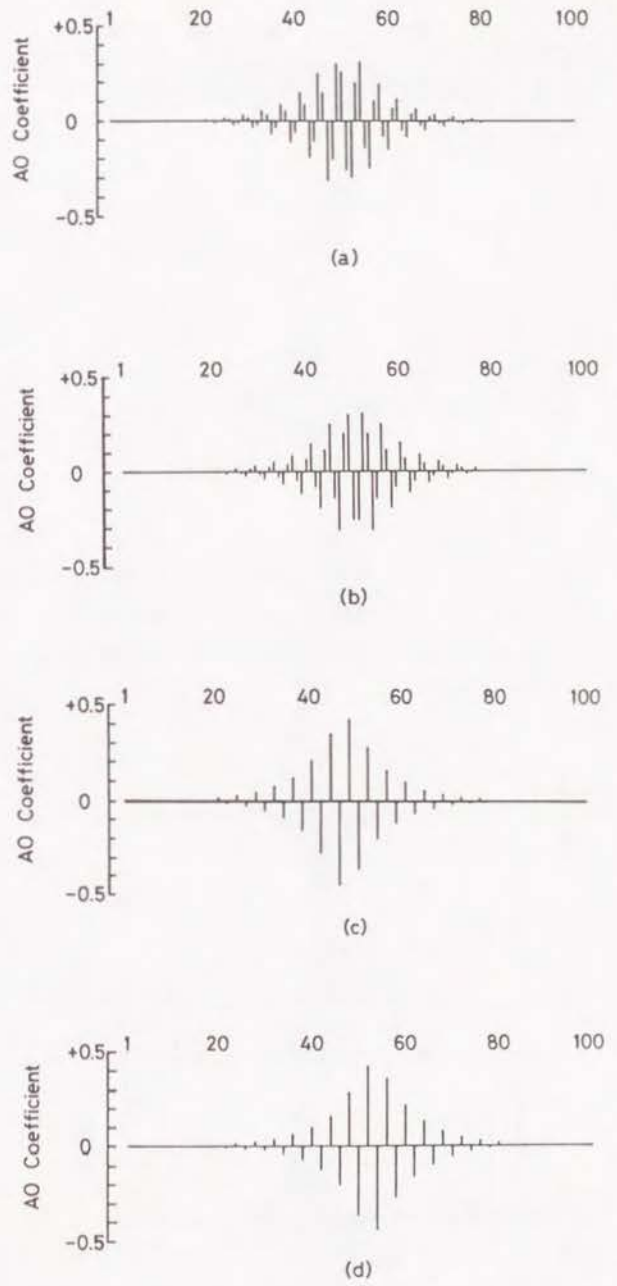

Fig. 3. Shape of (a) the HOMO, (b) the LUMO, (c) ψ_{S-}, and (d) ψ_{S+} for N = 6.

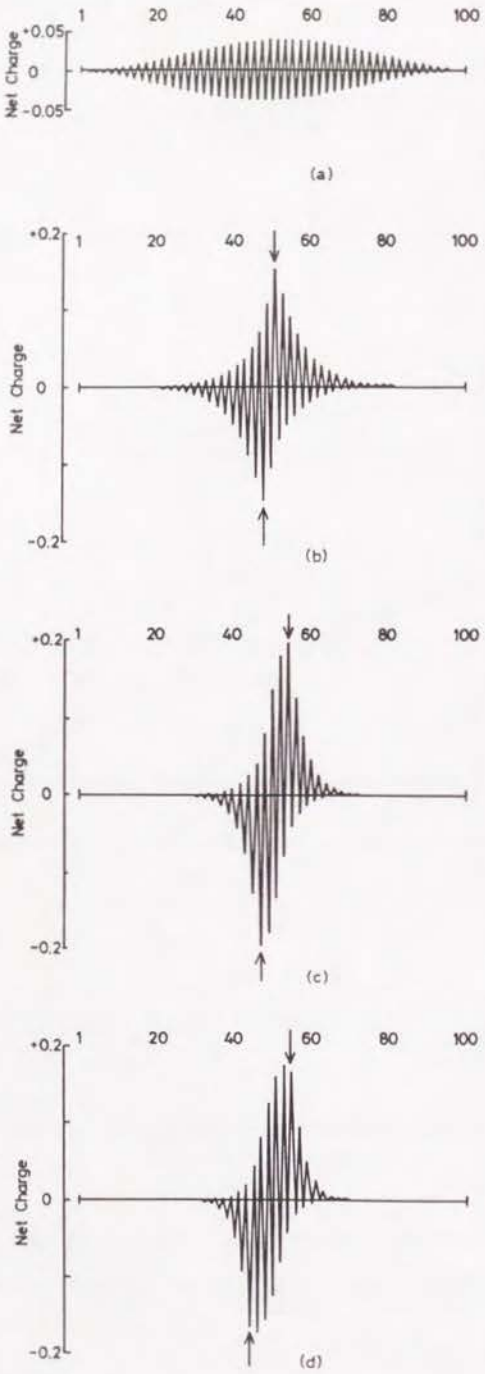

Fig. 4. Charge distribution of the zwitterionic state for (a) $N = 0$, (b) $N = 2$, (c) $N = 6$, (d) $N = 10$, (e) $N = 14$, (f) $N = 18$, and (g) $N = 22$. The number of the abscissa designates the carbon number in the chain.

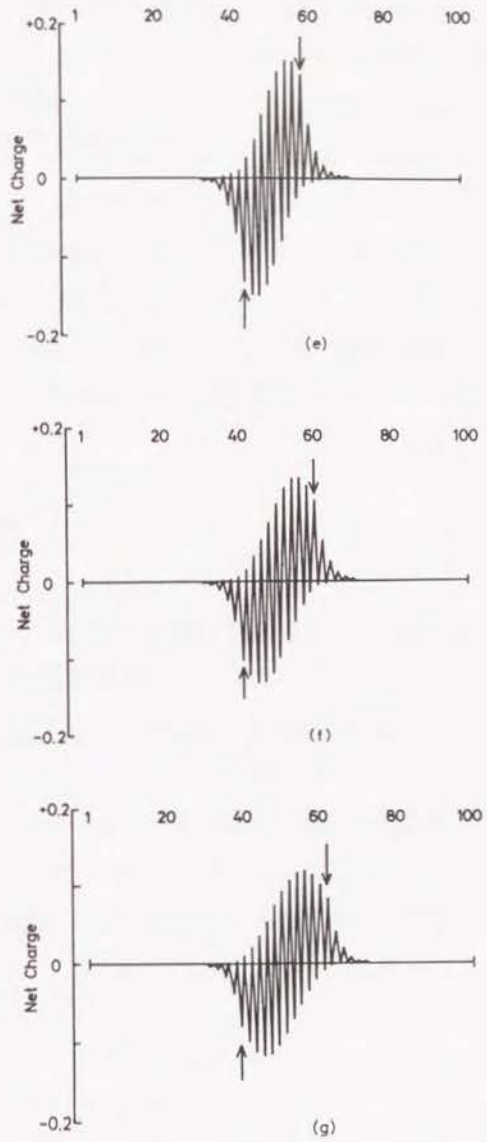

Fig. 4. (*Continued*).

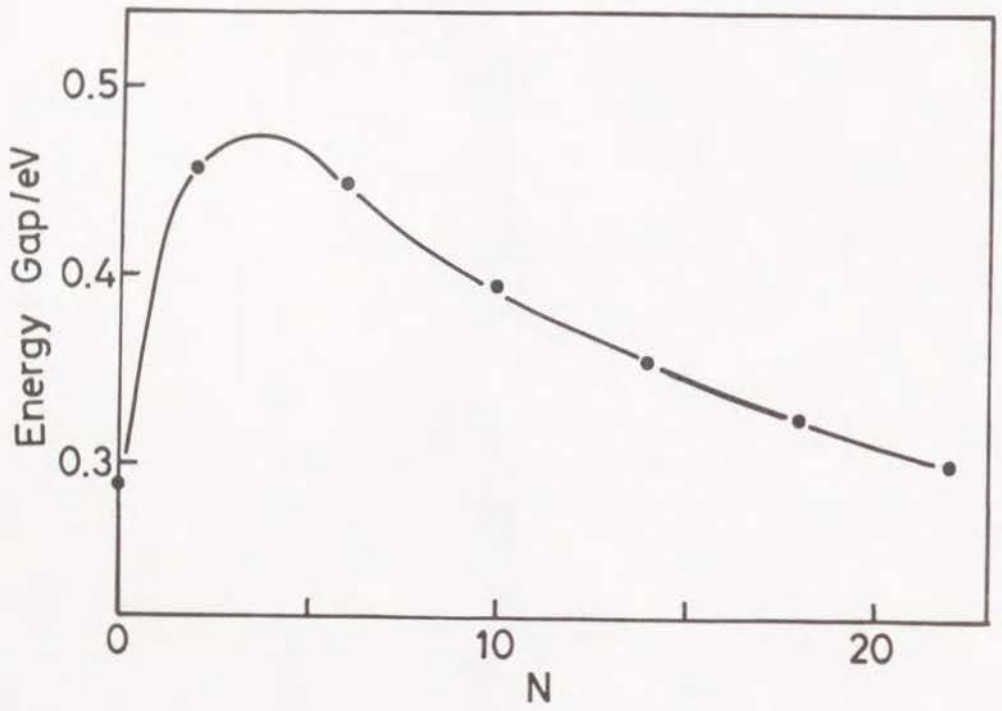

Fig. 5. Energy gap between the midgap levels depending on the intersoliton distance, N.

decreases as the intersoliton distance becomes large. It is of much interest that the energy gap for $N = 6$ is 0.45 eV, which is extremely close to an absorption peak at 0.43 eV observed in photoexcited *trans*-$(CH)_x$. Vardeny et al.[18] assigned the additional peak at 0.43 eV to an electronic transition from a state in the gap to the nearest band of continuum levels, where only one midgap level associated with the soliton is considered. If the Coulomb interaction is added to a Hamiltonian, however, the soliton level would split into doubly occupied and vacant levels. We therefore conclude that the absorption peak is due to the electronic transition between the midgap levels.

Conclusion

In conclusion we have investigated the midgap levels appearing in photoexcited *trans*-$(CH)_x$ on the basis of the concept of the orbital mixing. We have reexamined using the PPP Hamiltonian that the zwitterionic state in photoexcited *trans*-$(CH)_x$ is stabilized through the creation of the S^+-S^- pair. The distance between the S^+-S^- pair is estimated to be approximately 10 Å from the analysis of the energy for the zwitterionic state, and the soliton pair therefore makes a bound state owing to the Coulomb attraction.

References

1. W. P. Su and J. R. Schrieffer, *Proc. Natl. Acad. Sci. U.S.A.*, **77**, 5626(1980).
2. T. Tani, P. M. Grant, W. D. Gill, G. B. Street, and T. C. Clarke, *Solid State Commun.*, **33**, 499(1980).
3. L. Lauchlan, S. Etemad, T. C. Chung, A. J. Heeger, and A. G. MacDiarmid, *Phys. Rev.*, B**24**, 3701(1981).
4. W. P. Su, J. R. Schrieffer, and A. J. Heeger, *Phys. Rev.*, B**22**, 2099(1980).
5. A. R. Bishop, D. K. Campbell, P. S. Lomdahl, B. Horovitz, and S. R. Phillpot, *Phys. Rev. Lett.*, **52**, 671(1984), and *Synth. Met.*, **9**, 223(1984).
6. M. Sasai and H. Fukutome, *Prog. Theor. Phys.*, **79**, 61(1988).
7. For example, B. Hudson and B. Kohler, *Synth. Met.*, **9**, 241(1984).
8. For example, L. Salem, C. Leforestier, G. Segal, and R. Wetmore, *J. Amer Chem. Soc.*, **97**, 479(1975).
9. T. Yamabe, K. Akagi, T. Matsui, K. Fukui, and H. Shirakawa, *J. Phys. Chem.*, **86**, 2365(1982).
10. K. Tanaka, K. Yoshizawa, and T. Yamabe, *Int. J. Quantum. Chem.*, **40**, 305(1991).
11. R. Pariser and R. G. Parr, *J. Chem. Phys.*, **21**, 466, 767(1953).
12. J. A. Pople, *Trans Faraday Soc.*, **49**, 1375(1953).
13. J. Orenstein and G. L. Baker, *Phys. Rev. Lett.*, **49**, 1043(1982).
14. K. Fukui, *Theory of Orientation and Stereoselection*, Springer Verlag, West Berlin, 1975.
15. R. B. Woodward and R. Hoffmann, *The Conservation of Orbital Symmetry*, Academic, New York, 1970.
16. J. Orenstein, Z. Vardeny, G. L. Baker, G. Eagle, and S. Etemad, *Phys. Rev.*, B**30**, 786(1984).
17. D. Moses, F. Feldlum, E. Ehrenfreund, A. J. Heeger, T. C. Chung, and A. G. MacDiarmid, *Phys. Rev.*, B**26**, 3361(1982).

18. Z. Vardeny, J. Orenstein, and G. L. Baker, *Phys. Rev. Lett.*, **50**, 2032(1983).

Chapter 3

Interaction of Two Solitons on Two *trans*-Polyacetylene Chains

Introduction

Photoexcitation processes and their relaxation in *trans*-polyacetylene, $(CH)_x$, have been examined experimentally[1-3] and theoretically[4,5] in relation to the soliton model.[6] The basic idea in $(CH)_x$ is that the soliton-like kinks are accompanied by zero, one, or two electrons, labeled S^+, S^0, or S^-, respectively. S^0 has spin 1/2 as observed with electron spin resonance (ESR) measurements. The spin concentration is one unpaired electron for every 3200 carbons in a reduced pressure in, e.g., usual Shirakawa-$(CH)_x$.[7] On the other hand, S^+ and S^-, which act as charge carriers in the doped or photoexcited $(CH)_x$, have no spin.

Moraes et al.[3] have examined photoinduced ESR of *trans*-$(CH)_x$ and observed a decrease in ESR intensity, that is, a decrease in the number of S^0 under irradiation of the samples containing short conjugation lengths and many localized gap states. In contrast they did not observe a decrease for samples carefully prepared and handled. They concluded that the extent of the photoinduced ESR signal depends on the preparation and handling of samples.

To understand the macroscopic electrical transport in *trans*-$(CH)_x$, however, the interchain interactions and the hopping of electrons between two chains are indispensable ideas. In the ground state of *trans*-$(CH)_x$, an antiferromagnetic order between chains is favored from the calculation by Baeriswyl and Maki.[8] Yamabe et al.[9] have estimated the time required for

intersoliton hopping to be 10^{-13} and 10^{-14} s for π-type and σ-type interacting chains, respectively, with 4 Å separation. On the other hand, Su[10] has considered a pair of oppositely charged solitons on two chains and calculated the electrostatic energy from the simple charge-density profile of the soliton, where it is assumed that the charge-density profiles are not affected by the Coulomb interactions. However, there is a possibility that the Coulomb attraction leads to the deformation of the charge-density profiles of the solitons.

The purpose of the present paper is to study the electronic structures of a pair of neutral solitons and of oppositely charged solitons interacting on two neighboring $(CH)_x$ chains, and, at the same time, to investigate their bound states on the basis of quantum chemical calculations. Because the nearest chain-chain distance is estimated as 4.2 Å,[11] these interactions should be considered as long-range interaction or, in other words, a dissociation problem in terms of the classification in quantum chemistry.

Model Chains and Method of Calculation

To describe the interchain interactions, we consider two finite odd polyenes, both of which consist of 53 carbon atoms as the model system. As shown in Fig. 1, the lower chain has a topological kink fixed at the chain center; which is generated due to defects in the bond alternation. Another kink is located in the upper chain and it is free to migrate around an equilibrium point. Its position is given by the number of translations (N) from the center. Here we assume for simplicity that the kinks are localized on one carbon atom without decaying tails in the chains. Double and single bond lengths are fixed at 1.364 and 1.429 Å, respectively, and bond angles at 120°.[12] The chain-chain spacing is set as 4.2 Å.[11]

In the present study, we consider only π-type interactions between these two modelled $(CH)^x$ chains using the Pariser-Parr-Pople (PPP) approximation,[13,14] including π-π Coulomb repulsion interactions. We

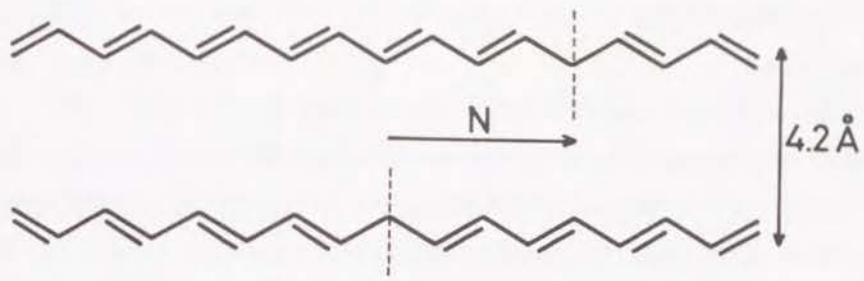

Fig. 1. The model system employed where the location of kinks are shown schematically for $N = 2$. Here N signifies the number of translations separating the two kinks.

confine ourselves to wavefunctions with both the total spin and the total charge being zero; that is, a pair of oppositely charged solitons and a singlet-spin pair of neutral solitons existing in each chains. The spin-restricted Hartree-Fock (RHF) and the unrestricted Hartree-Fock (UHF) hierarchies are used to study the pair of oppositely charged kinks and that of neutral kinks, respectively.

The RHF solution is appropriate to describe the oppositely charged solitons on the two $(CH)_x$ chains, since this case can be associated with ionic dissociation in usual molecular reactions. On the other hand, the UHF method is often used for the open-shell molecules, where the number of electrons with α-spin ($n\alpha$) is not equal to that with β-spin ($n\beta$). In the case where $n\alpha = n\beta$, the UHF solution is normally identical to the RHF solution.[15]

However, even when $n\alpha = n\beta$, there can be a UHF solution different from the RHF solution if appropriately selected initial conditions are used for the self-consistent-field calculation This UHF solution allows different spatial orbitals for different spins (DODS). This kind of DODS many-electron wavefunction represents an antiferromagnetic-type long range interaction between subsystems; that is, the total system is divided into two subsystems each having α or β spin.[16,17] Moreover, the energy of the DODS solution is sometimes even more stable than that of the RHF solution. In this sense, such a case should be called the *un*-dimerization of spins or counter-spin Peierls phenomenon. Hence the DODS solution has also been considered for our model chains to check the appearance of neutral solitons with opposite spins on the two $(CH)_x$ chains

The total energy is calculated from the π-electronic energy and the effective nuclear repulsions[14] containing a part of the energy of the σ-core. For the core resonance integrals, t_{rs}, we use the overlap-integral type assuming non-neighboring terms being equal to zero

$$t_{rs} = -0.4314\, S_{rs}(I_r + I_s)\,, \tag{1}$$

where S_{rs} is the overlap integral between atomic π-orbitals χ_r and χ_s, and I_r and I_s are the ionization potentials for these orbitals. Other parameters are taken to be identical to those in the original papers of Pariser and Parr.[13]

Results and discussion

In the present calculation, the picture of a pair of neutral solitons energetically more stable than that of the oppositely charged solitons has been successfully described by employing an appropriate initial condition. The calculated total energies as a function of the intersoliton separation are shown in Fig. 2 for a pair of charged solitons and that of neutral solitons. In addition to the present results, the case of the triplet soliton pair ($n\alpha = n\beta + 2$) has been found to be a little unstable compared with the singlet pair.

The potential curve for the pair of neutral solitons is shallower than that for the pair of charged solitons. This result is understandable considering the attractive Coulomb interactions between the oppositely charged solitons the neighboring chains. The depth of the potential curve in the pair of charged solitons is about 0.5 eV. The energy difference between the two curves at $N = 0$ is 4.6 eV, which is smaller than the band gap energy, 5.8 eV, calculated under the PPP approximation. Note the SCF method often overestimates gap energies.[18] On the basis of this result, we can expect a sudden conversion of two neutral solitons in the ground state of the system into an oppositely charged soliton pair on two chains on photoexcitation, as illustrated in Fig. 3,

$$2S^0 \rightarrow S^+ + S^-\,, \tag{2}$$

where the thermal movement of the chains would make the hopping of electrons easier. Thus the contribution from this process to the decrease in the ESR signal during the photoexcitation of $(CH)_x$[3] is comprehensible.

Incidentally, this process is in contrast to the model of Street and Mott

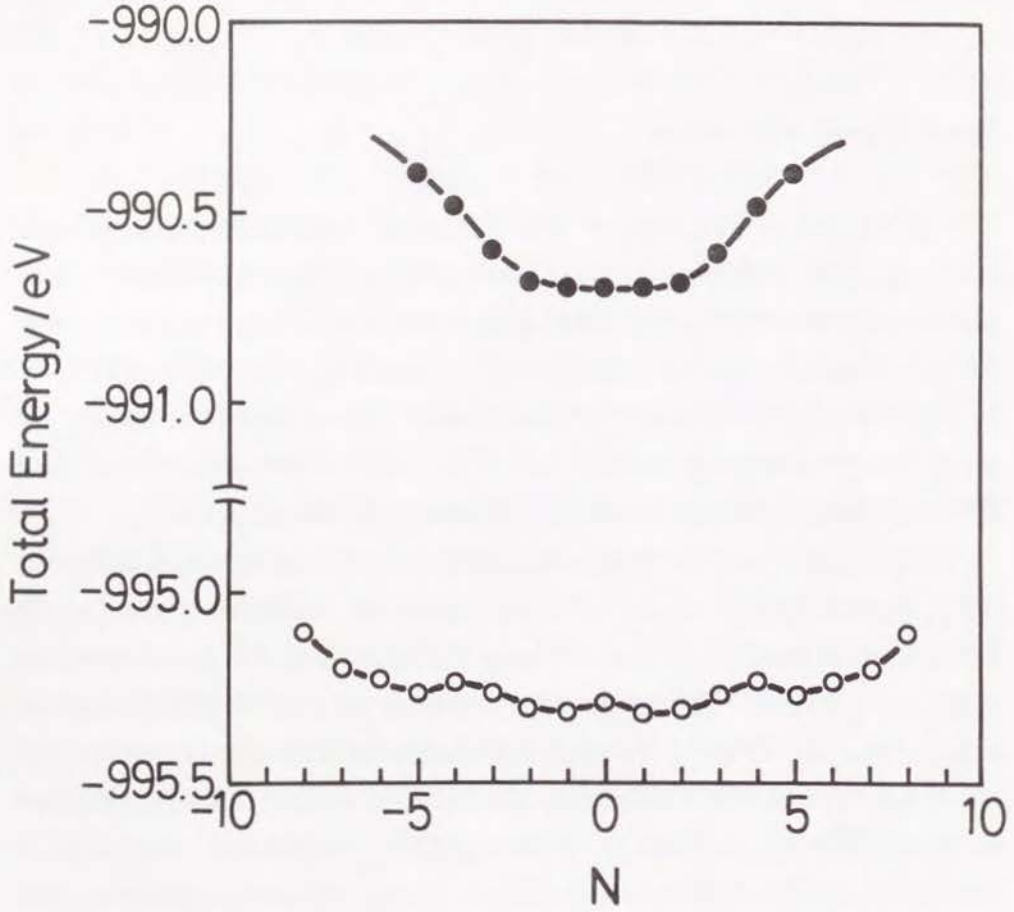

Fig. 2. Energy diagram depending on N. See the caption of Fig. 1 for a singlet pair of neutral solitons (open circle) and a pair of charged solitons (closed circle).

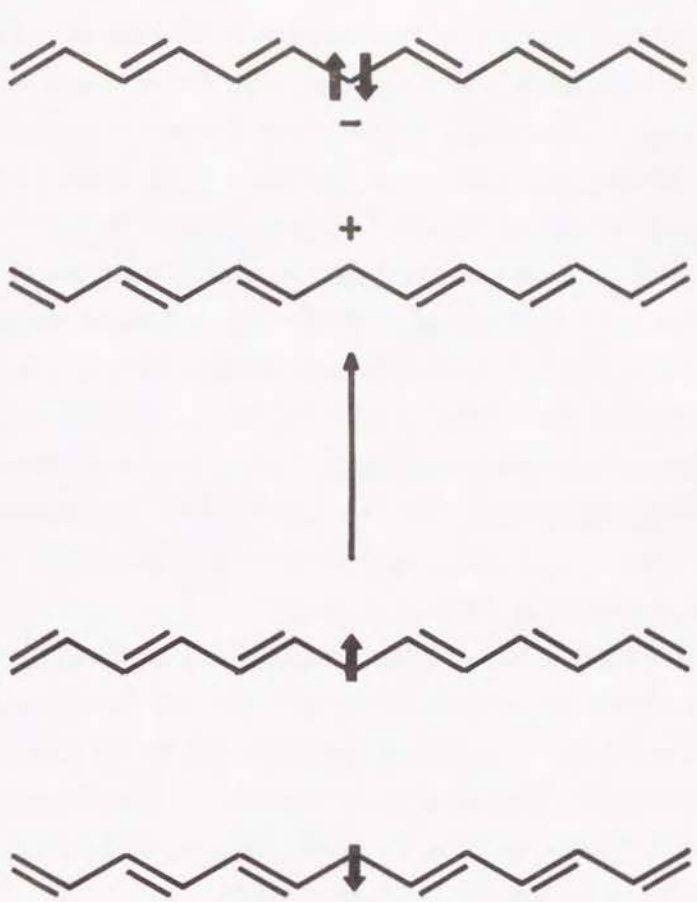

Fig. 3. The concept of the change in the interchain soliton state. Thick arrows represent the spins.

when they interpreted the photoinduced ESR phenomenon in chalcogenide glasses such as As_2S_3 and As_2Se_3.[19] For these chalcogenide glasses, all the defect centers are occupied by two or zero electrons and the defect with one unpaired electron occurs by photoexcitation. In the case of *trans*-$(CH)_x$, however, the defects are mostly singly occupied, that is, neutral solitons in the ground state. According to Anderson,[23] such a phenomenon in chalcogenide glasses stems from the fact that the effective interelectron correlation energy is negative because of a strong electron-phonon interaction.

Furthermore, we have examined the electronic structures of a pair of charged solitons and that of neutral solitons. Figure 4 shows the profiles of charge density of the pair of charged solitons for $N = 0$ and 5. For $N = 0$ the two kinks are located at the center of both the chains. Positive and negative charges are induced symmetrically around the kink centers on the upper and the lower chains, respectively. For $N = 5$ the profile is naturally deformed into an asymmetrical shape; the charge tails are drawn towards the kink in the opposite chain due to the Coulomb attraction.

The spin density of a pair of neutral solitons are shown in Fig. 5. The locations of the kinks are same as in Fig. 4. The spin density profiles are more diffused and flat compared with charge density for the pair of charged solitons. For $N = 0$ the profile of the spin density is symmetrical. Unlike that of the pair of charged solitons, the profile for $N = 5$ is almost the same as that for $N = 0$ except for the shift of the spin center.

Conclusion

The interaction of two solitons on two $(CH)_x$ chains has been analyzed based on the RHF and the UHF methodologies for π-electrons in an appropriate model system. The major findings are summarized as follows.

(i) The state involving a singlet pair of neutral solitons existing in each chain is energetically more stable than that including a pair of oppositely charged solitons. The latter is regarded as an excited state, the transition

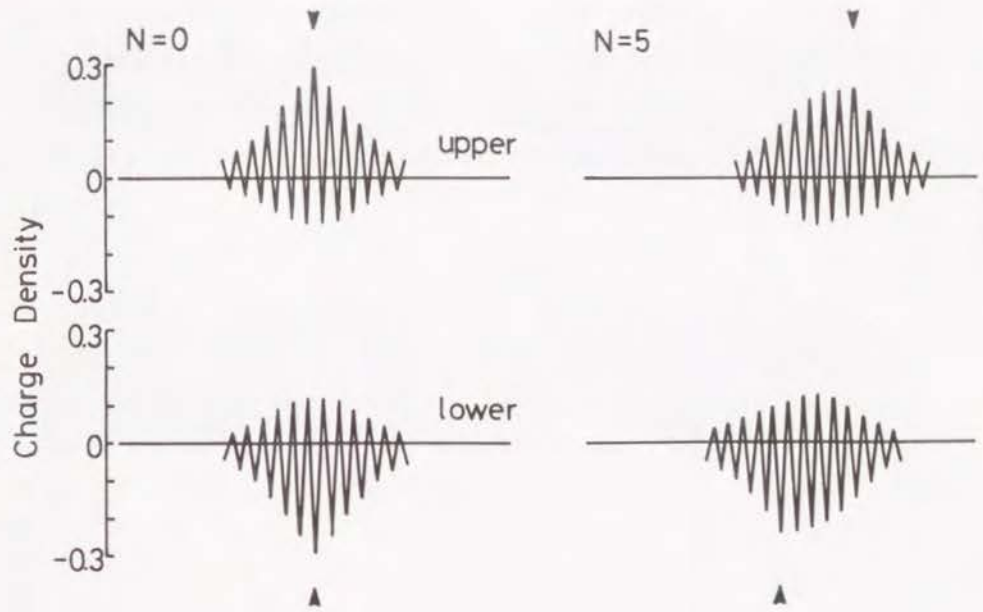

Fig. 4. Profiles of the charge density for a pair of oppositely charged solitons. The wedges represent the kink centers in the chain.

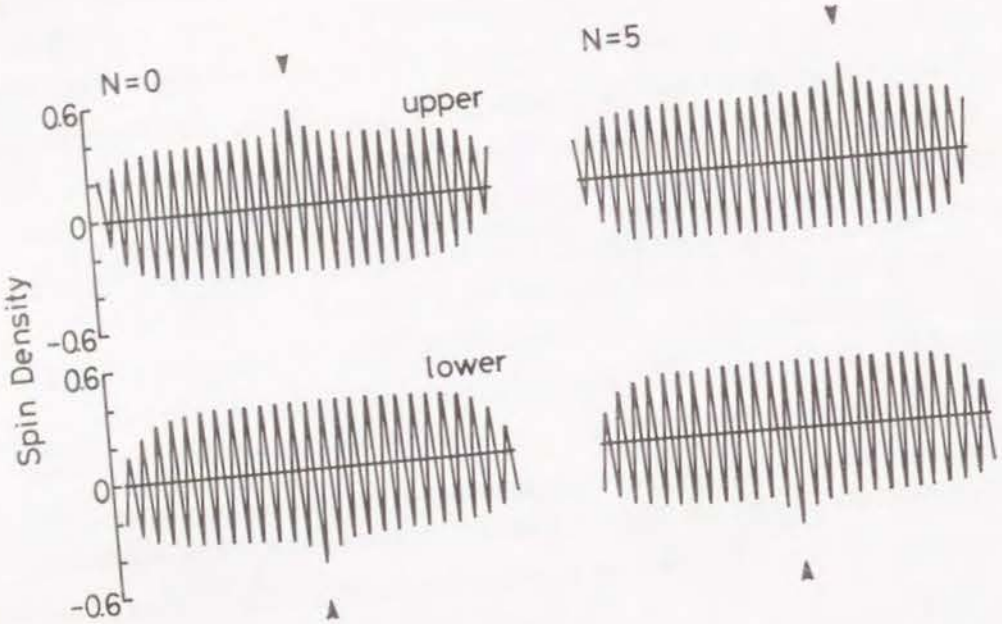

Fig. 5. Profiles of the spin density for a pair of neutral solitons. The positive and the negative spin densities indicate the α-spin and the β-spin, respectively. See also the caption of Fig. 4.

energy to which is smaller than the band gap. This explains qualitatively the decrease in the ESR signal found in photoexcited $(CH)_x$

(ii) There is a difference in the distribution mode of the spin density and the charge density for the above two states, because of the different mode of the interaction between the two kinds of soliton pairs.

The significance of soliton problems related to interchain interactions in $(CH)_x$ has not been fully analyzed hitherto. A study of some interesting aspects is now being undertaken in our laboratory and will be reported elsewhere.

References

1. L. Lauchlan, S. Etemad, T. -C. Chung, A. J. Heeger, and A. G. MacDiarmid, *Phys. Rev.,* B**24**, 3701(1981).
2. J. Orenstein, Z. Vardeny, G. L. Baker, G. Eagle, and S. Etemad, *Phys. Rev.,* B**30**, 786(1984).
3. F. Moraes, Y. W. Park, and A. J. Heeger, *Synth. Met.*, **13**, 113(1986).
4. W. P. Su and J. R. Schrieffer, *Proc. Natl. Acad. Sci. U.S.A.*, **77**, 5626(1980).
5. A. R. Bishop, D. K. Campbell, P. S. Lomdahl, B. Horovitz, and S. R. Phillpot, *Phys. Rev. Lett.*, **52**, 671(1984).
6 W. P. Su, J. R. Schrieffer, and A. J. Heeger, *Phys. Rev.,* B**22**, 2099(1980).
7. I. B. Goldberg, H. R. Crowe, P. R. Newman, A. J. Heeger, and A. G. MacDiarmid, *J. Chem. Phys.*, **70**, 1132(1979).
8. D. Baeriswyl and K. Maki, *Phys. Rev.*, B**28**, 2068(1983).
9. T. Yamabe, K. Tanaka, S. Yamanaka, T. Koike, and K. Fukui, *J. Chem. Phys.*, **82**, 5737(1985).
10. W. P. Su, *Phys. Rev.*, B**35**, 9245(1987).
11. K. Shimamura, F. E. Karasz, J. A. Hirsch, and C. D. Chien, *Macromol. Chem., Rapid Commun.,* **2**, 473(1981).
12. T. Yamabe, K. Akagi, T. Matsui, K. Fukui, and H. Shirakawa, *J. Phys. Chem.*, **86**, 2365(1982).
13. R. Pariser and R. G. Parr, *J. Chem. Phys.*, **21**, 466,767(1953).
14. J. A. Pople, *Trans Faraday Soc.*, **49**, 1375(1953).
15. J. Kouteck´y, *J. Chem. Phys.*, **46**, 2443(1967).
16. I. A. Misurkin and A. A. Ovchinnikov, *Mol. Phys.*, **27**, 237(1974).
17. M. Kertész, J. Koller, and A. Azman, *Phys. Rev.*, B**19**, 2034(1979).
18. See, for instance, M. Kertész, *Adv. Quantum Chem.*, **15**, 161(1982).
19. R. A. Street and N. F. Mott, *Phys. Rev. Lett.*, **35**, 1293(1975).
20. P. W. Anderson, *Phys. Rev. Lett.*, **34**, 953(1975).

Chapter 4

A Stability Condition for the Hartree-Fock Solution of the Infinite One-Dimensional System

Introduction

Since the first formulation of the stability condition for the Hartree-Fock (HF) theory by Thouless[1] and the rederivation specified for the closed-shell electronic systems,[2] a good deal of research concerning the analyses of molecular structures[2-5] and chemical reactions[6,7] have been performed by way of the examination of the instability problem on the HF solutions obtained for these systems. As is well known, this problem is algebraically interpreted as the instability of the HF solution of the concerned molecular systems based on the variational principle.

From the viewpoint of the frontier orbital theory, for instance, the singlet instability of the original HF solution (namely, a single Slater determinant) accompanied by the molecular structure will predict the adequacy of introduction of the excited configuration from, in most cases, the highest occupied molecular orbital (HOMO) to the lowest unoccupied MO (LUMO) into the electronic wavefunction. This instability is to be removed by actual deformation of nuclear rearrangement in the molecular structure to a lower spatial symmetry according to the orbital pattern of the LUMO or other unoccupied MOs contributing to the excited configurations added.[8] The Jahn-Teller distortion[9,10] can be regarded as an example of the manifestation of the singlet instability occurring in the degenerated HOMO-LUMO systems.

On the other hand, in the infinite systems such as polymers and crystals, it

is difficult to treat this kind of problem due to infinite number of the energy levels involved and, hence, infinite number of the excited configurations to be considered. Therefore, the instability problem has not been explicitly treated hitherto for the infinite polymer chain systems.

In this article, we present a simple formulation of the stability condition for the HF solution of the infinite one-dimensional systems with a specific condition that the variable space is selected only around the Fermi surface in the same spirit with the above viewpoint based on the frontier orbital theory. In the following, the formulation is presented in detail, where it will be found that the stability condition for the infinite system can be replaced by that obtained from minor determinants of the original one, and that the new stability condition contains only two physical parameters. Furthermore, an example will be given with respect to the HF solution of *trans*-polyacetylene having isodistant C-C bond length, i.e., metallic polyacetylene (m-$(CH)_x$), so as to check the validity of the present formulation.

Formalism

The complete stability condition for the HF solution of the infinite one-dimensional system can be derived in principle from the formula of stability matrix for the closed-shell MO system first developed by Paldus and Čížek.[2] With a set of the atomic orbitals (AOs) in a unit cell, the crystal orbital (CO) of the one-dimensional polymer concerned is determined by Bloch's theorem. Labeling the νth AO in jth unit cell as $\chi(\nu, r - jd)$, the μth CO, $\Psi_{k\mu,l}$ in the lth band can be written as

$$\Psi_{k_\mu,l} = \frac{1}{\sqrt{N}} \sum_{j}^{N} \exp[ik_\mu jd] \sum_{\nu}^{\text{unit cell}} C_{k_\mu,l,\nu}\chi(\nu, r - jd),$$
$$\mu = 0 \cdots N\text{-}1. \tag{1}$$

Both the AOs and the COs are labeled by integer modulus N representing the

total number of the cells. The notations k_μ, d, and $C_{k\mu,l,\nu}$ indicate the μth wave vector, the lattice constant, and the CO coefficient, respectively. Applying the formulation of Paldus and Čížek[2] to the CO in Eq. (1), the stability matrix elements concerning an arbitrary monoexcitation are derived as follows:

$$a^s_{p_1p_i,p_2p_i'} = \Delta\varepsilon(p_1, p_1')\delta_{p_1p_2}\delta_{p_ip_i'} + 2\langle p_1'p_2|\hat{v}|p_1p_2'\rangle - \langle p_1'p_2|\hat{v}|p_2'p_1\rangle,$$

$$b^s_{p_1p_i,p_2p_i'} = 2\langle p_1'p_2'|\hat{v}|p_1p_2\rangle - \langle p_1'p_2'|\hat{v}|p_2p_1\rangle,$$

$$a^t_{p_1p_i,p_2p_i'} = \Delta\varepsilon(p_1, p_1')\delta_{p_1p_2}\delta_{p_ip_i'} - \langle p_1'p_2|\hat{v}|p_2'p_1\rangle, \tag{2}$$

$$b^t_{p_1p_i,p_2p_i'} = -\langle p_1'p_2'|\hat{v}|p_2p_1\rangle,$$

where the superscripts s and t in the left-hand side are associated with the singlet and the triplet excitations, respectively. The notation p_i indicates an arbitrary occupied CO labeled by both k_μ and l which accommodates the electron i. The prime for p_i designates an arbitrary unoccupied CO. Similarly, $p_i \equiv (l, k_\mu)$ used in the Kronecker delta defines the extended CO level containing both the band level component l and the wave vector k_μ. Furthermore, $\Delta\varepsilon(p_i, p_i')$ and $\hat{v}$ represent the energy difference between the p_i and p_i' levels and the two-particle operator of the Coulomb repulsion, respectively. The bracket stands for the molecular integrals as usual after Ref. 2. Using these expressions the stability matrix is defined as

$$I^x = \begin{bmatrix} a^x_{p_1p_i,p_2p_i'} & b^x_{p_1p_i,p_2p_i'} \\ \bar{b}^x_{p_1p_i,p_2p_i'} & \bar{a}^x_{p_1p_i,p_2p_i'} \end{bmatrix}, \qquad x = s \text{ or } t, \tag{3}$$

where $\bar{a}$ and $\bar{b}$ represent the complex conjugate to the submatrices a and b, respectively. If I^x is positive definite, namely, if all the eigenvalues of I^x are positive, the HF solution of the concerning infinite system is stable and, if

negative definite or indefinite, it is unstable.

Let us now consider $\Delta\varepsilon(p_i, p_i')$ and the molecular integrals in the right-hand side of Eq. (2). It should be noticed that the values of the molecular integrals are small due to multiplication of the usual molecular integrals in the MO theoretical scheme by $1/N$. On the other hand, in the ordinary semiconducting or insulating polymers, $\Delta\varepsilon(p_i, p_i')$ has the value of a couple of electron volts. Hence for finite subspaces of I^x, the stability condition becomes trivial since all the molecular integrals converge on zero and, hence, the minor determinants become positive definite.

On the contrary, if we give attention to the complete matrix I^x considering the total space, it is possible for I^x to become negative definite or indefinite. Hence, the instability of the HF solution may possibly occur by inclusion of a great deal of electron correlation even in semiconducting or insulating polymers with an infinite chain length. This situation makes difficult to analyze the characteristic problem for I^x. However, these are originated from the correlation working in the macroscopic scale, being a considerably special case.

In the present study, we rather confine ourselves to the instability problem of almost gapless polymers or, what is called, metallic polymers. For such systems, the following two conditions for the selection of minor determinants in I^x can be plausibly employed.

(1) p_i and p_i' are selected only in the neighborhood of the Fermi level and $\Delta\varepsilon(p_i, p_i')$ will converge on $1/N$. Then the subspace in I^x is factorized into smaller ones with the use of the relationship similar to that developed by Cizek and Paldus[2] among the nonzero elements.

(2) p_i' is related to p_i with the minimal quasimomentum δk and the nesting vector Q as illustrated in Fig. 1,

$$p_i' = p_i + \Delta k \tag{4}$$

where

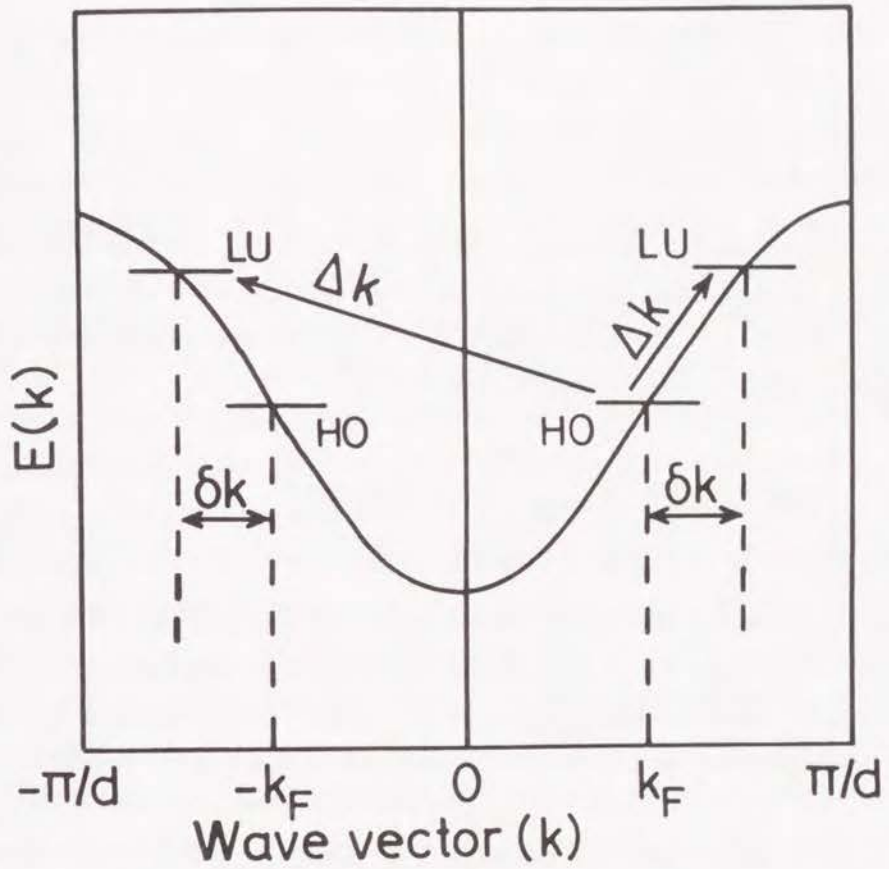

Fig. 1. The lowest unoccupied (p_i') and the highest occupied (p_i) states around the Fermi level. The short and the long arrow lines exemplify the excitation from p_i = (HO, k_F) to p_i' = (LU, $\pm k_F \pm \delta k$), for instance, with the nesting vectors 0 and $2k_F$, respectively. The interval between the HO and the LU levels are exaggerated for clarification.

$$\Delta k = \begin{cases} \pm(Q + \delta k) & \text{for } Q = 0, \quad \pm \text{ for } p_i = (\mathrm{HO}, \pm k_F), \\ \mp(Q + \delta k) & \text{for } Q = 2k_F, \quad \mp \text{ for } p_i = (\mathrm{HO}, \pm k_F), \end{cases} \tag{5}$$

and

$$\delta k = 2\pi/Nd \tag{6}$$

which can usually be determined from the Born-von Karman periodic boundary condition and the discreteness of the momentum in the reciprocal space. Under the above condition, $\Delta\varepsilon(p_i, p_i')$ on the continuous band dispersion, $E(k_\mu)$, is approximately obtained as

$$\Delta\varepsilon(p_1, p_1 + \Delta k) \equiv \left\{\frac{dE(k_\mu)}{dk_\mu}\right\} dk = \{D(E_F)/m\}^{-1} \tag{7}$$

for any Δk in Eq. (5), where $D(E_F)$ is the density of states (DOS) at the Fermi surface on single band dispersion, and m the degeneracy there. Furthermore, the molecular integrals in Eq. (2) can be estimated as follows utilizing the fact that δk is very small corresponding to the order of $1/N$:

$$\begin{aligned} &\langle p_1 + \Delta k, p_2|\hat{v}|p_1, p_2 + \Delta k\rangle \equiv \langle p_1 \pm Q, p_2|\hat{v}|p_1, p_2 \pm Q\rangle, \\ &\langle p_1 + \Delta k, p_2|\hat{v}|p_2 + \Delta k, p_1\rangle \equiv \langle p_1 \pm Q, p_2|\hat{v}|p_2 \pm Q, p_1\rangle, \\ &\langle p_1 + \Delta k, p_2 + \Delta k|\hat{v}|p_1, p_2\rangle \equiv \langle p_1 \pm Q, p_2 \pm Q|\hat{v}|p_1, p_2\rangle, \\ &\langle p_1 + \Delta k, p_2 + \Delta k|\hat{v}|p_2, p_1\rangle \equiv \langle p_1 \pm Q, p_2 \pm Q|\hat{v}|p_2, p_1\rangle, \end{aligned} \tag{8}$$

where the sign of $\pm Q$ is determined after the rule in Eq. (5). With the use of the above approximations, the matrix elements of the stability matrix I^x in Eq. (3) can be easily setup. It should, however, be emphasized that the condition described above is applicable to the instability problem only around the Fermi level.

Stability condition for m-$(CH)_x$

It has been well known that the structure of the *trans*-$(CH)_x$ with the isodistant carbon-carbon bond lengths is energetically unstable and will spontaneously deform into a bond-alternant conformation based on the simple discussion by Peierls[11] and by conventional HF-CO calculations of various approximation levels.[12] The former conformation will show metallic properties due to the degeneracy of the highest occupied CO (HOCO) and the lowest unoccupied CO (LUCO), and it shall be called m-$(CH)_x$ (metallic $(CH)_x$). Here in this section, the structural instability of m-$(CH)_x$ is examined as the simplest application from the viewpoint of the instability of the HF solution in order to check the validity of the present formulation.

The band structure employed for m-$(CH)_x$ is calculated by the one-dimensional SCF-CO method at the level of the CNDO/2 approximation[13] based on the polymer structure optimized within the frame of m-$(CH)_x$.[14] These are shown in Figs. 2 and 3, respectively. The HO band is a typical half-filled one of π nature and, hence, the Fermi wave vector k_F becomes $\pi/2d$ in this case.

We consider the stability for m-$(CH)_x$, selecting several minimum excited configurations around the Fermi level as shown in Fig. 1. The lowest-lying eigenvalues obtained for the singlet and triplet stability problems for two kinds of the nesting vectors are listed in Table I. The results show that the stability matrices for monoexcitations classified by the nesting vectors, 0 and $2k_F$, become positive definite and negative indefinite, respectively. That is, the HF solution of m-$(CH)_x$ is unstable for the nesting vector $2k_F$ at the optimized structure, and this solution is associated with a saddle point on the energy surface.

In order to examine these eigenvalues in detail, the fluctuated HOCOs of the π type at the Fermi level defined by the following expression are considered:

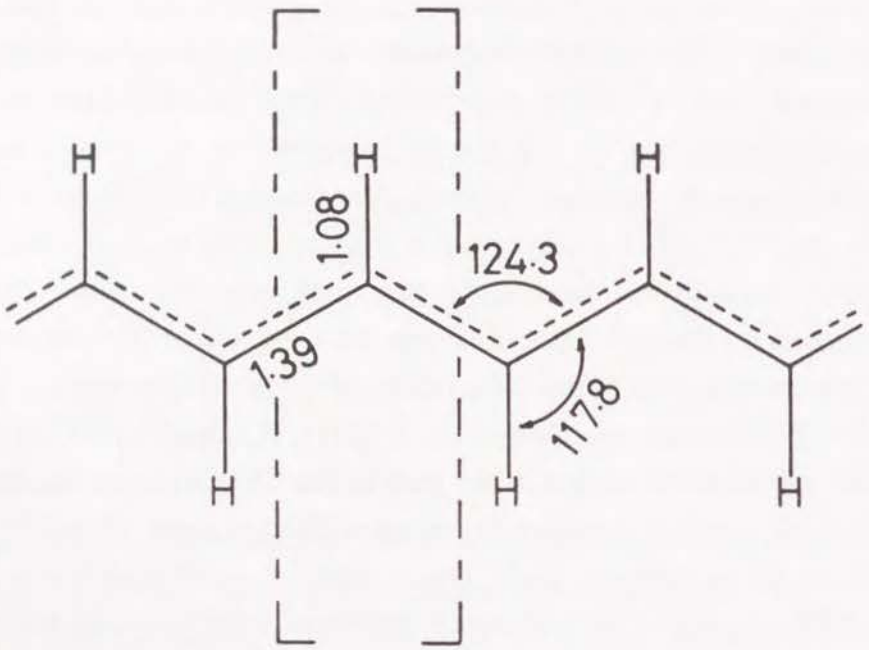

Fig. 2. The optimized geometry of m-$(CH)_x$ employed from Ref. 14. The dash-dot line indicates the unit cell of the polymer. The values of the bond lengths and angles are in Å and degrees, respectively.

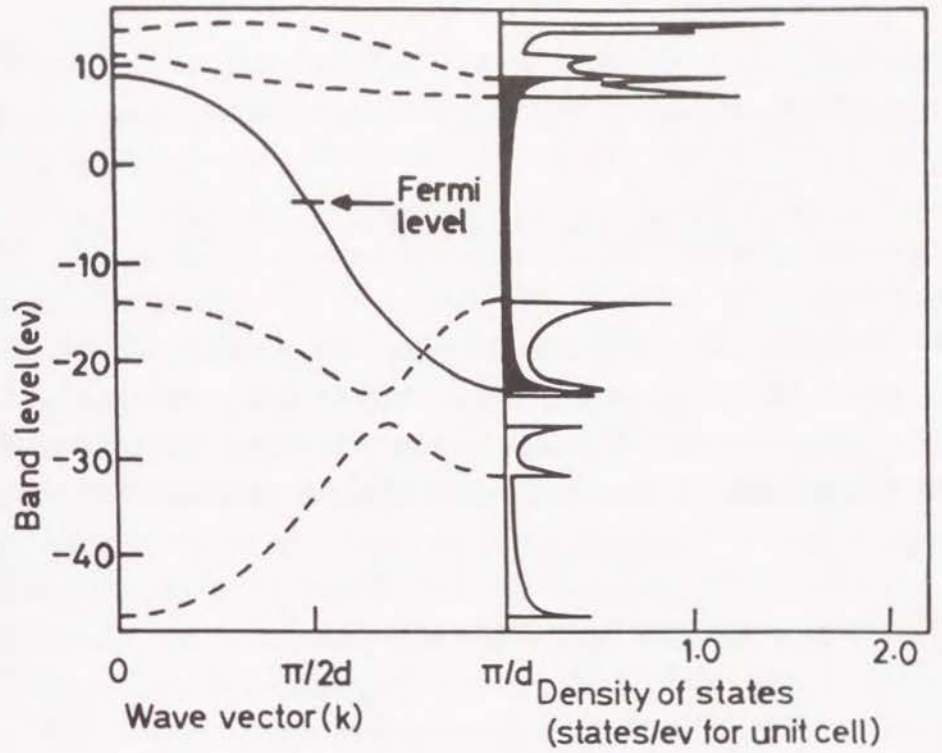

Fig. 3. The band structure and the DOS of m-$(CH)_x$. The dashed and solid lines indicate σ and π bands, respectively. The shaded area in the DOS represents the contribution from the π band.

$$\Psi_+ = \Psi_{k_F,\,\mathrm{HO}} + \lambda^+ \Psi_{k_F+\Delta k,\,\mathrm{HO}}$$

$$= \frac{1}{\sqrt{N}} \sum_j^N \left\{ \exp[ik_F jd] + \lambda^+ \exp[i(k_F + \Delta k)jd] \right\} \chi(\pi,\, r - jd), \tag{9}$$

$$\Psi_- = \Psi_{-k_F,\,\mathrm{HO}} + \lambda^- \Psi_{-k_F+\Delta k,\,\mathrm{HO}}$$

$$= \frac{1}{\sqrt{N}} \sum_j^N \left\{ \exp[-ik_F jd] + \lambda^- \exp[i(-k_F + \Delta k)jd] \right\} \chi(\pi,\, r - jd),$$

where λ^+ and λ^- indicate the complex fluctuation parameters and Δk is the quasimomentum transfer as defined in Eq. (5). Using Eq. (9), we can easily derive the representations of the density matrix elements originating from Ψ_+ and Ψ_- in a similar manner to those in the ordinary molecular orbital theory as follows:

$$P_{j,j}(\Psi_+) = 1/N\{1 + \lambda^2 + 2\lambda\cos(\theta^+ + \Delta kjd)\},$$

$$P_{j,j}(\Psi_-) = 1/N\{1 + \lambda^2 + 2\lambda\cos(\theta^- + \Delta kjd)\}, \tag{10}$$

$$P_{j,j+1}(\Psi_+) = 1/N\{1 + \lambda^2 \exp[-i\Delta kd]$$

$$+ 2\lambda\exp[-i\Delta kd/2]\cos[\theta^+ + \Delta k(j + 1/2)]\}\exp[-ik_F d],$$

$$P_{j,j+1}(\Psi_-) = 1/N\{1 + \lambda^2 \exp[-i\Delta kd]$$

$$+ 2\lambda\exp[-i\Delta kd/2]\cos[\theta^- + \Delta k(j + 1/2)]\}\exp[ik_F d],$$

where the subscript j simply represents a π-nature orbital of carbon in the jth cell in a chain of the infinite m-$(CH)_x$ and $P_{j,j}$ and $P_{j,j+1}$ stand for the π-AO density and the π-bond order between the nearest neighboring carbons, respectively. The variables λ, θ^+, and θ^- are connected with λ^+ and λ^- by

the following relationships:

$$\lambda^+ = \lambda\exp[i\theta^+], \quad \lambda^- = \lambda\exp[i\theta^-]. \tag{11}$$

Consequently, we can classify the fluctuated HOCOs as the determinantal functions of the Slater determinant of m-$(CH)_x$ utilizing the density matrix elements, $P_{j,j}(\Psi_+) + P_{j,j}(\Psi_-)$ and $P_{j,j+1}(\Psi_+) + P_{j,j+1}(\Psi_-)$.

Let us discuss the case of the singlet characteristic problem of m-$(CH)_x$ for the nesting vector $Q = 2k_F$ by means of Eq. (9). From the diagonalization of the stability matrix in Eq. (3), the arguments θ^+ and θ^- of the eigenvector $(\lambda^+, \lambda^-, \lambda^{+*}, \lambda^{-*})$ and the eigenvalues are determined, where the asterisk for λ designates the complex conjugate. Table II shows the classification of the fluctuated HOCOs with respect to all the arguments and the eigenvalues of the singlet stability matrix. As Fig. 4 shows, the classes of the lowest-lying and the next lowest-lying eigenvalues obviously correspond to the off-diagonal charge density wave (CDW) and the diagonal CDW, respectively. Incidentally, the appearance of the off-diagonal CDW has been found by Kertész[15] only in a numerical manner. As a whole, bond-alternating structure is expected to be more stable than that of m-$(CH)_x$, which is consistent with the structure of *trans*-$(CH)_x$ actually observed.[16,17] It is further noted that this tendency holds even if the C-C bond distance varies in the frame of m-$(CH)_x$ as seen in Fig. 5. Hence $(CH)_x$ would have no stable solution even under very high pressure.

Conclusion

The stability condition for the Hartree-Fock solution of the infinite one-dimensional system has been established. In particular, the special case in which the HOCO and the LUCO are degenerated associated with the polymer of metallic properties has been explicitly dealt with. It has been shown that, in this case, only two physical parameters, that is, the DOS and the Coulomb

Table I. The lowest-lying eigenvalues of the stability matrices for m-$(CH)_x$.

Nesting vector (Q)	Type of excitation	The lowest-lying eigenvalues (in eV)
0	singlet	62.68
0	triplet	56.45
$2k_F$	singlet	-23.89[a]
$2k_F$	triplet	-36.35

[a]Off-diagonal CDW (see Table II).

Table II. Calculated data of the singlet stability matrix and the classification of the fluctuated HOCOs for m-$(CH)_x$.

Arguments of eigenvectors $\theta+$	$\theta-$	Eigenvalues (in eV)	Classification
0	π	149.25	totally symmetric
$\pi/2$	$\pi/2$	149.25	totally symmetric
0	0	-11.44	diagonal CDW
$\pi/2$	$-\pi/2$	-23.89	off-diagonal CDW

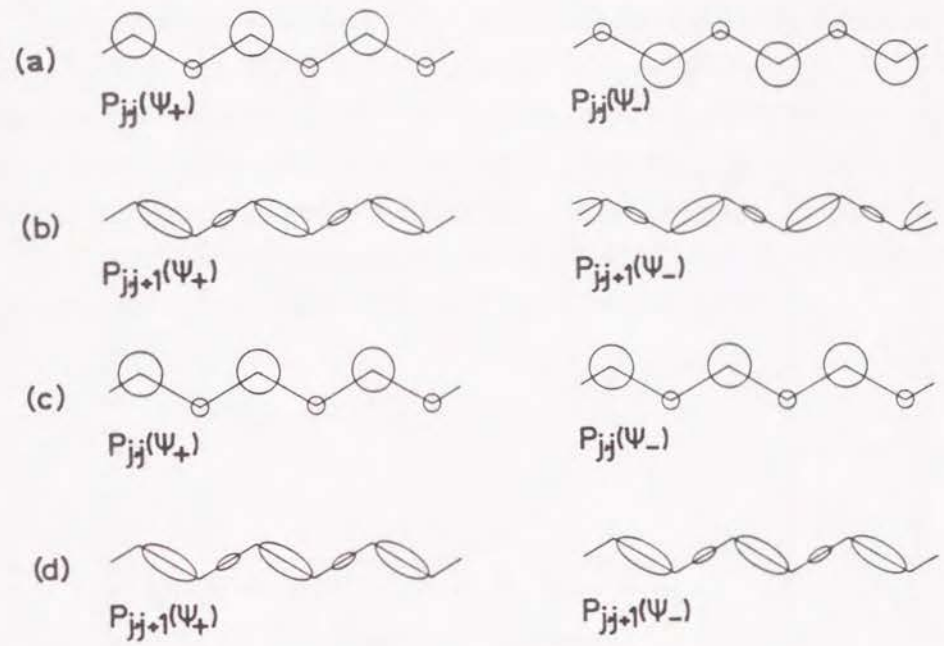

Fig. 4. The charge distribution mode of the fluctuated HOCOs at the Fermi level for the case of (a) $\theta^+ = 0$, $\theta^- = \pi$, (b) $\theta^+ = \pi/2$, $\theta^- = \pi/2$, (c) $\theta^+ = 0$, $\theta^- = 0$, and (d) $\theta^+ = \pi/2$, $\theta^- = -\pi/2$. See Table II with respect to the classification of these cases. The circles and the ovals schematically indicate $P_{j,j}$ and $P_{j,j+1}$, respectively.

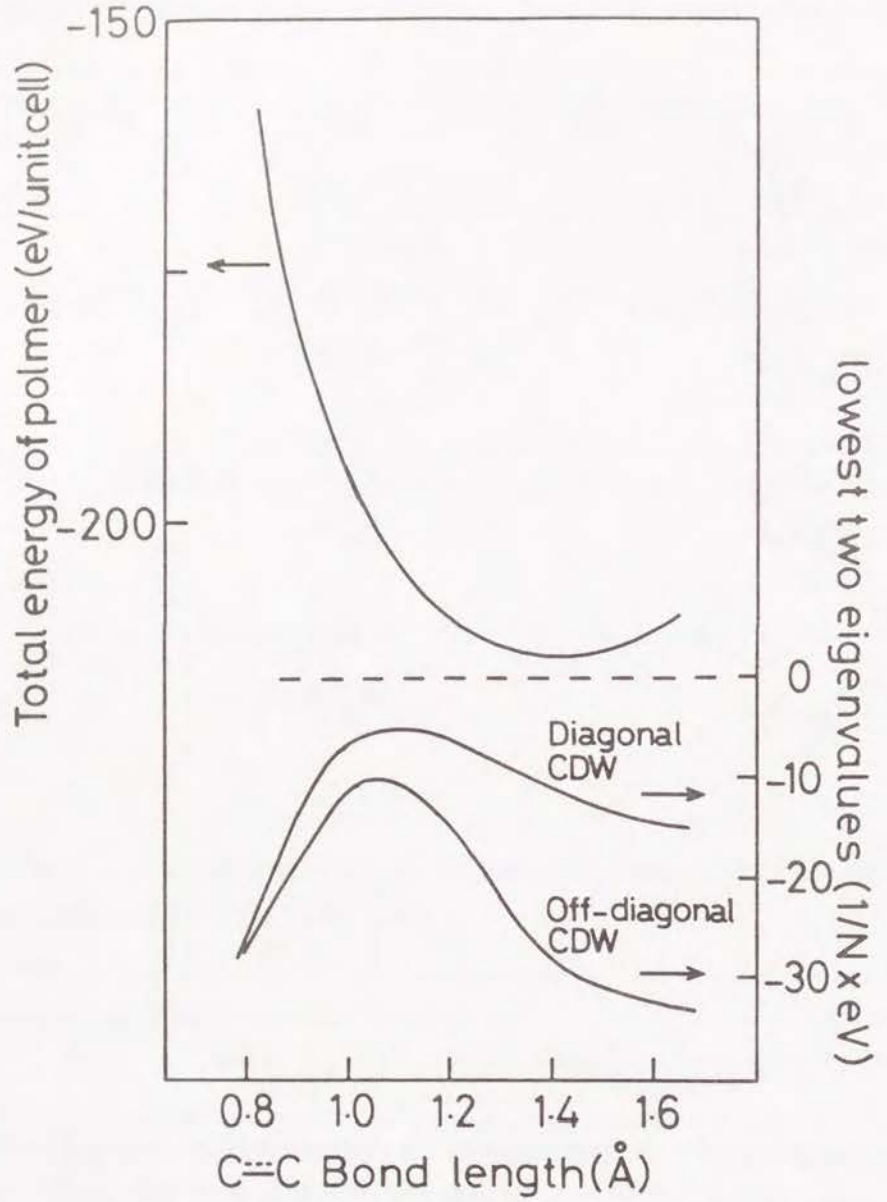

Fig. 5. The total energy of m-$(CH)_x$ and the lowest two eigenvalues of the singlet stability matrices concerned as a function of the C-C bond distances.

repulsion integrals both at the Fermi level, are required in order to check the condition.

Along the present criterion, the instability condition of metallic *trans*-type polyacetylene was able to be examined in a systematic manner including the case of the off-diagonal CDW which has been expected in this polymer based on the numerical calculations. This signifies that the dimerization of *trans*-polyacetylene can be clearly figured out as an instability within the framework of the Hartree-Fock scheme not necessarily invoking an explicit treatment of the non-adiabatic process described by, e.g., Peierls distortion.

References

1. D. J. Thouless, *The Quantum Mechanics of Many Body Systems*, Academic, New York, 1961, Chap. 2.
2. J. Čizek and J. Paldus, *J. Chem. Phys.*, **47**, 3976(1967).
3. J. Paldus and J. Čizek, *J. Polym. Sci.* Part C **29**, 199(1970).
4. P. Karadkov and O. Castano, *Theor. Chim. Acta*, **70**, 25(1986).
5. M. Benard and W. G. Raidraw, *Theor. Chim. Acta*, **70**, 17(1986).
6. K. Yamaguchi and T. Fueno, *Chem. Phys. Lett.*, **38**, 47(1976).
7. K. Yamaguchi and T. Fueno, *Chem. Phys. Lett.*, **38**, 52(1976).
8. K. Fukui and K. Tanaka, *Bull. Chem. Soc. Jpn.*, **50**, 1391(1976).
9. H. A. Jahn and E. Teller, *Proc. R. Soc. London Ser.*, A **161**, 220(1937).
10. H. A. Jahn, *Proc. R. Soc. London Ser.* A **164**, 117(1938).
11. R. E. Peierls, *Quantum Theory of Solids*, Oxford University, London, 1955, Chap. 5.
12. See, for example, K. Tanaka and T. Yamabe, *Adv. Quantum Chem.*, **17**, 251(1985).
13. A. Imamura and H. Fujita, *J. Chem. Phys.*, **61**, 115(1974).
14. K. Karpfen and R. Holler, *Solid State Commun.*, **37**, 179(1981).
15. M. Kertész, J. Koller, and A. Ažman, *Int. J. Quantum Chem.*, **18**, 645(1986).
16. H. Shirakawa, T. Ito, and S. Ikeda, *Polym. J.*, **4**, 460(1973).
17. C. R. Fincher, Jr., C. -E. Chen, A. J. Heeger, A. G. MacDiarmid, and J. B. Hastings, *Phys. Rev. Lett.*, **48**, 100(1982).

Chapter 5

Unrestricted Hartree-Fock Method for Infinite Systems with Antiferromagnetic Array: Analysis of Antiferromagnetic State of *trans*-Polyacetylene

Introduction

Peierls[1] has discussed that regular-chain structure is unstable in one-dimensional (1-D) metals whose energy band is partially occupied and would be distorted into dimerized structure with a lower symmetry, which causes the metal-insulator transition called Peierls distortion. Overhauser[2,3] has subsequently shown that the paramagnetic (metallic) state is always unstable with respect to formation of a static spin density wave (SDW), the instability of which occurs for SDW having a wavevector $Q = 2k_F$, where k_F is the radius of the Fermi sphere. Actually, charge-density-wave (CDW) and SDW states are observed to appear in the insulating phase of some conducting polymers[4] and organic superconducting crystals[5] at low temperatures as characteristic phenomena occurring in 1-D systems. These facts are explained on the basis of the electron-hole correlation[5] due to the nesting of the Fermi surface. In 1-D systems, for instance, the Fermi surface completely overlaps by the translation of $2k_F$. In contrast, the nesting is incomplete in two- or three-dimensional solids and, therefore, such instabilities become less general.

In molecular systems, chemical reactions are well realized on the basis of the interaction between occupied and unoccupied molecular orbitals (MO) in a similar sense. In particular, the frontier orbital theory[6] and the Woodward-

Hoffmann rule[7] tell us that the concept of phase and symmetry in the highest occupied MO (HOMO) and the lowest unoccupied MO (LUMO) is extremely important in the theory of chemical reactions. The instability problems associated with molecular systems such as polyene rings, hydrogen molecule and small hydrocarbons have been extensively studied by Čížek and Paldus,[8] Fukutome,[9] and Yamaguchi.[10]

In our previous paper,[11] we have obtained a stability condition for the Hartree-Fock (HF) solution of infinite 1-D systems. By the application of the formulation, we have analytically confirmed that the off-diagonal CDW is the most stable solution in *trans*-polyacetylene, $(CH)_x$ and, consequently, the bond-alternating structure is more stable than that of metallic and diagonal CDW states. Moreover, in other papers[12,13] we have presented a simple description of a photoinduced charged soliton pair, S^+-S^-, generated in *trans*-$(CH)_x$ on the basis of the HOMO-LUMO interaction within finite chains.

Recently theoretical and experimental investigations on organic ferromagnetism have been extensively carried out.[14] We have described ferromagnetic states of poly(*m*-phenylcarbene)[15] and poly(*m*-aniline)[16] by application of the unrestricted Hartree-Fock (UHF) crystal orbital (CO) method under the condition that $n\alpha > n\beta$ in the unit cell, where $n\alpha$ and $n\beta$ designate the number of electrons with α- and β-spins. On the other hand, antiferromagnetic states ($n\alpha = n\beta$) are difficult to describe owing to the lack of electron correlation in the usual UHF method. One of the simplest and most effective methods to represent electron correlation without losing the simplicity of the one-electron approximation is the alternant MO (AMO) method proposed by Löwdin and co-workers,[17-19] where suitable linear combinations of sets of paired bonding and antibonding MOs are taken to yield semilocalized AMOs, to which electrons with α- and β-spin are subsequently assigned.

Since Overhauser[2,3] showed that the metallic state is always unstable with respect to formation of SDW states, Berggren et al.,[20,21] Harris and Falicov,[22] Misurkin and Ovchinnikov,[23] André et al.[24] , and Subbaswamy and Grabowski[25] have investigated the antiferromagnetic states of simple 1-D

chains such as a linear hydrogen chain and polyene on the basis of the AMO method. They have treated the problem of the 1-D systems with only one electron per atom; polyene has been hence calculated using the Hubbard model. Incidentally, the AMO method has been suggested to lead to erroneous results when it is applied to the system having more than two electrons per atom.[23] On the other hand, Kertész et al.[26-28] have solved this kind of problem by the introduction of a special choice of starting density matrix into the UHF CO method. In this method, however, the way of making the starting density matrix is rather empirical, and it is not therefore an easy task to set up the initial condition especially in complicated systems.[26]

In this paper, we present an intrinsic method for obtaining the self-consistent-field (SCF) antiferromagnetic solution, that is, the SDW solution of polymers and crystals within the UHF CO method by taking effective electron correlation into account on the basis of the nesting of the Fermi surface. This method can be easily applied to more complicated polymers and crystals and will facilitate the energetical comparison between ferromagnetic and antiferromagnetic states. We examine the antiferromagnetic state of *trans*-$(CH)_x$ with isodistant C-C bond length with respect to the energetical stability, correlation gap, and spin density distribution.

Method of calculation

The CO with spin σ based on the Bloch's theorem is described as

$$\varphi_s^{\sigma}(k, x) = \frac{1}{\sqrt{N}} \sum_{j=1}^{N} \sum_{\mu}^{n} e^{ikja} c_{\mu s}^{\sigma}(k) \chi_{\mu}(x - ja), \tag{1}$$

where $\chi_\mu(x - ja)$ is the μth atomic orbital in the jth unit cell, a the unit vector of translational symmetry; s the band level; N the number of cells; $c_{\mu s}{}^{\sigma}(k)$ the CO coefficient. We employed the MINDO/3 parametrization,[29] which has

been successfully applied to a large number of molecules concerning heat of formation, ionization potential, dipole moment, and so on,[30] throughout the present paper. The values of the overlap integrals and the electron-repulsion integrals were considered as far as the fourth-nearest-neighboring cell. The number of the representative vectors was chosen as 21 with regular intervals ($\pi/10a$) in the Brillouin zone.

The procedure of the present method is composed of two SCF steps. In the first step the RHF CO equation was solved for diamagnetic state, where the unit cell had to be doubled for successive description of an antiferromagnetic state as shown below. In the RHF solution $\varphi_s{}^{\alpha}(k, x)$ is equal to $\varphi_s{}^{\beta}(k, x)$ and the system is diamagnetic. We then perform the following canonical transformation to introduce electron correlation into the system.

$$\psi_{occ}{}^{\alpha}(k, x) = \cos\theta_1 \varphi_s{}^{\alpha}(k, x) + \sin\theta_1 \varphi_s{}^{\alpha}(k+Q, x),$$

$$\psi_{uno}{}^{\alpha}(k, x) = -\sin\theta_1 \varphi_s{}^{\alpha}(k, x) + \cos\theta_1 \varphi_s{}^{\alpha}(k+Q, x), \tag{2}$$

$$\psi_{occ}{}^{\beta}(k, x) = \cos\theta_2 \varphi_s{}^{\beta}(k, x) - \sin\theta_2 \varphi_s{}^{\beta}(k+Q, x),$$

$$\psi_{uno}{}^{\beta}(k, x) = \sin\theta_2 \varphi_s{}^{\beta}(k, x) + \cos\theta_2 \varphi_s{}^{\beta}(k+Q, x), \quad (0 < \theta_1, \theta_2 < \pi/2)$$

where the subscripts, *occ* and *uno*, stand for the CO associated with an occupied level and an unoccupied one, respectively, and Q a phase parameter. In a non-variational form, the electron densities ρ^{α} and ρ^{β} from the highest occupied band thus generated are expressed as

$$\rho^{\alpha} = \sum_k [cos^2\theta_1 |\varphi_s^{\alpha}(k, x)|^2 + sin^2\theta_1 |\varphi_s^{\alpha}(k + Q, x)|^2$$

$$+ cos\theta_1 sin\theta_1 (\varphi_s^{\alpha}(k, x)\varphi_s^{\alpha}(k + Q, x)^* + h.c.)]$$

(3)

$$\rho^{\beta} = \sum_k [cos^2\theta_2 |\varphi_s^{\beta}(k, x)|^2 + sin^2\theta_2 |\varphi_s^{\beta}(k + Q, x)|^2$$

$$- cos\theta_2 sin\theta_2 (\varphi_s^{\beta}(k, x)\varphi_s^{\beta}(k + Q, x)^* + h.c.)]$$

The strongest correlation is introduced at $\theta_1 = \theta_2 = \pi/4$, where the spin density is written down as

$$\rho^{\alpha} - \rho^{\beta} = \sum_k \left(\varphi_s^{\alpha}(k,x)\varphi_s^{\alpha}(k+Q,x)^* + h.c.\right), \tag{4}$$

because $\varphi_s{}^{\alpha}(k, x) = \varphi_s{}^{\beta}(k, x)$ in the first SCF solusion . Using Eq. (1), we obtain the spin density distribution,

$$\rho^{\alpha} - \rho^{\beta} \propto cosQja\,. \tag{5}$$

Here the wavelength of the SDW is $2\pi/Q$. Here it is considered that the mixing of the COs occurs only around the Fermi level, i.e., at $Q = 0$ or $2k_F$ in the same spirit of the frontier orbital theory[6] and the "g-ological" analysis of 1-D electrical conductors.[31] The translational vector of the SDW is found to be $2a$ and infinity in the cases of $Q = 2k_F$ and 0, respectively. In the latter case, the SDW does not occur.

The mixing of the COs is thus carried out around the Fermi level with $Q = 2k_F$. Figure 1 is a schematic representation of the mixing of occupied and unoccupied states in a single unit cell, where Q becomes the nesting vector. In the actual calculation a doubled unit cell must be considered since it is necessary to represent an antiferromagnetic state because opposite spins are located on different sublattices as discussed above. Here let us pay attention to the CO patterns shown in Fig. 2. The mixing of the COs around the Fermi level induces a significant change in the CO patterns for $Q = 2k_F$. Electron correlation such as an alternant effect proposed by Löwdin[17] is

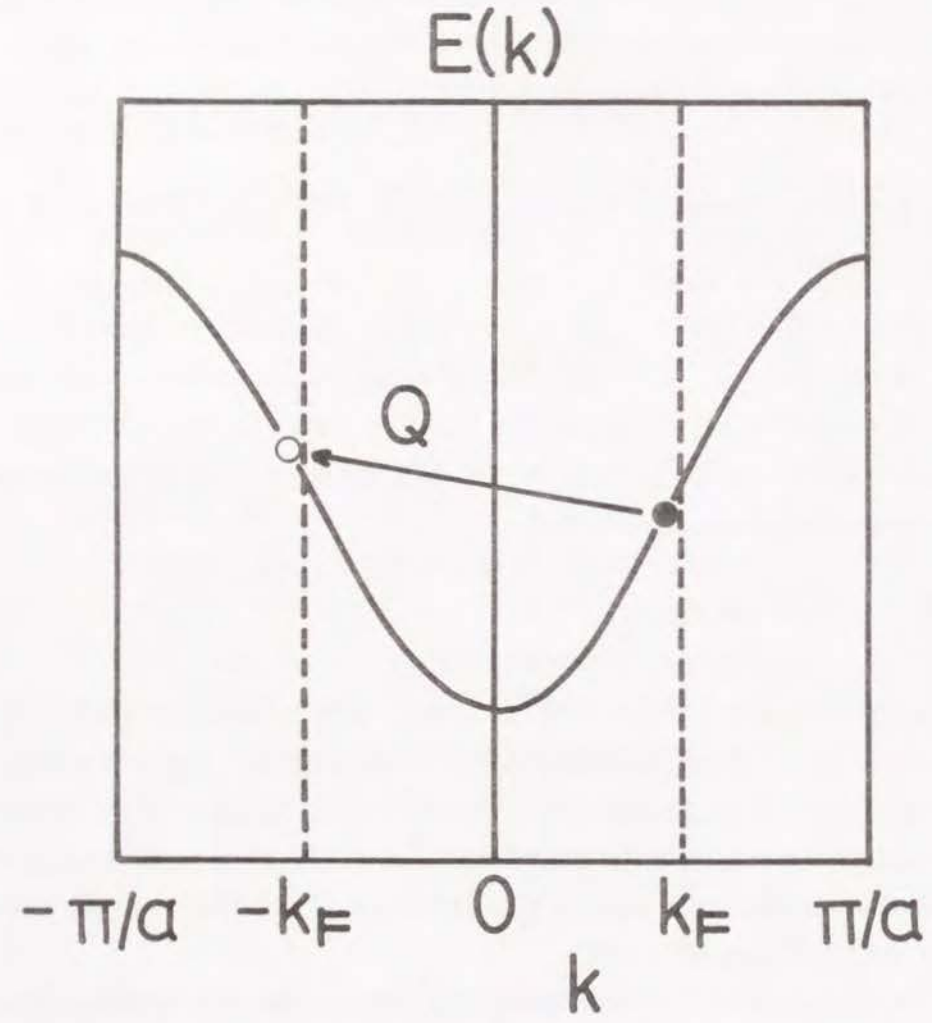

Fig. 1. Schematic representation of the interaction between occupied states (solid circle) and unoccupied states (open circle). The nesting vector $Q = 2k_F$.

described well by these semi-localized orbitals, that is, electrons with opposite spins can repel each other in accordance with their repulsive interaction which is not included in both of the RHF and the usual UHF methods. In this case, classical Coulomb repulsion between antiparallel spins plays a crucial role in the dynamism of electrons in solids. In this sense, the CO patterns shown in Fig.2 are adequate for describing electron correlation between antiparallel spins.

In the next step, the second SCF equation is solved starting from the initial density matrix constructed by the canonically transformed COs in Eq. (2) and the rest of the COs ntransformed. The canonical transformation, i.e., the mixing between the highest occupied CO and the lowest unoccupied CO, is performed only around the Fermi level as is described in the above. Moreover, in Eq. (2), mixing parameter, θs are set to be $\pi/4$ for the maximum correlation effect.[17-19] Such inclusion of the electron correlation spontaneously leads to a rearrangement of the inner-shell COs untransformed originally.

Results and discussion

Since the antiferromagnetic state of *trans*-$(CH)_x$ has not been fully analyzed from the viewpoint of its coordinate dependence,[22,23,28] we employed an isodistant model structure of *trans*-$(CH)_x$ by the use of the present scheme. Our main purpose here is to check the coordinate dependence of the total energy, the correlation gap, and the spin density distribution in the antiferromagnetic state. The C-C bond length ($r_{C\text{-}C}$) is changed from 1.2 to 1.8 Å, and the C-H bond length and the bond angles are fixed at 1.09 Å and 120°, respectively.

The first SCF solution gave metallic structure within the bond lengths calculated, that is, a gapless energy band structure, not giving a diagonal CDW-type solution. The antiferromagnetic SCF solution was obtained via the second SCF equation based on the canonical transformation of Eq. (2).

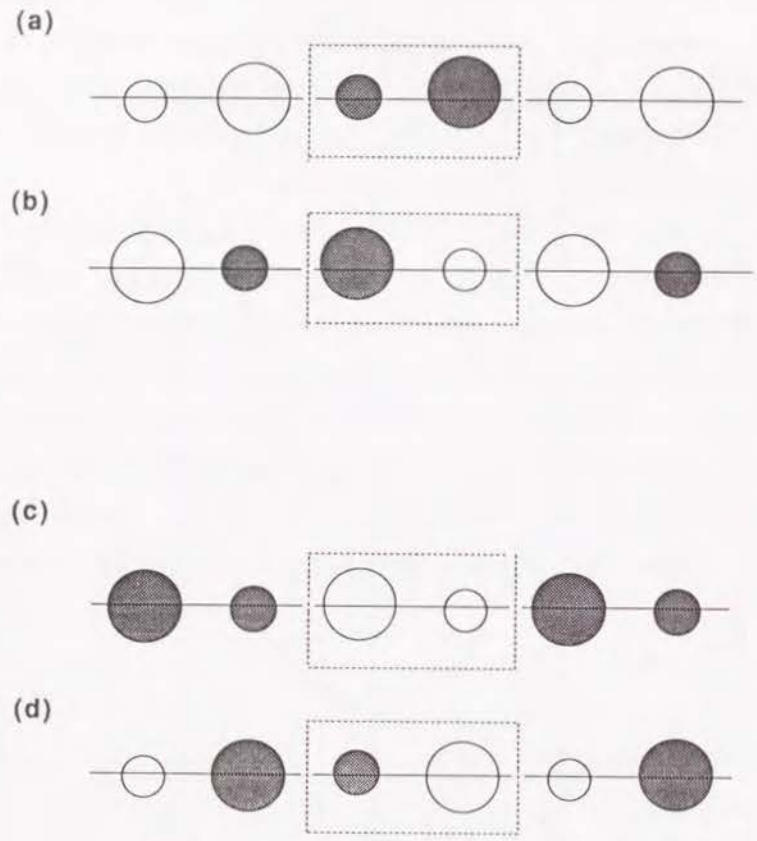

Fig. 2. Orbital patterns of the canonically transformed COs of pπ nature. (a) $\psi_{occ}{}^{\alpha}(k, x)$, (b) $\psi_{uno}{}^{\alpha}(k, x)$, (c) $\psi_{occ}{}^{\beta}(k, x)$, and (d) $\psi_{uno}{}^{\beta}(k, x)$. The size of circles signifies the magnitude of atomic orbital coefficients. Broken lines indicate the doubled unit cell.

The convergency of the second SCF process was excellent because the initial density matrix reflects exact electron correlation to a certain extent. In order to complete the energetical comparison, the total energy for the bond-alternating structure ($r_{C\text{-}C}$ = 1.46 Å, $r_{C=C}$ = 1.35 Å)[32] was also calculated.

The total energy of the metallic and antiferromagnetic states as function of $r_{C\text{-}C}$ is shown in Fig. 3, where the antiferromagnetic state of this polymer is always more stable than the metallic one. Furthermore, it is interesting that both the metallic and the antiferromagnetic states are most stable at $r_{C\text{-}C}$ = 1.40 Å. In contrast with the conclusion of the previous investigations,[22,23] the present check clearly shows that the bond-alternating structure is more stable than the antiferromagnetic state in accordance with a large number of experimental results.[33] As suggested by Subbaswamy and Grabowski,[25] failure of the earlier investigations seems to originate in crude level of approximation and parametrization. Therefore, the order of energetical stability is found as, metallic < antiferromagnetic < off-diagonal CDW.

The band structure for the most stable antiferromagnetic state ($r_{C\text{-}C}$ = 1.40 Å) are shown in Fig. 4. Broken lines in Fig. 4(b) indicate the dispersion curves of a metallic state, whereit is seen that the inclusion of the electron correlation leads to opening a gap near the Fermi level known as a correlation gap. The dispersion curves of σ-nature in Fig.4(a), does not substantially change from those of the metallic state. In spite of this, judging from the alternating phase-patterns of the inner-shell COs, inclusion of electron correlation is found to affect the σ-electronsalthough the extent of the alternation is smaller. It is of great interest that the alternating patterns of the COs with σ-nature does not induce an energy gap at k = $\pi/2a$ as shown in Fig. 4(a). On the basis of these results, we find that the electron-hole correlation, i.e., the interaction between occupied and unoccupied states plays an essential role in this kind of instability problem associated with 1-D systems.

The spin density distribution of π- and σ-nature and the correlation band gap (E_g) as a function of the bond length is listed in Table I. The spin density and E_g become larger as $r_{C\text{-}C}$ increases as is expected. The spin

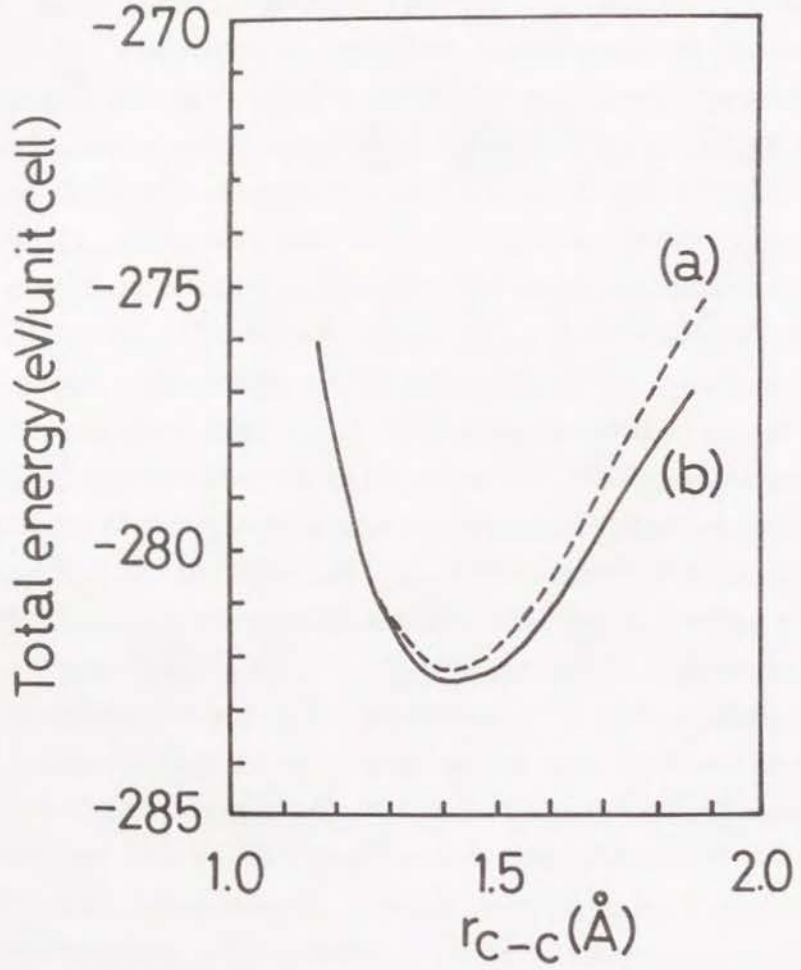

Fig. 3. Total energy per unit cell in an isodistant structure of *trans*-$(CH)_x$. (a) metallic and (b) antiferromagnetic states. Total energies of the metallic, antiferromagnetic ($r_{C\text{-}C}$ = 1.40 Å), and bond-alternating ($r_{C\text{-}C}$ = 1.46 Å, $r_{C=C}$ = 1.35 Å) states are -282.337 eV, -282.423 eV, and -282.530 eV, respectively.

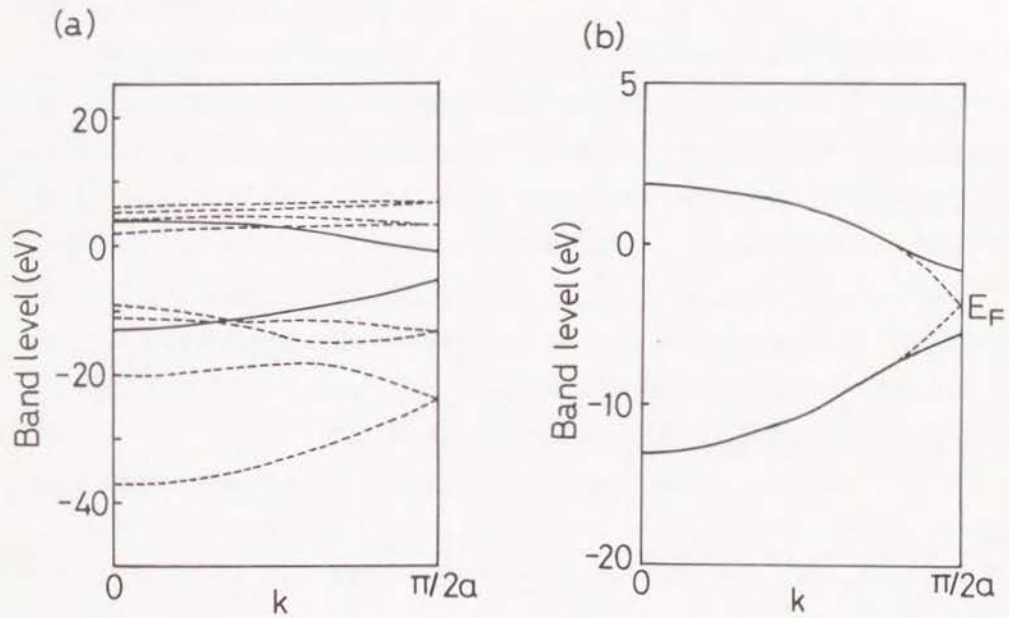

Fig. 4. Band levels of the antiferromagnetic state of *trans*-$(CH)_x$ ($r_{C\text{-}C}$ = 1.40 Å). Solid and broken lines indicate π- and σ-bands, respectively in (a). Broken lines in (b) indicate π-bands of the metallic state.

Table I. Spin densities with π- and σ-nature and band gap (E_g) as a function of the C-C bond length ($r_{C\text{-}C}$).

$r_{C\text{-}C}$ (Å)	C_1		C_2		E_g (eV)
	π	σ	π	σ	
1.2	–0.085	–0.012	0.085	0.012	3.97
1.3	–0.094	–0.013	0.094	0.013	4.07
1.4	–0.099	–0.014	0.099	0.014	4.30
1.5	–0.569	–0.170	0.569	0.170	8.20
1.6	–0.683	–0.229	0.683	0.229	9.08
1.8	–0.861	–0.387	0.861	0.387	10.47
Bond-alternating ($r_{C\text{-}C}$ = 1.46 Å, $r_{C=C}$ = 1.35 Å)					
	0	0	0	0	6.51

densities are relatively small up to $r_{C\text{-}C}$ = 1.4 Å, and the spin densities of π- and σ-nature cooperate for the formation of the antiferromagnetic state. It is remarkable that the spin density as well as E_g suddenly becomes large between $r_{C\text{-}C}$ = 1.4 and 1.5 Å, which indicates the beginning of correct dissociation of the C-C bond.

An antiferromagnetic solution for the bond-alternating structure was not obtained as suggested by Kertész et al.,[28] which means that the RHF method rather correctly describes the electronic state of the bond-alternating structure. Interestingly, E_g of the optimal antiferromagnetic state is smaller than that of the bond-alternating structure as shown in Table I, being in a strong contrast with the result obtained by Kertész et al.[28] They have reported that the antiferromagnetic state of *trans*-$(CH)_x$ has a very large E_g of 13.53 eV (at $r_{C\text{-}C}$ = 1.39 Å), and that, on the other hand, the bond-alternating structure has E_g of 7.24 eV. Suhai[34] also obtained similar results. The E_g value for the bond-alternating structure is reasonable because the Hartree-Fock method has a tendency to overestimate a band gap. However, the E_g of the antiferromagnetic state seems physically inappropriate because such a large E_g would lead to the erroneous conclusion that the antiferromagnetic state is more stable than the bond-alternating structure.[34] We believe that rather arbitrary overestimation of inclusion of electron correlation in Refs. 28 and 34 has led to their large E_g values.

Conclusion

We have presented an intrinsic UHF CO scheme for polymers and crystals having antiferromagnetic spin array. It has been found extremely profitable to introduce the idea of the AMO method, i.e., taking suitable linear combinations of sets of paired occupied and unoccupied states into the UHF CO method for 1-D systems having many electrons per atom.

We have calculated the antiferromagnetic state of *trans*-$(CH)_x$ by the use of this method. The antiferromagnetic state is always more stable than the

metallic state as is expected, but less stable than the bond-alternating state by 2.47 kcal/unit cell, being consistent with the experimental studies. Correlation gap for the antiferromagnetic state of *trans*-$(CH)_x$ has been estimated to be 4.30 eV for the equilibrium geometry ($r_{C\text{-}C}$ = 1.40 Å), the result of which is in contrast with the conclusion of the previous investigations. Furthermore, the spin density is relatively small in the equilibrium structure.

Although the usual UHF method has a difficulty to set up an initial asymmetrical density matrix for the SCF iterations, the present method is more useful in the physical point of view and the convergency of the SCF process. This method is expected to be easily applied to a number of 1-D polymers and crystals, the results of which will be reported elsewhere.

References

1. R. E. Peierls, *Quantum Theory of Solids*, Oxford University, London, 1955, Chap. 5.
2. A. W. Overhauser, *Phys. Rev. Lett.*, **4**, 462(1960).
3. A. W. Overhauser, *Phys. Rev.*, **128**, 1437(1962); **167**, 691(1968).
4. See, for example, A. J. Heeger, *Polyacetylene New Concepts and New Phenomena*, T. A. Skotheim Ed., *Handbook of Conducting Polymers*, Marcel Dekker, New York, 1986, vol. 2, p. 729.
5. See, for example, D. Jérome, *Science*, **252**, 1509(1991).
6. K. Fukui, *Theory of Orientation and Stereoselection*, Springer-Verlag, West Berlin, 1975.
7. R. B. Woodward and R. Hoffmann, *The Conservation of Orbital Symmetry*, Academic, New York, 1970.
8. J. Čížek and J. Paldus, *J. Chem. Phys.*, **47**, 3976(1967).
9. H. Fukutome, *Prog. Theor. Phys.*, **47**, 1156(1972), **49**, 22(1973), **50**, 1433(1973).
10. K. Yamaguchi, *Chem. Phys. Lett.*, **33**, 330(1975), **35**, 230(1975).
11. K. Tanaka, H. Kobayashi, S. Yamanaka, K. Yoshizawa, and T. Yamabe, *J. Chem Phys.*, **91**, 3724(1989).
12. K. Tanaka, K. Yoshizawa, and T. Yamabe, *Int. J. Quantum Chem.*, **40**, 305(1991).
13. K. Tanaka, K. Yoshizawa, T. Takeuchi, and T. Yamabe, *Int. J. Quantum Chem.*, **40**, 315(1991).
14. See, for example, Proccedings of the International Conference on Science and Technology of Synthetic Metals, Tübingen, Germany, M. Hanack, S. Roth, and H. Schier, Ed., *Synth Met.*, **43**, 3229-3304(1991).
15. K. Tanaka, T. Shichiri, and T. Yamabe, *J. Mol. Struc. (Theochem)*, **188**, 313(1989).
16. K. Tanaka, K. Yoshizawa, A. Takata, and T. Yamabe, *Synth. Met.*, **43**, 3297(1991).
17. P. O. Löwdin, *Phys. Rev.*, **97**, 1509(1955).

18. R. Pauncz, J. de Heer, and P. O. Löwdin, *J. Chem. Phys.*, **36**, 2247, 2257(1962).
19. J. de Heer, *Rev. Mod. Phys.*, **35**, 631(1963).
20. K. -F. Berggren and F. Marino, *Phys. Rev.*, **184**, 484(1969).
21. B. Johansson and K. -F. Berggren, *Phys. Rev.*, **181**, 855(1969).
22. R. A. Harris and L. M. Falicov, *J. Chem. Phys.*, **51**, 5034(1969).
23. I. A. Misurkin and A. A. Ovchinnikov, *Mol. Phys.*, **27**, 237(1974).
24. J. -M. André, J. -L. Brédas, J. Delhalle, Y. Kalenov, and L. Piela, *Int. J. Quantum Chem.: Quantum Chem. Symposium,* **14**, 419(1980).
25. K. R. Subbaswamy and M. Grabowski, *Phys. Rev.*, B**24**, 2168(1981).
26. M. Kertész, *Acta Phys. Hung.*, **41**, 107(1976).
27. M. Kertész, J. Koller, and A. Ažman, *Phys. Rev.*, B**14**. 76(1976).
28. M. Kertész, J. Koller, and A. Ažman, *Phys. Rev.*, B**19**, 2034(1979).
29. R. C. Bingham, M. J. S. Dewar, and D. H. Lo, *J. Am. Chem. Soc.*, **97**, 1285(1975).
30. D. V. Lewis, *Chem. Rev.*, **86**, 1111(1986).
31. J. Solyom, *Adv. Phys.*, **28**, 201(1979).
32. S. Suhai, *J. Chem. Phys.*, **73**, 3843(1980).
33. See, for example, C. R. Fincher, C. E. Chen, A. J. Heeger, A. G. MacDiarmid, and J. B. Hastings, *Phys. Rev. Lett.*, **48**, 100(1982).
34. S. Suhai, *Chem. Phys. Lett.*, **96**, 619(1983).

PART II

MOLECULAR DESIGN OF ORGANIC FERROMAGNETS BASED ON CRYSTAL ORBITAL METHOD

INTRODUCTION

Magnets have fascinated and served mankind for almost 3000 years.[1] In contrast, the progress of the theory of magnetism has been very slow, in spite of the efforts made throughout history. The thermal properties of magnetic substances were first investigated in a systematic manner by Pierre Curie, who found magnetization M to be proportional to the applied field H. He studied χ, the constant of proportionality, known as the magnetic susceptibility, finding for paramagnetic substances:

$$\chi = \lim_{H \to 0} M/H = C/T.$$

As we know, the great development of science and technology in this century is indebted mainly to the invention of quantum mechanics. Progress in the modern understanding of magnetism has greatly depended on progress in quantum theory. Any modern theory of magnetism must be based on two concepts inherent in quantum mechanics: electron spin and Pauli exclusion principle. In 1927 Pauli invented his spin matrices; the next year Heisenberg explained ferromagnetism by means of exchange, the combination of the Pauli principle and physical overlap of the electronic wavefunctions.

$$H_{12} = -J_{12} S_1 \cdot S_2,$$

where J_{12} is exchange energy between the nearest neighbor spins and S_i electronic spin. Subsequently, Hartree, Fock, Heitler, London, and many others performed atomic and molecular calculations as the direct application of quantum theory. In 1929 Slater showed that a single determinant gives a variational many-electron wavefunction for use in problems of atomic and molecular structure.

The simplest model of magnetism in metal is the following: electrons in well-localized magnetic d or f shells interact with one another via the nearest neighbor exchange mechanism of Heisenberg, whilst an entirely distinct set

of quasi-free electrons in Bloch states accounts for the metallic properties without partaking of the magnetic ones. However, it is not possible to ignore the itinerancy of the electrons in any sensible theory of magnetism in metals for several reasons, and therefore the concept of "direct exchange" has to be modified. Recent theory of magnetism is based on the band picture, by which the magnetism of the iron group can be described. The study of Slater on nickel-copper alloys offers strong evidence for the band theory of ferromagnetism in metals. Ruderman and Kittel developed the effective long-range interaction between nuclear spins in 1954. The extension of their treatment to the *s-d* or *s-f* electronic interaction was performed by Kasuya and Yoshida (RKKY interaction).

The known case of ferromagnetism has involved spins of either *d* or *f* electrons, which have been considered to presumably play an essential role in the mechanism of the magnetic interactions. One can imagine that ferromagnetic materials based on organic molecules and polymers would show fundamentally new properties that would provide valuable insights into the nature of magnetism. An important guide to the spin alignment in π-conjugated systems was established in the 1950s.[2] In order to design such materials, we first consider an odd alternant hydrocarbon, i.e., one where the conjugated atoms are odd in number and can be divided into two classes (starred and unstarred) such that no two atoms of the same class are directly linked. When the number of starred atom (n_s) is larger than that of unstarred atoms (n_u) in an alternant hydrocarbon, it has (n_s - n_u) degenerate non-bonding molecular orbitals (NBMO) according to the theorem of Coulson and Rushbrooke. It is further found that the ground state of such molecules has the total spin $S = (n_s - n_u)/2$ following the Heisenberg model employing negative exchange energy, or the valence bond theory. In line with these guides or others, several theoretical models were presented in the 1960s for designing ferromagnets based on organic molecules or polymers having only *p*-electrons. Following McConnell,[3] it is possible that radicals on the alternant hydrocarbons may pancake on top of one another in the crystal lattice so that atoms of positive spin density are exchange coupled most

strongly to atoms of negative spin density in neighboring molecules.

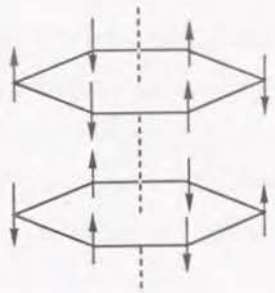

This suggests a ferromagnetic exchange interaction favoring parallel spin angular momentum on neighboring molecules. The importance of this model must be recognized in terms of the intermolecular spin control. Another model of McConnell[4] is a mixed stack of donor ($D^{\bullet+}$) and acceptor ($A^{\bullet-}$) radical ions with high symmetry, $\cdots D^{\bullet+}A^{\bullet-}D^{\bullet+}A^{\bullet-}D^{\bullet+}A^{\bullet-}\cdots$. Moreover, Mataga[5] suggested that large alternant hydrocarbons composed of *meta*-substituted diphenylcarbene or triphenylmethyl radical moieties will have a very high-spin ground state in the manner illustrated below.

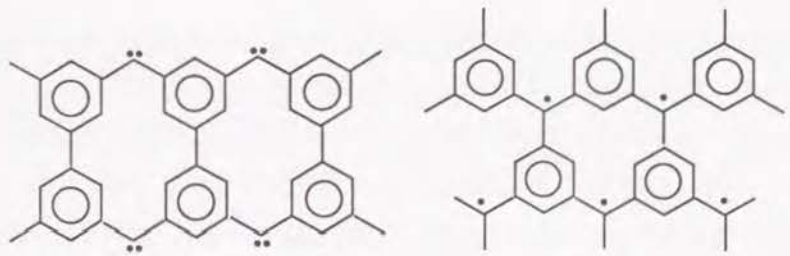

With guidance from Mataga's model, Iwamura and coworkers[6] prepared several high-spin phenylcarbene oligomers via a route of the *in situ* photolysis of polydiazo derivatives. The best characterized compound is a nonet ($S = 4$) tetracarbene. The electron spin resonance and the magnetic susceptibility measurements in either a 2-methyltetrahydrofuran matrix or a benzophenone

crystal confirmed the nonet ground state. The parallel spins are divided into two types: well-localized σ-spins and relatively delocalized π-spins. The *meta*-substitution in this type of molecules is essential to the topological degeneracy of the NBMOs. However, the temperature dependence of the susceptibility exhibited only independent-spin or antiferromagnetic behavior. Furthermore, Ovchinnikov[7] proposed nitrogen- and boron-substituted high-spin model polymers based on Mataga's suggestion.

In Part II, design of organic ferromagnets is attempted based on the band theory.

In Chapter 1 (*Synth. Met.*, **44**, 1(1991)), the electronic structure and magnetic properties, particularly interplane magnetic coupling, of stacked diphenylcarbene is theoretically studied on the basis of the crystal orbital method and the McConnell's rule. It is revealed that the ferromagnetic interplane interaction is anticipated throughout chain for the translation pitch angle of $\theta = 60°$ and 180° in contrast with the antiferromagnetic interaction for $\theta = 120°$. Furthermore, more realistic polymer conformation based on the observed polycrystalline structure of diphenylcarbene derivatives is also examined.

In Chapter 2 (*Polym. J.*, submitted), the electronic structure of poly(*m*-aniline), which is originally designed by our group, is examined using the unrestricted Hartree-Fock one-dimensional tight-binding crystal orbital method. It is concluded that the ferromagnetic state is energetically more favorable than the non-magnetic state both in the cationic and dehydrogenated forms. The ferromagnetic band is extremely narrow owing to the nature of NBMO. The spin is mainly located on nitrogen, but considerable portion of the spin flows into the benzene ring through spin polarization mechanism. Synthesis and a series of characterizations of poly(*m*-aniline) will be discussed in Part III.

References

1. See, for instance, D. C. Mattice, *The Theory of Magnetism I*, Springer-Verlag, Berlin 1981. Useful reviews about the history of magnetism have been given in the fascinating introduction of this book.
2. H. C. Longuet-Higgins, *J. Chem. Phys.*, **18**, 265(1950), C. A. Coulson and H. C. Longuet-Higgins, *Proc. Roy. Soc.*, A**192**, 16(1947), C. A. Coulson and G. S. Rushbrooke, *Proc. Cambridge Phil. Soc.*, **36**, 193(1940).
3. H. M. McConnell, *J. Chem. Phys.*, **39**, 1910(1963).
4. H. M. McConnell, *Proc. Robert A. Welch Found. Conf. Chem. Res.*, **11**, 144(1967).
5. N. Mataga, *Theor. Chim. Acta* (*Berl.*), **10**, 372(1968).
6. T. Sugawara, S. Bandow, K. Kimura, H. Iwamura, and K. Itoh, *J. Am. Chem. Soc.*, **108**, 368(1986), Y. Teki, T. Takui, K. Itoh, H. Iwamura, and K. Kobayashi, *ibid*, **108**, 2147(1986).
7 A. A. Ovchinnikov, *Theor. Chim. Acta* (*Berl.*), **47**, 297(1987).

Chapter 1

Theoretical Study on Ferromagnetic Interaction in Stacked Diphenylcarbene Polymer

Introduction

In recent years, the possibility of synthesizing organic ferromagnets has been extensively discussed from both theoretical and experimental points of view.[1-4] Two main categories have been considered as candidates for ferromagnetic polymers: one exhibits ferromagnetic properties by means of peculiar topological backbone of π-conjugated polymers and the other by means of the interaction among the spins located in the side chains. Poly(*m*-phenylcarbene), having the backbone in which benzene rings are connected at the *meta*-positions through carbene moiety, belongs to the former. In a previous paper,[7] we have studied the magnetic properties of this polymer employing the tight-binding crystal orbital (CO) method based on the unrestricted Hartree-Fock (UHF) scheme and demonstrated that the ferromagnetic state is well described by the mean-field approximation such as the Hartree-Fock scheme, as well as by the Heisenberg-type effective Hamiltonian scheme.[6]

A third possible category would be the stacking polymers consisting of infinitely stacking monomeric radical units. Almost two decades ago, McConnell proposed an interesting guideline for design of this type of ferromagnetic polymer.[7] According to his rule, the ferromagnetic order in the whole polymer chain would be achieved when the product of the spin densities becomes negative between the interacting spin sites each belonging to the nearest neighboring (stacking) radical units by circumventing the

exchange integral of spins being usually negative (favoring antiferromagnetic array) as is referred to in detail later. There have been, however, no attempts to synthesize these stacking-type ferromagnetic polymers.

Meanwhile, Iwamura et al.[8] have synthesized three kinds of isomers of the cyclophane-type diphenylcarbene dimers, bis(phenylmethylenyl)[2,2] para-cyclophane, in order to investigate relationship between the stacked orientation and the spin multiplicity of these dimeric units, to reveal based on the electron spin resonance (ESR) analysis that the ground state of the pseudo-*ortho* and pseudo-*para* dimers are of quintet state in comparison with that of the pseudo-*meta* dimer of singlet state. These results agree well with McConnell's rule. On the other hand, Yamaguchi et al.[9] have calculated the effective exchange integral values of similar carbene-stacked dimers.

With respect to the carbene-stacked polymer even no theoretical assessment has been performed and, hence, McConnell's rule has never been applied to the prediction of ferromagnetism in these polymers. In the present work, we have first investigated the magnetic properties of diphenylcarbene-stacking polymer of infinite length, poly(diphenylcarbene) (PDPC) which has longitudinal π-electron interactions of each phenyl ring as shown in Fig. 1, by using the one-dimensional tight-binding self-consistent-field crystal orbital (SCF-CO) method. It is the main concern of this article to discuss the favorable configuration of PDPC to yield the ferromagnetic state as a whole. Moreover, we have examined the magnetic interaction for the stacking structure of tilted diphenylcarbene based on the experimental report on the crystalline structure of a diphenylcarbene derivative.[10]

Method of calculation

All of the calculations were performed on the basis of the one-dimensional tight-binding SCF-CO method under the MINDO/3 level approximation,[11] including all the valence electrons, the program for which was made in the authors' laboratory. The computer system used was FACOM M-780/30

equipped at the Data Processing Center of Kyoto University. This method has been successfully applied to the analysis of poly(*m*-phenylcarbene) also indicating the ferromagnetic state[5] as mentioned above. The number of representative wave vectors was chosen as 21 with regular intervals in the Brillouin zone. Monomeric diphenylcarbene (DPC) was taken as the unit cell of stacking polymer. The overlap and the electron repulsion integrals were considered as far as the second nearest-neighboring cell of all the calculations. The UHF scheme was employed for the calculation of the polymer, the monomeric unit of which is of triplet state.

The structures and the atomic numberings of the polymer skeletons employed are shown in Fig. 1. One benzene ring in the monomeric unit was arranged to stack in parallel with the benzene ring in the adjacent unit with the translation distance R and the pitch angle θ around the z-axis. Three R values (2.5, 2.8, and 3.1 Å) and four θ values (0°, 60°, 120°, and 180°) for each R were employed in the calculation. The interplanar spacing of 3.1 Å was taken from the experimental data of, for instance, the stacking distance in [2,2]paracyclophane.[12] For all the C-C and C-H bond lengths, the standard values were utilized; 1.40 and 1.08 Å, respectively. The C-C-C and the C-C-H angles in the benzene ring were fixed at 120°, and the bond angle at the carbenic carbon was set to 140° according to the theoretical study on *m*-phenylene-bisphenylmethylene.[13]

The dihedral angle between two benzene rings in a DPC molecule has been found to be 72.0° from the analysis of electron nuclear double resonance.[14] Our separated calculation, however, for two kinds of dihedral angles (72.0° and 0°) with respect to DPC monomer yielded no essential difference in the spin distribution throughout the molecular structure. Hence, the monomeric unit was assumed to be planar in the present study for simplicity.

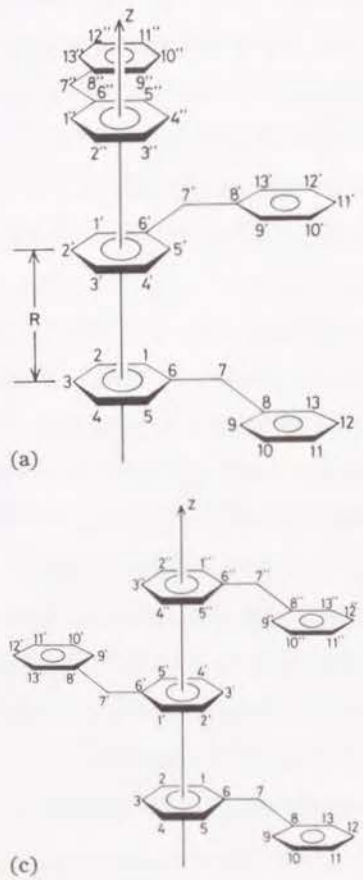

Fig. 1. Structures and numberings of PDPC for (a) $\theta = 60°$, (b) $\theta = 120°$, and (c) $\theta = 180°$. R denotes the translation distance between the two monomeric units and θ the pitch angle around the z-axis of the translation.

Results and discussion

Ferromagnetic intercell interaction

The spin densities on selected atomic orbitals of PDPC are listed in Table I. It is seen that both the π and σ spins on the carbenic carbon (C7) consist of the up-spin (positive value) for all the configurations, indicating the triplet-spin configuration. In the benzene ring the positive and negative π spins appear alternately in an antiferromagnetic order. The spin densities of the two up-spin electrons on C7 are almost constant for all the combinations of R and θ.

We are now in a position to discuss the spin coupling between the monomeric units of the polymer. In order to estimate qualitatively the ferromagnetic property of the whole polymer, we utilized McConnell's rule[7] in which the interspin interaction is described as the expanded form of the Heisenberg Hamiltonian for the combination of monomeric units A and B:

$$H^{AB} = -\sum_{i,j} J_{ij}^{AB} S_i^A S_j^B = -S^A S^B \sum_{i,j} J_{ij}^{AB} \rho_i^A \rho_j^B \quad , \tag{1}$$

where S^A and S^B are the total spin operators for the monomeric units A and B, ρ_i^A and ρ_j^B are the π-spin densities on atoms i and j of the units A and B, and J_{ij}^{AB} is the exchange integral between i and j. When the Hamiltonian in Eq. (1) is negative, the total system favors the ferromagnetic array of spins Since the summation in Eq. (1) is rather complicated, we assume that the spin couplings only between the nearest carbons between the stacked DPCs A and B play a dominant role. Hence the right-hand side of Eq. (1) can be approximated to

$$H^{AB} \equiv -2J_{eff} S^A S^B \sum_{i,j} \rho_i^A \rho_j^B = -2J_{eff} S^A S^B \Delta(\mathrm{A, B}) \quad , \tag{2}$$

where J_{eff} is the effective exchange integral, being negative in general, and only the products of π-spin densities are considered. The calculated

Table I. Calculated data of spin density at R = 2.5 and 3.1 Å and Δ(A, B).

θ		60°		120°		180°	
R		2.5Å	3.1Å	2.5Å	3.1Å	2.5Å	3.1Å
C1	π	0.423	0.215	0.239	0.206	0.374	0.212
C2	π	-0.348	-0.140	-0.141	-0.131	-0.308	-0.138
C3	π	0.410	0.199	0.275	0.192	0.388	0.200
C4	π	-0.350	-0.141	-0.144	-0.132	-0.309	-0.139
C5	π	0.429	0.221	0.248	0.213	0.380	0.219
C6	π	-0.342	-0.194	-0.252	-0.189	-0.322	-0.193
C7	σ	0.974	0.970	0.965	0.970	0.979	0.970
	π	0.647	0.684	0.638	0.684	0.660	0.684
C8	π	-0.167	-0.181	-0.153	-0.182	-0.183	-0.182
C9	π	0.186	0.206	0.175	0.207	0.206	0.207
C10	π	-0.117	-0.127	-0.104	-0.128	-0.134	-0.128
C11	π	0.161	0.184	0.151	0.184	0.180	0.185
C12	π	-0.116	-0.127	-0.103	-0.127	-0.133	-0.127
C13	π	0.180	0.200	0.168	0.200	0.199	0.201

Δ(A, B)			
R = 2.5Å	-0.875	0.285	-0.714
2.8Å	-0.281	0.207	-0.259
3.1Å	-0.202	0.191	-0.197

summation, Δ(A, B) in Eq. (2), becomes positive at θ = 120° while those at θ = 60° and 180° negative. These results indicate that the ferromagnetic intercell interaction can appear in the orientations with θ = 60° and 180°.

The orbital patterns of the singly occupied CO (SOCO) of PDPC accommodating electrons with the up-spin at R = 2.5 Å are shown in Fig. 2 for three values of θ with the spin configurations, the up- and the down-spins being represented by up- and down-arrows, respectively. The spin-configurations are also shown in Fig. 3, where up- and down-spins are expressed as up- and down-arrows, respectively. These spin-configurations through the stacking polymer are determined by Eq. (2). The orbital patterns demonstrate a good agreement with the spin configurations, that is, the spins appear according to the contribution of the patterns of the up-spin SOCO and it is again obvious that the ferromagnetic intercell interaction is manifested for θ = 60° and 180°.

The result of the present analysis has also demonstrated that the CO method in the framework of the UHF scheme is applicable to the calculation of the magnetic order in organic compounds, as well as the valence bond (VB) method based on the Heisenberg model.

PDPC with tilted monomeric unit

The DPC derivative has already been synthesized in a polycrystalline state and the average spin multiplicity has been reported as approximately 1.0 (the triplet state) based on the magnetic field dependence of the magnetization.[10] This molecular packing mode was found to have a layered structure and benzene rings are overlapped taking pseudo-geminal orientation (θ = 0°) with a certain tilt angle from the X-ray analysis.[10] Here we calculated the magnetic properties of DPC derivative. The translation distance was fixed to be 3.2 Å. The calculation for this model system was performed using the geometry shown in Fig. 3 and the results are listed in Table II. For the case of θ = 0° the antiferromagnetic intermolecular interaction is anticipated based on the analysis by Eq. (2). In the present stacking, however, the above approximation in Eq. (2) is not good because the tilting of benzene rings

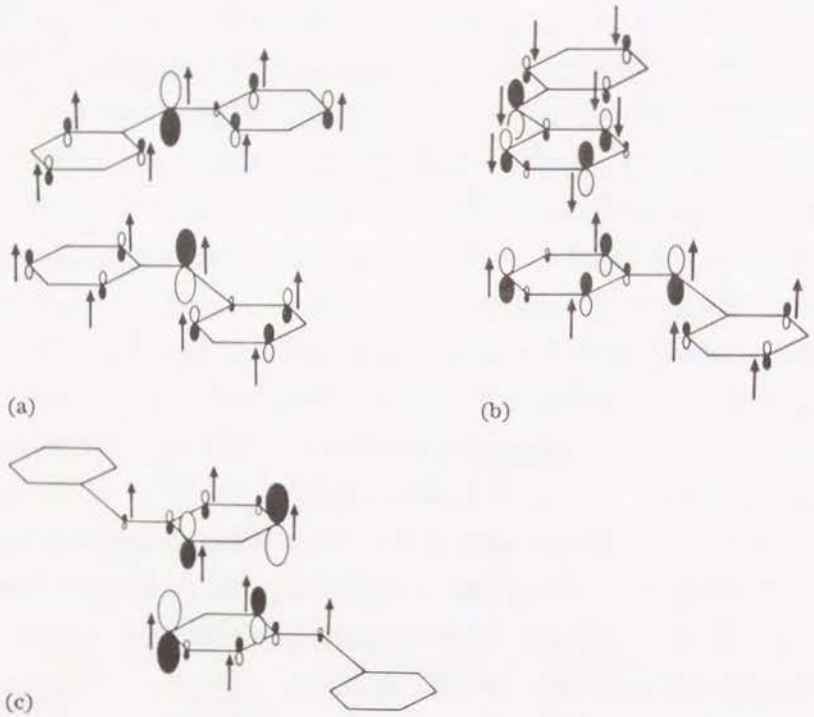

Fig. 2. Orbital patterns of the up-spin SOCO for (a) $\theta = 60°$, (b) $\theta = 120°$, and (c) $\theta = 180°$ at $R = 2.5$ Å. The up- and down-arrows denote up- and down-spins, respectively.

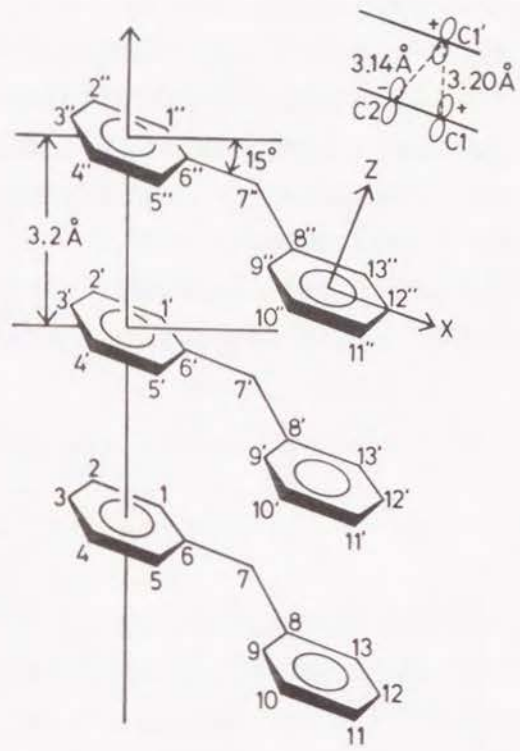

Fig. 3. Structure and numbering of PDPC with the tilt angle of 15°. Note the z-axis perpendicularly penetrates the molecular plane. A schematic side view of the magnetic interaction between C1' and C1, C2 is also illustrated.

Table II. Calculated data for the stacked polymer with tilted DPC.

Spin density[a]	C1	π	0.189	C8	π	-0.169
	C2	π	-0.113	C9	π	0.195
	C3	π	0.175	C10	π	-0.114
	C4	π	-0.114	C11	π	0.174
	C5	π	0.195	C12	π	-0.112
	C6	π	-0.170	C13	π	0.188
	C7	σ	0.964			
		π	0.677			
Δ(A, B)			0.407			

makes the distance between C1' and C2 (3.14 Å) to the same level as that between C1' and C1 (3.20 Å), the interaction between C1' and C2 being ferromagnetic as is also illustrated in Fig. 3. We therefore include both of these interactions in calculation of Eq. (2) assuming that the effective exchange interactions are the same. As a result, the value of Δ(A, B) is suppressed to be +0.407 while that for the same system without tilting is +0.775, signifying that the tilting of the stacking polymer reduces the antiferromagnetic interaction. This agrees with the experimental results in ref. 10, i.e., the triplet carbenes in the tilted array interact antiferromagnetically. However, it has also been claimed that the quinted state of these carbene pairs in this system is thermally attainable at low temperatures.

Conclusion

The electronic structures and magnetic properties of PDPC have been studied on the basis of the tight-binding crystal orbital method for various conformation. The ferromagnetic array of PDPC can appear in the stacked orientations of $\theta = 60°$ and 180° if the stacking condition in the solid state is adequately controlled. At the same time, it has been demonstrated that the unrestricted Hartree-Fock scheme proved to be able to handle the ferromagnetic polymer in a comparable manner to the Heisenberg model and give valuable information on the design of magnetic organic polymers.

References

1. A. A. Ovchinnikov, *Theor. Chim. Acta(Berl.)*, **47**, 297(1978).
2. N. Tyutyulkov, O. E. Polansky, P. Schuster, S. Karabunarliev, and C. I. Ivanov, *Theor. Chim. Acta(Berl.)*, **67**, 211(1985).
3. H. Iwamura and A. Izuoka, *J. Chem. Soc. Jpn.*, **1987**, 595.
4. J. S. Miller, A. J. Epstein, and W. M. Reiff, *Chem. Rev.*, **88**, 201(1988).
5. K. Tanaka, T. Shichiri, and T. Yamabe, *J. Mol. Structure (THEOCHEM)*, **188**, 313(1989).
6. K. Nasu, *Phys. Rev.*, B**33**, 330(1986).
7. H. M. McConnell, *J. Chem. Phys.*, **39**, 1910(1963).
8. A. Izuoka, S. Murata, T. Sugawara, and H. Iwamura, *J. Am. Chem. Soc.*, **107**, 1786(1985).
9. K. Yamaguchi, H. Fukui, and T. Fueno, *Chem. Lett.*, **1986**, 625.
10. T. Sugawara, H. Tukada, A. Izuoka, S. Murata, and H. Iwamura, *J. Am. Chem. Soc.*, **108**, 4272(1986).
11. R. C. Bingham, M. J. S. Dewar, and D. H. Lo, *J. Am. Chem. Soc.*, **97**, 1285(1975).
12. E. Ciliberto, K. A. Doris, W. J. Pietro, G. M. Reisner, D. E. Ellis, I. Fragalà, F. H. Herbstein, M. A. Patner, and T. J. Marks, *J. Am. Chem. Soc.*, **106**, 7748(1984).
13. J. Higuchi, *Bull. Chem. Soc. Jpn.*, **43**, 3773(1970).
15. C. A. Hutchison Jr. and B. E. Kohler, *J. Chem. Phys.*, **51**, 3327(1969).

Chapter 2

Crystal Orbital Study on Electronic and Magnetic Structures of Poly(*m*-aniline)

Introduction

Recently organic ferromagnetism has become of general interest and has attracted a great deal of attention of material scientists.[1] In order to synthesize ferromagnets from C, H, N and O with only 2*p*-orbitals, we must pay attention to the topology of molecular structures, because *p*-orbitals have at most three-fold degeneracy. Therefore, a class of organic polymers and oligomers having degenerate orbitals, or non-bonding molecular orbitals (NBMO) due to the topology of molecular systems has been investigated experimentally[2,3] and theoretically.[4-10] Poly(*m*-phenylcarbene) belongs to this class of polymers, and it has been shown by the application of various levels of calculation that the ground state with a very high spin multiplicity, that is, a ferromagnetic state is the most stable.[4,9,10] In fact, Iwamura and coworkers have succeeded the demonstration of a ferromagnetic alignment between the spins located on its oligomer chain by the magnetic susceptibility[2] and the ESR[3] measurements.

Previous theoretical studies on this type of molecules and polymers have mainly concentrated on the systems composed only of carbon and hydrogen atoms. For example, Klein et al.[6] have discussed the existence of high-spin hydrocarbons on the basis of the valence bond (VB) and the molecular orbital (MO) theories and so on. Moreover, Kouteck´y et al.[7] have examined the biradical character of various hydrocarbons by analyzing the natural orbitals

within the framework of the Pariser-Parr-Pople method. However, the first experimental report on the successful preparation of organic ferromagnets suggests that hetero atom such as nitrogen or oxygen in the π-conjugated systems play an important role as a spin supplier. For example, Korshak et al.[11] have prepared a ferromagnetic polymer containing a stable nitroxide radical (tetramethylpiperidine-N-oxyl) which has been reported to show spontaneous magnetization at low temperatures (4.2K). Torrance et al.[12] have also prepared a ferromagnetic compound by polymerizing triaminobenzene with iodine. Considering the structures of these polymers and traditional stable organic radicals such as diphenylpicrylhydrazyl (DPPH) and tetraphenylpyrrole radicals,[13] the spins located on the nitrogen site in the π-conjugated systems are rather stable and could be available for designing organic ferromagnets. From a theoretical viewpoint, Tyutyulkov et al.[14,15] have treated some potential ferromagnetic polymers containing hetero atom using the Hückel method.

Poly(*m*-aniline)[16,17] is an interesting material in relation to an approach to a possible ferromagnetic model-polymer. In particular, its cationic and dehydrogenated forms may well have free radicals interacting ferromagnetically owing to the topological backbone of the polymer. We have reported a synthetic method of poly(*m*-aniline) in the previous paper.[16] Moreover, we have concluded from the analysis of *g*-values in the ESR measurements that free radicals are actually created on the nitrogen sites of the cationic and the dehydrogenated forms of poly(*m*-aniline).[17] Although the bulk ferromagnetic properties have not been observed, its cationic and dehydrogenated forms attract interest toward the synthesis of an organic ferromagnet.

In the present work, we examine the electronic structure and the magnetic properties of poly(*m*-aniline) and its cationic and dehydrogenated forms using the one-dimensional tight-binding self-consistent-field crystal orbital (SCF-CO) method. The unrestricted Hartree-Fock (UHF) method was employed as one of the convenient tools available for clarifying the magnetic properties of the polymer systems in the ferromagnetic states artificially set up here.

The aim of this paper is first to find a plausibility of ferromagnetic states of both the cationic and the dehydrogenated forms from the energetical viewpoint and then to stress the comparison and relation between the electronic and magnetic properties of poly(*m*-aniline) and those of usual polyaniline, that is, poly(*p*-aniline).[18] In particular, we will show that the difference in the linkage of the aniline monomer between poly(*m*-aniline) and poly(*p*-aniline) remarkably affects their band structures and magnetic properties.

Method of calculation

The calculations were performed on the basis of the one-dimensional tight-binding SCF-CO method under the CNDO/2 approximation including all the valence electrons.[19,20] The geometrical structure of the neutral form was optimized by using the energy gradient method assuming the polymer skeleton being planar for simplicity.

Here, as a basic skeleton for ferromagnetic polymers, we considered the cationic and the dehydrogenated forms of poly(*m*-aniline), of which the spins are expected to align to show ferromagnetism. Although the electron extraction or the dehydrogenation could lead to a slight change in the geometry of the polymer, we tentatively employed the optimized geometry of the neutral form as the geometrical structure of the cationic and the dehydrogenated forms. The restricted Hartree-Fock (RHF) and the unrestricted Hartree-Fock (UHF) methods were used for the calculation of the non-magnetic states and the ferromagnetic states, respectively.

The unit cells for the polymers are shown in Fig. 1. Helical symmetry as well as translational symmetry was taken into account to describe these geometries. The values of the overlap integrals and the electron-repulsion integrals were considered as far as the fifth-nearest-neighboring cell. The number of the representative vectors was chosen as 21 with regular intervals ($\pi/10a$, where a is the unit vector of the translational symmetry or the helical

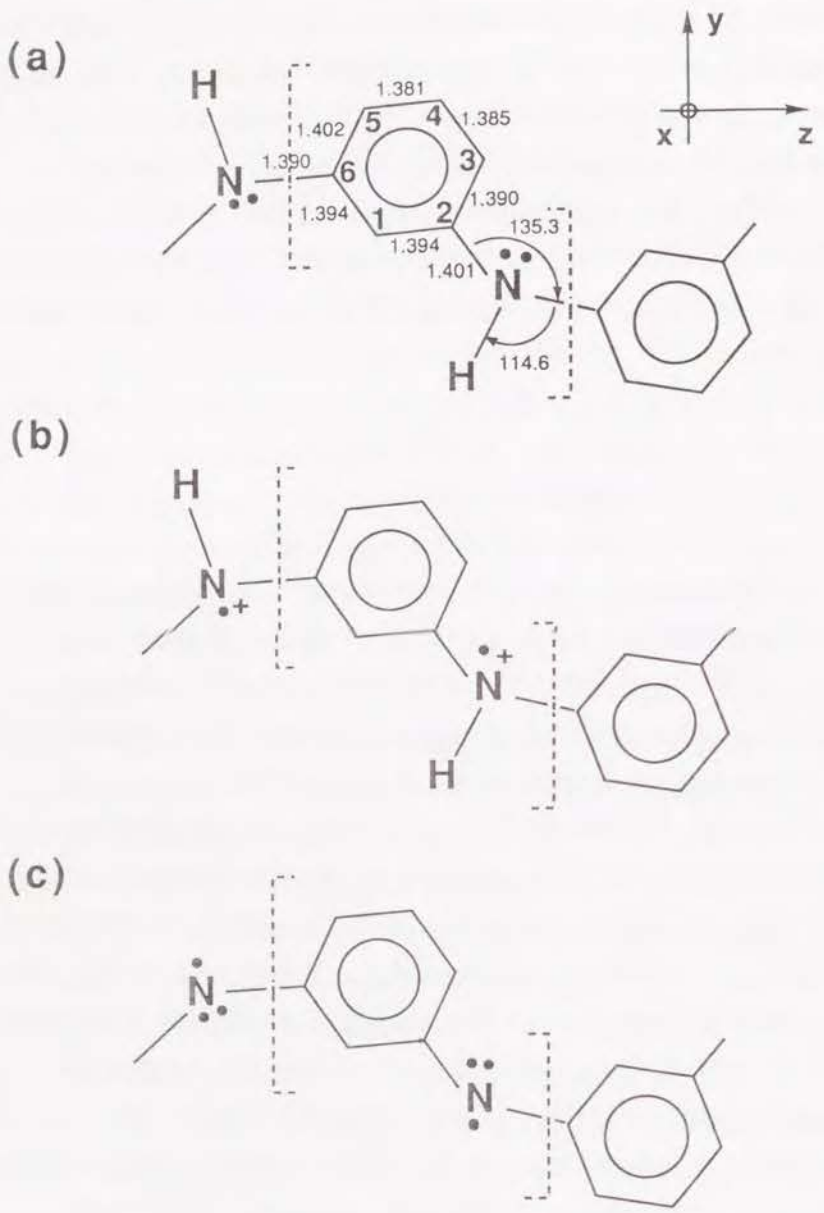

Fig. 1. Polymer skeletons and the coordinate axes employed for the present calculations. (a) neutral, (b) cationic, and (c) dehydrogenated forms of poly(*m*-aniline). The unit cell is bracketed. Bond lengths and bond angles are designated in Å and degree, respectively.

symmetry) in the Brillouin zone. The band levels are drawn in the reduced zone with $0 \leq k \leq \pi/a$.

Results and discussion

Band structures of the neutral forms of poly(m-aniline) and poly(p-aniline)

The band levels and the density of states (DOS) for the neutral form of poly(*m*-aniline) obtained by the RHF method are shown in Fig. 2. The band structure gives a background that this polymer is insulating, because there is a considerably large band gap between the highest occupied (HO) band and the lowest unoccupied (LU) band. Although the HO band is of π-nature, the band width is 1.27 eV being considerably narrow in contrast with that of poly(*p*-aniline). Considering these results, the conduction carriers will be rather hard to move because of this narrow band width and, therefore, poly(*m*-aniline) would not become a good electrical conductor like poly(*p*-aniline).[18]

The calculation was also performed on poly(*p*-aniline) with a reduced structure, what is called a leucoemeraldine form[18] in the same manner. The calculated band gap and the band width of the HO band for the neutral, the cationic and the dehydrogenated forms of poly(*m*-aniline) and neutral poly(*p*-aniline) are listed in Table I. Since the Hartree-Fock theory usually overestimates the band gap,[21] we should empirically use a 1/3 to 1/4 value of the calculated gap for the estimation of the actual gap. Accordingly, the actual band gaps for poly(*m*-aniline) and poly(*p*-aniline) are estimated to be 4.6-3.4 and 4.1-3.1 eV, respectively.

We also find in Table I that the difference in the topology of the polymer system remarkably affects the HO band width; poly(*m*-aniline) has a extremely narrow band compared with poly(*p*-aniline). The band width is usually determined by the interaction between the unit cells, especially by the overlap of the atomic orbitals (AO). Here we realize that what determines the HO band width is how the phenyl rings are connected by nitrogen, because

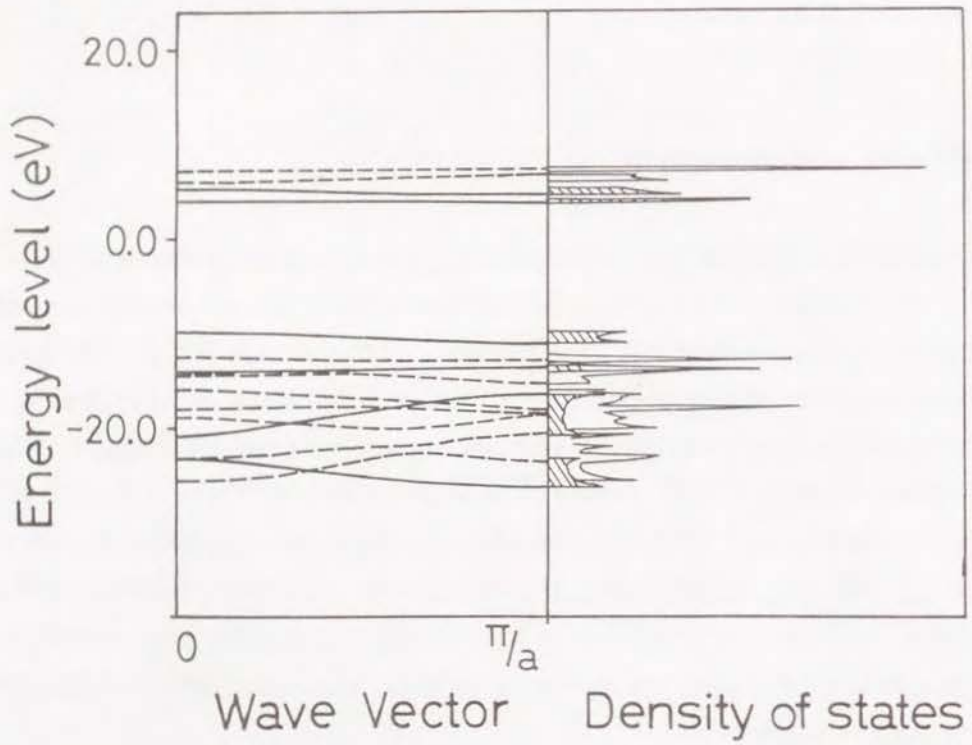

Fig. 2. The band structure of the neutral form of poly(*m*-aniline) calculated by the RHF method. Solid and dotted lines indicate π and σ bands, respectively. The density of states (DOS) is shown together, where the hatched area indicates the π DOS.

Table I. Calculated band gap and HOCO band width (in eV).

	poly(*m*-aniline)	poly(*p*-aniline)
Band gap	13.70	12.20
Band width		
Neutral form	1.27	5.10
Cationic form	1.59	-
Dehydrogenated form	0.98	-

Table II. Total energies (in eV) per unit cell of the ferromagnetic state and the non-magnetic state in the cationic and the dehydrogenated forms of poly(*m*-aniline). Two aniline units form the unit cell in these calculations.

	Cationic form	Dehydrogenated form
Ferromagnetic	-3131.981	-3116.304
Non-magnetic	-3129.321	-3112.188

the nitrogen is considered to greatly contribute to the HO crystal orbital(HOCO). We therefore consider that the HO band width of poly(*m*-aniline) is mainly determined by the NBMO-like orbital, as will be discussed below. Considering the results obtained about the HO band width, the difference between poly(*m*-aniline) and poly(*p*-aniline) comes only from the topology of the linkage of the aniline monomers.

Magnetic properties of the cationic and the dehydrogenated forms of poly(m-aniline)

First we performed the comparison of the total energies with respect to the ferromagnetic and the non-magnetic states, the result of which is listed in Table II. We see that the ferromagnetic states are energetically more stable than the non-magnetic states for both the cationic and the dehydrogenated forms. We have not shown here the antiferromagnetic state for these forms on account of technical difficulty in performing the present mean-field-type calculation. Based on these examinations, we therefore assume that these two forms take the ferromagnetic states hereafter.

The band levels of the cationic and the dehydrogenated forms of poly(*m*-aniline) obtained by the UHF method with the unit cell consisting of one aniline unit are shown in Figures 3(a) and 3(b), respectively. We find that the feature of the neutral ground state remains in these two forms and, consequently, these two forms give very similar band structures. The ferromagnetic bands (the HO α-spin bands) of the cationic and the dehydrogenated forms are 1.59 eV and 0.98 eV in width, respectively. The bands are so flat like in the neutral form that the magnetic spins will be localized spatially.

These narrow bands give the physical background for a macroscopic spin alignment,[15] and they are considered to stem from the contribution of the NBMOs as a consequence of the topological backbone of the polymer as explained in what follows. Here let us consider the band levels from a viewpoint of the orbital patterns of the HOCO. The orbital patterns of the HO bands for the three forms at $k = 0$ and $k = \pi/a$ are shown in Fig. 4. One

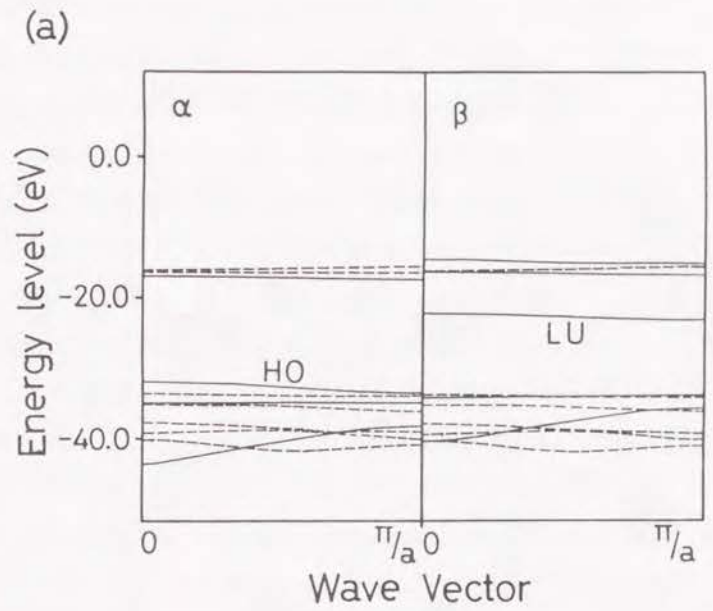

Fig. 3. The band structures of (a) the cationic and (b) the dehydrogenated forms of poly(*m*-aniline) calculated using the UHF method. α and β signify the up- and the down-spin bands, respectively.

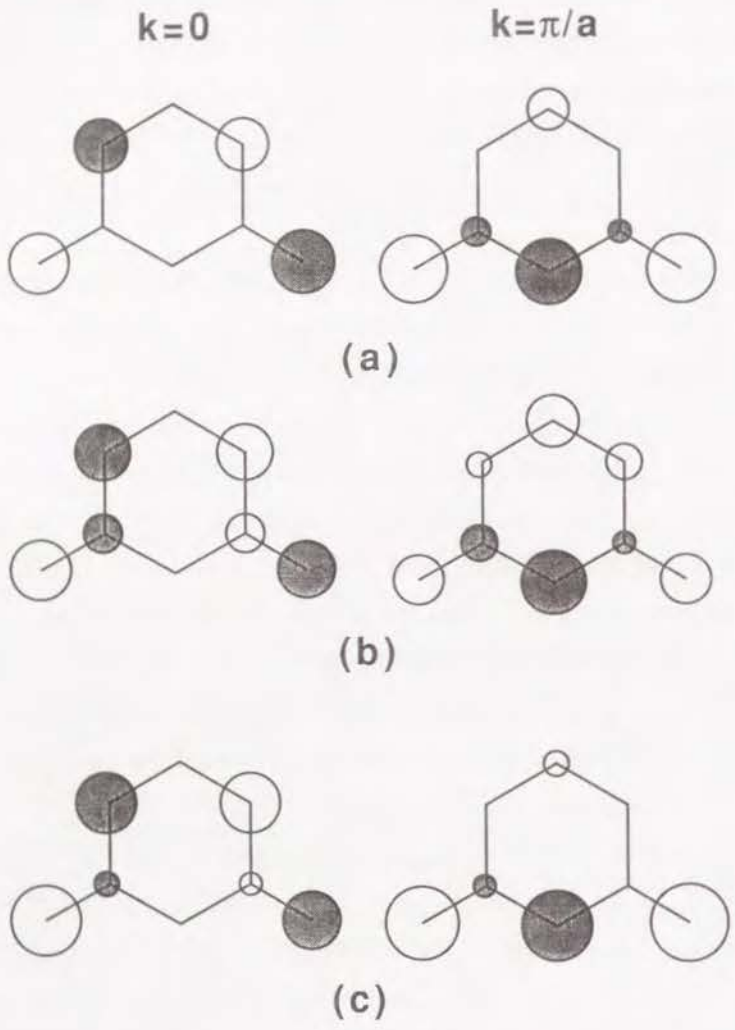

Fig. 4. Orbital pattern of the HOCO at $k = 0$ and π/a of (a) the neutral, (b) the cationic and (c) the dehydrogenated forms of poly(*m*-aniline). Round marks in the patterns indicate the phase and magnitude of π-AO coefficients.

can see that the patterns are different at $k = 0$ and $k = \pi/a$ and that those for the cationic and the dehydrogenated forms are very similar to the neutral one. The orbital patterns of the NBMOs of *meta*-quinodimethane biradical (C_{2v} symmetry) consisting of two degenerate orbitals (a_2 and b_1) are also shown in Figure 5 for the sake of comparison. The patterns of these two orbitals are very similar to those of the HOCO at $k = 0$ and $k = \pi/a$, respectively. If nitrogens are substituted for the starred carbons in this biradical, the degeneracy of these NBMOs is removed and the eigenenergy of the a_2 orbital becomes slightly higher than that of the b_1 orbital within the framework of the Hückel method. The energy level of the HOCO similarly goes down slightly with change in k from 0 to π/a. The dehydrogenated form has the narrowest HO band width 0.98 eV of the three, because the orbital patterns of the dehydrogenated form are most similar to the two degenerate molecular orbitals of *meta*-quinodimethane biradical. Comparing the HOCO patterns with the NBMOs of *meta*-quinodimethane biradical, we realize that the nature of the HO bands of the three forms of poly(*m*-aniline) are clearly constructed from the NBMOs.

Let us now look at the spin density distributions for the cationic and the dehydrogenated forms of poly(*m*-aniline) listed in Table III. Although the up-spin is mainly located on the nitrogen atom in the two radical forms of poly(*m*-aniline), considerable amount of spin flows into the benzene ring through spin polarization effect,[22] by which positive and negative spin densities appear alternately in the two forms. From this alternation of the spin density, the nature of the spin alignment should be called ferrimagnetic rather than ferromagnetic following the definition, because there are two spin sublattices in the magnetic structure.

From the electron spin resonance (ESR) measurement, we have reported that the *g*-values of the cationic and the dehydrogenated forms are 2.0038 and 2.0044 at 77 K, respectively.[17] The ESR results suggest that spin is more concentrated on the nitrogen site in the dehydrogenated form than in the cationic form. As shown in Table III, the calculated results agree well with such experimental results. Spins are considered to flow out more explicitly

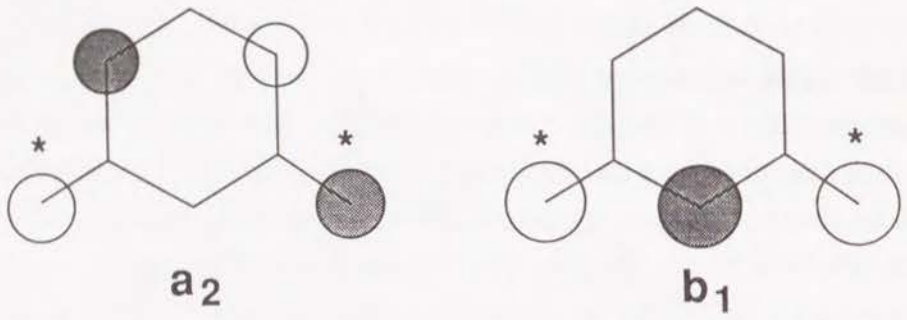

Fig. 5. Two degenerate NBMOs of *meta*-quinodimethane biradical. See the caption of Fig. 4.

Table III. Calculated spin densities of the cationic and the dehydrogenated forms of poly(*m*-aniline).

Atom	Cationic form	Dehydrogenated form
C_1	0.25	0.26
C_2	-0.09	-0.15
C_3	0.20	0.23
C_4	-0.10	-0.12
C_5	0.21	0.23
C_6	-0.10	-0.15
N	0.63	0.71

in the cationic form in association with the delocalization of a positive charge created in the lone pair of the nitrogen.

On the basis of the valence bond picture, one can illustrate for example the principal resonance structures as shown in Fig. 6. From Table IV, spin flows into the benzene rings more remarkably in the quinoid structures, (a) and (c). However, these quinoid structures are energetically less stable than the benzenoid ones and these resonance forms would not much contribute to the actual molecular structure accordingly.

Substituent effect

To examine the substituent effect on the magnetic property of the cationic form of poly(*m*-aniline), we consider fluorine introduced to each position as shown in Fig. 7. The standard bond length[23] was employed for the calculations. The obtained spin densities of these substituted cationic forms are not so different from those of the non-substituted one. However, we find that the HO band width largely depends on the substituted position as seen in Table V. Here let us again look at the orbital patterns shown in Figure 4 in order to analyze the substituent effect. On the basis of the result of the calculations, we see that the $p\pi$-orbital of the substituent interacts with the $p\pi$-orbital of the substituted carbon with out-of-phase in the HOCO pattern. Therefore, the orbital having a larger AO coefficient at the substituted position becomes unstable. Introducing substituents to the position 1 in Fig. 7, the energy level of the HOCO at $k = \pi/a$ is unstabilized; on the contrary, introducing substituents to the position 3 and 5, that at $k = 0$ is unstabilized. Consequently, the HO band width becomes narrower in the former case and wider in the latter case, since the energy level at $k = 0$ is higher than that at $k = \pi/a$ in the nonsubstituted poly(*m*-aniline) (see Figure 2). If a narrow band is really appropriate for the realization of macroscopic spin alignment,[15] introduction of the substituent to the position 1 can improve the magnetic properties of this polymer.

Substituted in position 4, on the other hand, a new CO with NBMO nature comes out as a result of the topological backbone similar to Torrance's

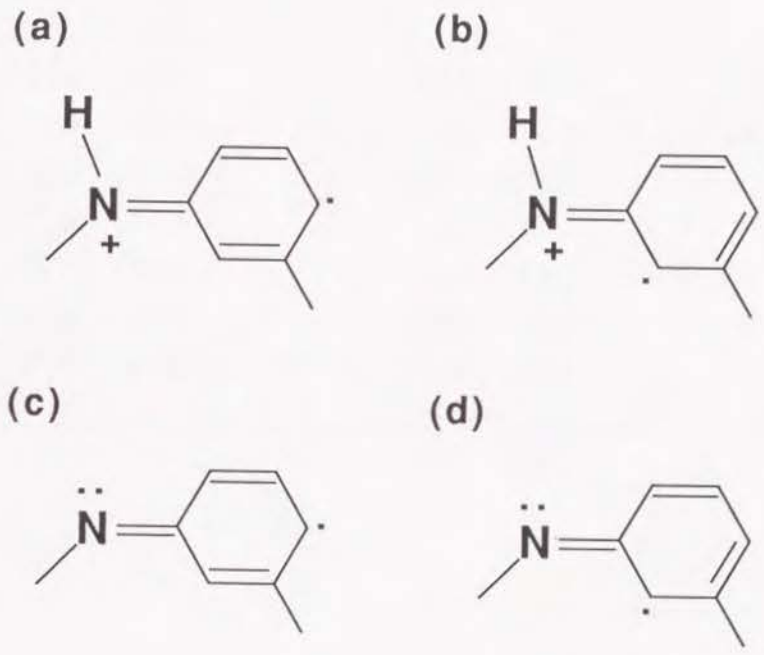

Fig. 6. Resonance structures of poly(*m*-aniline).

Table IV. Spin densities of resonance structures for cationic and dehydrogenated poly(*m*-aniline).

Atom	Cationic form (a)	(b)	Dehydrogenated form (c)	(d)
C1	0.26	0.27	0.29	0.27
C2	-0.11	-0.10	-0.15	-0.14
C3	0.37	0.23	0.37	0.25
C4	-0.12	-0.11	-0.13	-0.13
C5	0.20	0.18	0.24	0.20
C6	-0.07	-0.09	-0.20	-0.16
N	0.48	0.62	0.58	0.70

Table V. The HO band width of the cationic forms of poly(*m*-aniline) substituted by fluorine.

Non-substituted	I	II	III	IV
1.54	0.93	1.76	0.80	2.00

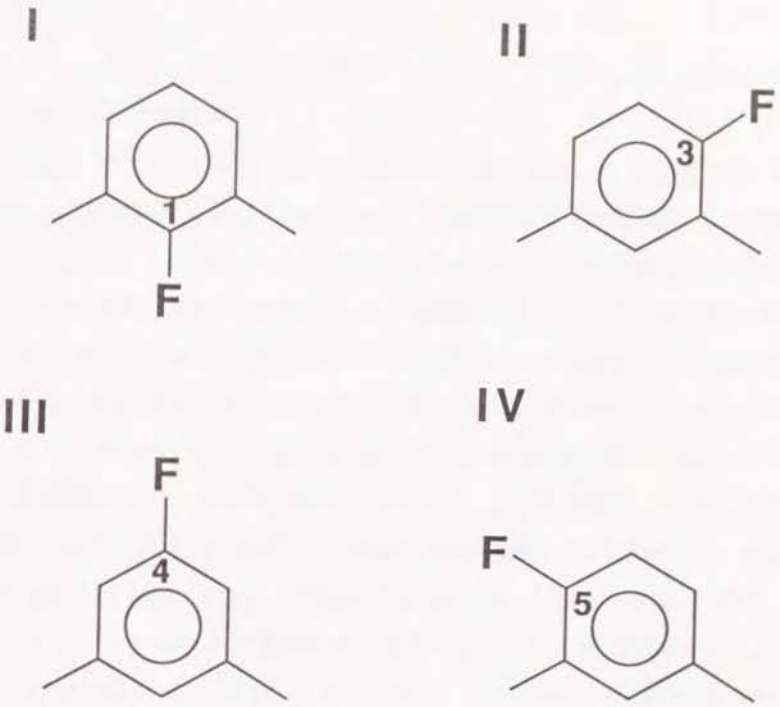

Fig. 7. Poly(*m*-aniline) substituted by fluorine.

polymer[12] with three-fold symmetry. The appearance of this CO would therefore contribute more largely to the narrowing of the HO band.

Conclusion

The electronic structure and the magnetic properties of the neutral, the cationic and the dehydrogenated forms of poly(*m*-aniline) have been examined using the one-dimensional tight-binding SCF-CO method under the CNDO/2 approximation. The band gap of poly(*p*-aniline) is smaller than that of poly(*m*-aniline) and, moreover, the band width of poly(*p*-aniline) is wider than that of poly(*m*-aniline). These results give a physical basis that poly(*p*-aniline) is more interesting in electrical conductivity rather than in magnetic properties, as we know from a large number of experimental investigations on poly(*p*-aniline). On the other hand, poly(*m*-aniline) has a narrow HO band. The narrow band and the topology suggest that poly(*m*-aniline) is adequate for a basic skeleton of a ferromagnetic polymer. The difference in the electronic and the magnetic properties is only due to the topology of the linkage of the aniline monomers.

In particular, we have discussed the magnetic properties of poly(*m*-aniline) associated with the possibility of an organic ferromagnet. It has been concluded that the ferromagnetic state would be energetically more favorable than the non-magnetic state in the cationic and the dehydrogenated forms. We have also clarified that the spin density distribution of the cationic and the dehydrogenated forms of poly(*m*-aniline) shows a ferrimagnetic nature in spin alignment. The spin is mainly located on nitrogen, but a considerable amount of spin also flows into the benzene ring through the spin polarization mechanism. Furthermore, the calculated result shows that a larger amount of spin is concentrated on nitrogen in the dehydrogenated forms than in the cationic forms. These results are in agreement with *g*-values observed with the ESR measurement.

Furthermore, on the basis of the analysis of the two degenerate molecular

orbitals of a *meta*-quinodimethane biradical, we have examined that the HO bands of the three forms of poly(*m*-aniline) consist of NBMOs. Moreover, we have found that the band width and the magnetic properties can be controlled by introducing substituents to the benzene ring. It is concluded that the cationic and the dehydrogenated forms of poly(*m*-aniline) are a potential organic ferromagnet.

References

1. See, for example, Proceedings of the Symposium on Ferromagnetic and High Spin Molecular Based Materials, 197th National American Chemical Society Meeting in Dallas, TX. J. S. Miller and D. A. Dougherty, Ed., *Mol. Cryst. Liq. Cryst.*, **176**, (1989)
2. T. Sugawara, S. Bandow, K. Kimura, H. Iwamura, and K. Itoh, *J. Am. Chem. Soc.*, **108**, 368(1986).
3. Y. Teki, T. Takui, K. Itoh, H. Iwamura, and K. Kobayashi, *J. Am. Chem, Soc.*, **108**, 2147(1986).
4. N. Mataga, *Theor. Chim. Acta(Berl.)* , **10**, 372(1968).
5. A. A. Ovchinnikov, *Theor. Chim. Acta(Berl.)*, **47**, 297(1978).
6. D. J. Klein, C. J. Nelin, S. Alexander, and F. M. Matsen, *J. Chem. Phys.*, **77**, 3101(1982)
7. J. Kouteck´y, D. Dohnert, P. E. S. Wormer, J. Paldus, and J. Čížek, *J. Chem. Phys.* **80**, 2244(1984).
8. N. Tyutyulkov, O. E. Polansky, P. Schuster, S. Karabunarliev, and C. I. Ivanov, *Theor. Chim. Acta(Berl.)*, **67**, 211(1985).
9. K.Nasu, *Phys. Rev.*, B**33**, 330(1986).
10. K. Tanaka, T. Shichiri, and T. Yamabe, *J. Mol.Struct.(Theochem)*, **188**, 313(1989) .
11. Y. V. Korshak, T. M. Medvedeva, A. A. Ovchinnikov, and V. N. Spector, *Nature*, **326**, 370(1987).
12. J. B. Torrance, S. Oostra, and A. Nazzal, *Synth. Met.*, **19**, 709(1987).
13. S. H. Pine, *Organic Chemistry*; McGraw-Hill, New York, 1987.
14. N. N. Tyutyulkov, C. I. Ivanov, I. Schopov, O. E. Polansky, and G. Olbrich, *Int. J. Quantum Chem.*, **34**, 361(1988).
15. N. N. Tyutyulkov, S. H. Karabunarliev, and S. I. Tsonchev, *Synth. Met.*, **32**, 51(1989).
16. K. Yoshizawa, K. Tanaka, and T. Yamabe, *Chem. Lett.*, **1990**, 1331.
17. K. Tanaka, K. Yoshizawa, A. Takata, and T. Yamabe, J. Yamauchi, *Synth. Met.*, **43**, 3297(1991).

18. See, for example, a historical survey on polyaniline, E. M. Geniès, A. Boyle, M. Lapkowski, and C. Tsintavis, *Synth. Met.*, **36**, 139(1990) and references therein.
19. J. M. André, J. Ladik, and J. Delhalle, *Electronic Structures of Polymers and Molecular Crystals*; Plenum, New York, 1975, p. 23.
20. A. Imamura and H. Fujita, H. *J. Chem. Phys.*, **61**, 115(1974).
21. M. Kertész, *Adv. Quantum Chem.*, **15**, 161(1982).
22. K. Yamaguchi, Y. Toyoda, and T. Fueno, *Synth. Met.*,**19**, 81(1987).
23. J. A. Pople and D. L. Beveridge, *Approximate Molecular Orbital Theory*; McGraw- Hill, New York, 1970.

PART III

SYNTHESIS AND MAGNETIC PROPERTIES OF POTENTIAL FERROMAGNETIC POLYMERS

INTRODUCTION

In this part, synthesis and a series of magnetic properties measurements of potential ferromagnetic polymers are discussed on the basis of the molecular design treated in the previous part.

It can be expected that conjugated polymers containing hetero atoms will be stable systems as a result of additional conjugation energy. In fact, most stable radicals are located on hetero atoms in π-conjugated systems, for example, 1,1'-diphenyl-2-picrylhydrazyl (DPPH) and tetraphenylpyrrole radicals and many other cation radicals of dyes. It is shown that the theorem of Coulson, Rushbrooke, and Longuet-Higgins mentioned in Part II can be expanded to conjugated systems containing nitrogen or oxygen. Therefore it is interesting for designing ferromagnetic polymers to construct a polymer from hetero atoms in π-conjugated systems as stable spin suppliers.

In Chapter 1 (*Synth. Met.*, **39**, 103(1990) and *J. Chem. Phys.*, **94**, 6868(1991)), the results of the magnetization and electron spin resonance (ESR) measurements of the simplest members of alkylene-aromatic polymers (AAP) have been described. In contrast with the previous claim of the observation of ferromagnetism, a distribution of the spin alignment giving $1 < S < 3/2$ on the average has been concluded from the magnetization measurement. The spin concentration certainly coming from carbon π spins has turned out to be relatively small (10^{17}-10^{18} spins•g^{-1}). The ESR observation has revealed a forbidden $\Delta m_s = \pm 2$ transition characteristic of a triplet or higher multiplet state of radical pairs in agreement with the observation of the local spin alignment. The relationship between the spin state and the chemical structure of AAPs has also been examined with the use of the ^{13}C NMR spectroscopy. It is concluded that in the present material there is a ferromagnetic coupling between a few of spins such as triphenylmethyl radicals forming spin clusters of triplet or higher spin multiplet state diluted in the whole bulk.

In Chapter 2 (*Chem. Lett.*, **1990**, 1311), synthesis of poly(*m*-aniline) is performed from *m*-chloroaniline using copper (I) chloride. A reddish-orange

colored polymer was confirmed to have a structure in which an aniline unit is linked in *meta*-positions judging from three C-H out-of-plane deformation modes at 840, 770, and 685 cm^{-1} in the infrared spectrum.

In Chapter 3 (*Synth. Met.*, **43**, 3297(1991)), it is confirmed from the *g*-values of the ESR that free radicals are actually created on nitrogen atoms in the cationic and dehydrogenated forms of poly(*m*-aniline) obtained from the method described in Chapter 2. The spin concentration has been estimated to be in the order of 10^{18}-10^{19} spins•g^{-1}, being relatively small probably due to the low molecular weight of the oligomer examined.

In Chapter 4 (*Chem. Mater.*, submitted), the synthetic method of poly(*m*-aniline) is improved on the basis of the method described in Chapter 2. The polymerization of *m*-bromoaniline using copper (I) iodide and potassium carbonate on the basis of the Ullmann reaction is described. An extreme loss of bromine was detected in the obtained polymer by elemental analysis and ESCA. The reaction is hence based on dehydrobromination although it is considered to proceed via a rather complex free-radical process. The polymer obtained is confirmed to have a poly(*m*-aniline) structure which is of interest as a basic skeleton toward an organic ferromagnetic polymer. The preliminary magnetic-property measurements, the existence of ferromagnetic coupling of the spins is suggested in the present materials.

In Chapter 5 (*J. Chem. Phys.*, submitted), the results of ESR and magnetic susceptibility measurements of poly(*m*-aniline) are presented. Ferromagnetic interaction among the spins in poly(*m*-aniline) is suggested on the basis of these measurements. From the *g*-value analysis, these spins are found to be localized on nitrogens although they are in some degree delocalized on phenyl rings. Doping of this polymer with iodine leads to an increase in the spin concentration up to 10^{20} spins•(g-polymer)$^{-1}$. Saturation magnetization of 0.30 emu•G•g^{-1} and spin clusters of $S = 1$ are observed in the iodine-doped polymer from the temperature- and field-dependence of the magnetization. Through-bond-interaction, depending on the topology of a polymer skeleton, is considered to operate between rather distant spins through the spin-polarization with antiferromagnetic array of the phenyl rings.

Chapter 1

Magnetic Properties of Simple Alkylene-aromatic Polymers

Introduction

In recent years, organic ferromagnetism has been attracting a considerable attention from both the theoretical and the experimental points of view.[1-4] For instance, Torrance et al.[5,6] have claimed that the iodine complex of poly(1,3,5-triaminobenzene) showed ferromagnetism up to 400°C, near which the material was decomposed. Ovchinnikov et al.[7] have reported that pyrolized polyacrylonitrile showed ferromagnetic behavior with Curie temperature of 480°C and saturation magnetization around 200 G•g^{-1}. Moreover, Ota et al.[8-10] have reported that heat-treated polycondensate of fused polynuclear aromatics (COPNA) resin prepared from pyrene and terephthalaldehyde or benzaldehyde indicated ferromagnetic behavior with saturation magnetization of 0.12-0.18 G and coercive force of 40-65 Oe.

To the authors' present knowledge, however, all of these studies suffer from poor reproducibility of the ferromagnetic property and relatively little has been known about the spin state for what are called organic ferromagnets. Moreover, Aleksandrova et al.[11] have claimed that the ferromagnetic behavior observed in pyropolymers can be explained by the presence of impurity iron in the polymer matrix, being undetectable by the usual atomic absorption analysis.

The COPNA resins ought to be more generally called alkylene-aromatic polymers (AAPs), because this kind of resin originally consists of condensed aromatic nuclei cross linked with methylene bridges. These AAPs are

obtained by the final heat treatment at relatively low temperature such as 200°C after the polymerization process. Elevation of the treatment temperature up to 500°C will increase the spin concentration and yield the ordinary paramagnetism as has been reported with respect to polyacenic semiconductive materials.[12]

Meanwhile, we have already confirmed[13] by the electron spin resonance (ESR) measurement over the wide magnetic-field range that the spin state of a typical AAP prepared from pyrene and benzaldehyde is free from metallic ferromagnetic impurity. It has been assigned that the spins in this material are of π type possibly occurring in the triarylmethyl radicals involved in the resin skeleton. Furthermore, in our preliminary report,[14] we have shown a possible existence of not a ferromagnetic state but a locally ordered spin state equal to or higher than the triplet state on the average through the magnetization measurement of the simplest AAPs prepared from resorcinol and terephthalaldehyde and benzaldehyde. The aim of the present paper is to complete the report of the magnetic properties of these AAPs based on the magnetization and the ESR analyses together with the chemical structure of AAPs based on the ^{13}C nuclear magnetic resonance (NMR) measurement.

Experiment

The precursors of the simplest AAP samples were prepared by catalytic dehydration of resorcinol/benzaldehyde (1/1.5 in molar ratio; labeled RBA) and resorcinol/terephthalaldehyde (1/0.8 in molar ratio; RTA) in benzene and methanol solvents, respectively, as shown in Fig. 1. Methanesulfonic acid was used as a catalyst. The RBA sample was preheated at 200 °C for 15 min and then once dissolved in tetrahydrofuran, whereas the RTA was dried at 110 °C for 1h. Both of these pretreated specimen were further heat treated at 200 °C in N_2 atmosphere for 2h. The content of metallic ferromagnetic impurities such as Fe, Co, and Ni in both the starting materials and the sample products were checked by x-ray fluorescence analysis. Their

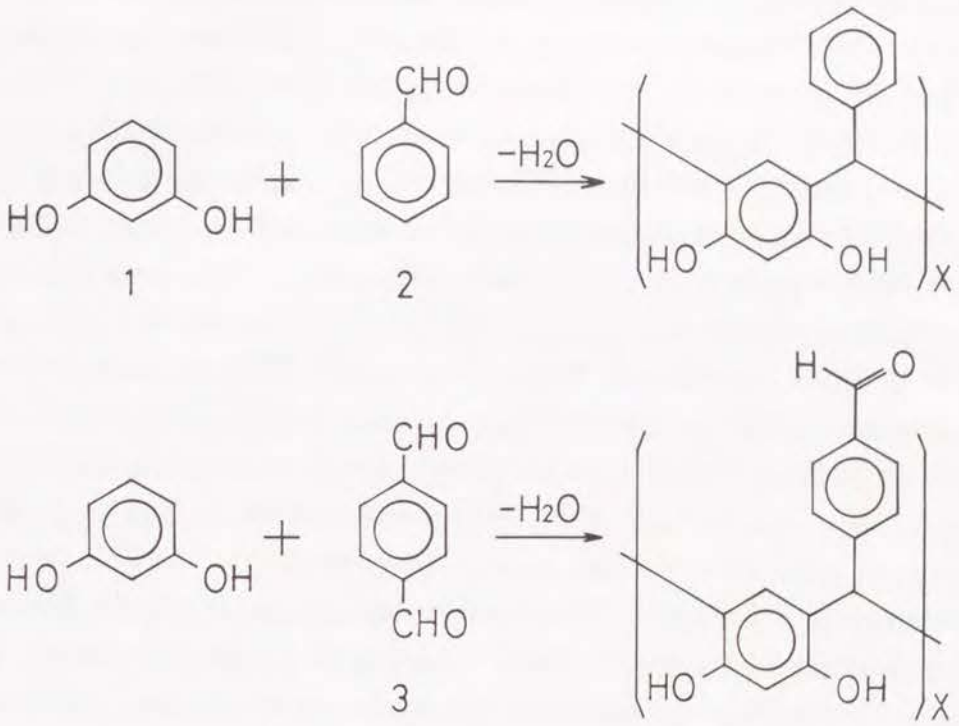

Fig. 1. Synthetic method of RBA and RTA. (1) resorcinol, (2) benzaldehyde, and (c) terephthalaldehyde.

contents were confirmed to be less than the lowest limit of detection. Furthermore, the ESR measurement scanning the range of 1000-3500 G did not detect typical ferromagnetic impurities such as transition metal oxide.

The ^{13}C NMR spectra of RBA in $(CD_3)_2SO$ solution were measured on JEOL FX100 in order to analyze the fundamental skeleton of AAPs. Tetramethylsilane (TMS) was used as a reference. Measurements of the magnetization and the magnetic susceptibility were performed using an Oxford's Faraday-type magnetic balance. A quartz cell was stuffed with the AAP sample powder (80 mg), and then liquid paraffin (80 mg) was added to fix the powder. The magnetization (M) curves were recorded at 4.5, 77, and 260 K up to the magnetic field (H) of 5.1 T. The correction of the diamagnetism of the quartz cell and liquid paraffin was performed as usual. The magnetic susceptibility was measured in the temperature range 4.2-260 K under the magnetic field of 1 T. Detailed prescription inherent in the magnetic susceptibility measurement is described later. The ESR spectra were recorded on a Varian E-112 spectrometer equipped with an Air Product liquid-helium-flow cryostat at the X band with the field modulation of 100 kHz. The as-prepared AAP sample powder was put into a 4.75 mm o.d. quartz tube. The sample tube was evacuated down to less than 10^{-4} Torr for 2 h and then charged with high purity helium gas (99.9999 %) as a heat medium up to 10 Torr before sealing. A Mn^{2+}/MgO solid solution was used as a reference for the g-value and the magnetic field calibration. The spin concentration was determined using $CuSO_4 \cdot 5H_2O$ as a standard. The 100 kHz field-modulation width was kept less than 25 % of the peak-to-peak linewidth (ΔH_{pp}).

Results and discussion

Structure

Table I lists the results of the elemental analysis for the RBA and RTA samples. The [H]/[C] and [O]/[C] molar ratios roughly agree with the

product-sample models illustrated in Fig. 1. The ^{13}C NMR spectrum for RBA resin before the final heat treatment and its simulation[15] are shown in Fig. 2. We assume an oligomeric structure for the simulation shown in the inset of Fig. 2(b) because resorcinol is a typical *ortho*-, *para*-directing reagent. In general it is difficult to analyze oligomers with the NMR spectroscopy; in the present study, however, the spectrum and the simulation agree fairly well. We consider that the AAPs treated at 200 °C also contain triphenylmethyl parts in their skeletons, where the hydrogen at that part would be easily eliminated driven by both the steric hindrance and the stability of the generated radical itself.[16] Thus the structures containing triphenylmethyl radicals illustrated in Fig. 3 are expected to be partially involved in RBA and RTA. Considering the topological linkage and the spin order in such polymer backbone (see Fig. 3), these radical spins will interact ferromagnetically with one another in some cases.

Magnetization and magnetic susceptibility

The magnetization curves of the RBA and RTA samples are shown in Fig. 4, in which ferromagnetic behavior is not observed. The saturation of magnetization did not appear up to 5.1 T for the present samples. The magnetization for paramagnetic species is a function of applied field and temperature, which is theoretically represented by

$$M(H, T) = N_s g \mu_B J B_J(J g \mu_B H / k_B T), \quad (1)$$

where $B_J(x)$ is the Brillouin function, N_s the spin concentration, g-the Landé g factor, μ_B the Bohr magneton, J ($= L + S$) the total angular momentum quantum number, and k_B the Boltzmann constant. Here we assume L (total orbital angular momentum quantum number) to be zero as for usual organic radical spins and, hence, J is reduced to S (total spin quantum number). Since N_s and J ($= S$) in Eq. (1) are unknown, the $M(H, T)$ curves for S = 1/2, 1, and 3/2 were forced to encounter the experimental data at 2 T for the Brillouin fitting to find the average values of S of the samples. It is obvious

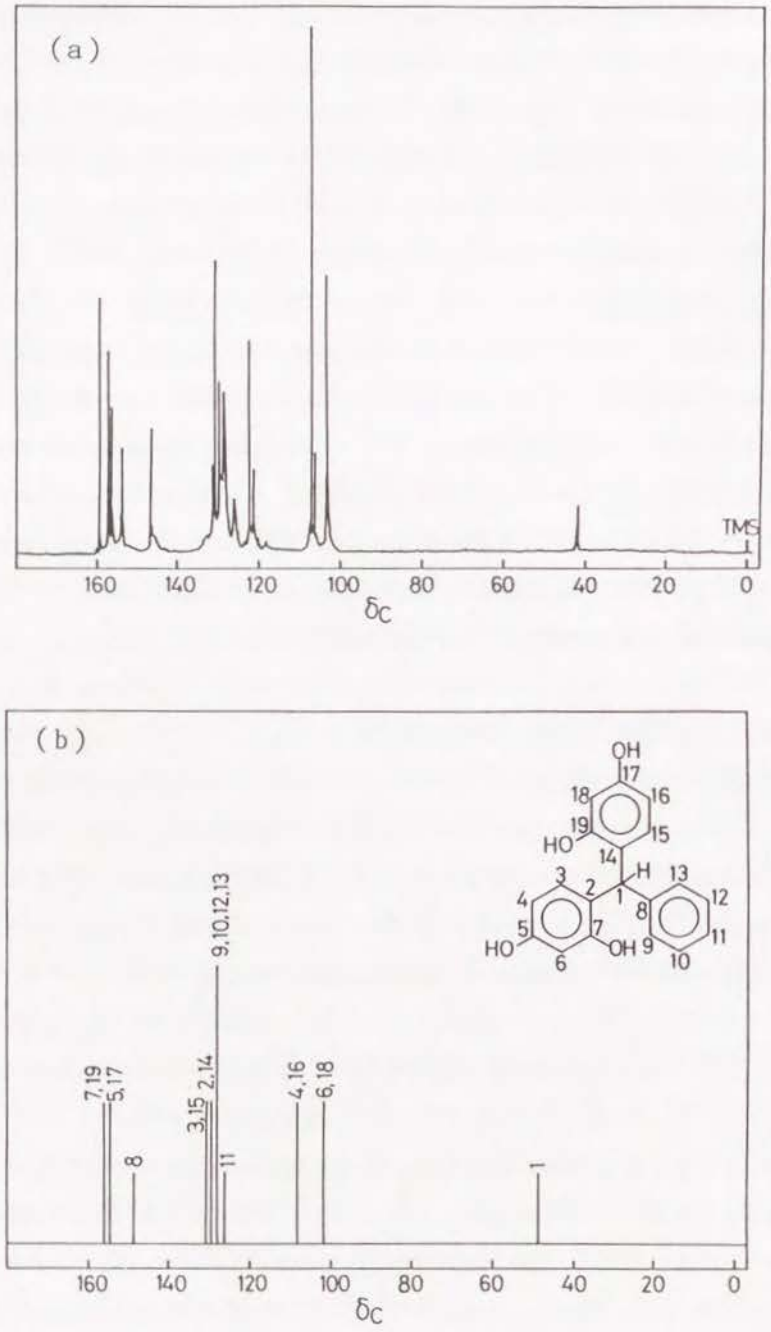

Fig. 2. ^{13}C NMR spectrum for (a) RBA resin before heat treatment and (b) its simulation. The signal of $(CD_3)_2SO$ solution is omitted from (a).

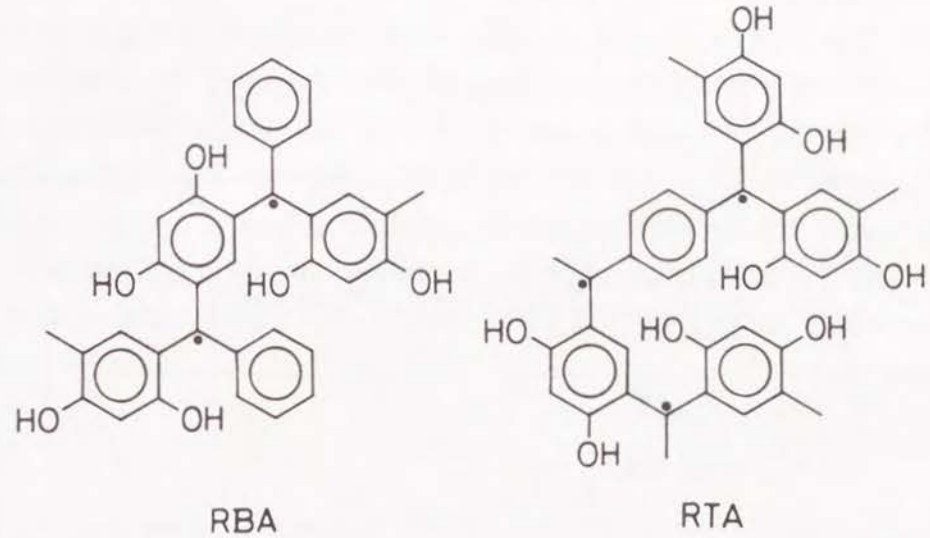

Fig. 3. Model of the local spin alignment among the triphenylmethyl radicals existing in AAPs.

from this simulation in Fig. 4 that there is weak and local spin alignment with $1 < S < 3/2$. This suggests that there is some distribution of the spin alignment with different S values in the present sample in addition to the conventional value of $S = 1/2$.

The magnetic susceptibilities measured can be divided into the temperature-independent diamagnetic term (χ_{dia}) and the temperature-dependent one after usual procedure. That is, χ_{dia} was determined from the gradient of the χT vs T plot. The latter temperature-dependent term was assumed to comply with the Curie-Weiss law as in general, and the Curie (C) and the Weiss (θ) constants were determined from the gradient and the intercept of the $1/(\chi - \chi_{dia})$ vs T plot, respectively. These relationships are expressed by

$$\chi = \chi_{dia} + C/(T - \theta). \tag{2}$$

The Curie-type spin concentration (N_C) was determined from the following formula:

$$C = N_C g^2 \mu_B^2 S(S + 1)/3k_B. \tag{3}$$

The value of S in Eq. (3) was set to that determined from the magnetization curve for each sample (= 1). All of the magnetic data are listed in Table II.

On the basis of the result of the magnetization curves, the existence of a local interspin interaction between a few of triphenylmethyl radicals with ferromagnetic coupling as illustrated in Fig. 3 is concluded. Since the structure of AAP is somewhat similar to that of the ferromagnetic model proposed by Mataga,[17] the nearest-neighboring radicals could magnetically couple as stated above. The Curie-type spin concentrations observed in the present samples are in the order of 10^{17} - 10^{18} spins•g^{-1} being very small, the order of which well agree with that obtained by the ESR measurement as described below. Difference in Curie constants or in spin concentrations of RBA and RTA certainly comes from that of the skeletons shown in Fig. 3,

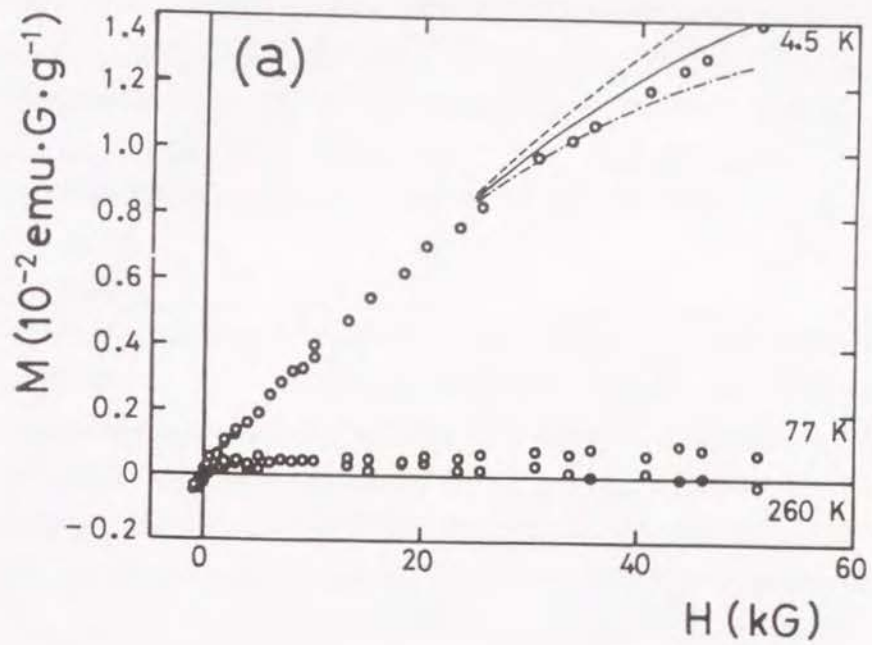

Fig. 4. Magnetization curves for (a) RBA and (b) RTA samples (indicated by circles) at 4.5, 77, and 260 K. Those based on the Brillouin functions are also shown (--- for $S = 1/2$, —— for $S = 1$, and -•-•- for $S = 3/2$) (see text).

Table I. Elemental analysis results of RBA and RTA (in molar ratio).

Samples	[H]/[C]	[O]/[C]
RBA	0.775	0.130
RTA	0.763	0.239

Table II. Diamagnetic susceptibility (χ_{dia}), Curie constant (C), Weiss constant (θ), and Curie-type spin concentration (N_C).

Sample	χ_{dia} (in emu•g^{-1})	C (in emu•K•g^{-1})	θ (in K)	N_C (in spins•g^{-1})
RBA	$-(6 \pm 3) \times 10^{-7}$	$(6 \pm 3) \times 10^{-7}$	$-(0.9 \pm 0.5)$	$(3.4 \pm 1.7) \times 10^{17}$
RTA	$-(6 \pm 3) \times 10^{-7}$	$(8.7 \pm 0.3) \times 10^{-6}$	$-(1.0 \pm 0.5)$	$(5.2 \pm 0.2) \times 10^{17}$

where it is understood that more numbers of spins could contribute in RTA. Because of small Weiss constants, the temperature dependence of the magnetic susceptibility of both RBA and RTA almost follows the Curie law and only a weakly antiferromagnetic interaction can be expected possibly among spin clusters involving a few of triphenylmethyl radicals.

ESR analysis

We have observed in the ESR spectra a usual $\Delta m_s = \pm 1$ signal and a forbidden $\Delta m_s = \pm 2$ signal could be observed at 15 K. The results of the ESR measurements are given in Table III. The spin concentration (N_s) for the present samples treated at 200 °C are in the order of 10^{17}-10^{18} spins•g^{-1}. Furthermore, the g values for the $\Delta m_s = \pm 1$ signals suggest that the spins are ascribed to carbon not to oxygen. These results are consistent with our previous ESR measurement of AAP prepared from pyrene and benzaldehyde.[13]

As shown in Fig. 5, the absorption for the $\Delta m_s = \pm 2$ indicating the half-field transition of triplet or higher multiplet state is clearly observed at 1555 G at 15 K in both RBA and RTA, probably because the environmental electrons around the triplet spins concerned become singlet or "calm" at such low temperature. The observation of these signals strongly supports the result of the magnetization measurement, that is, the existence of a local spin alignment between a few of triphenylmethyl radicals.

Let us now look at the $\Delta m_s = \pm 1$ transition. The signal of the $\Delta m_s = \pm 1$ transition for both the samples consists of a single line without fine nor hyperfine structures observed as shown in Fig. 6. The $\Delta m_s = \pm 1$ transition of the multiplet state is rather difficult to observe in randomly oriented materials because the intensity of the signal will be significantly weaker for randomly oriented triplets than for regularly oriented ones. Moreover, in amorphous polymers it is not expected that the spins of the multiplet state are arranged with specific distance. Since the zero-field-splitting constant depends on the distance between interacting spins, the signal is broadened owing to the wide distribution of the zero-field-splitting constant and would,

Table III. Peak-to-peak linewidth (ΔH_{pp}), g-value, and spin concentration (N_s).

Samples	Measurement temperature	ΔH_{pp} (in G)	g-value	N_s[a] (spins•g^{-1})
RBA	*RT*	4.24 ± 0.08	2.0029 ± 0.0001	$(5.6 \pm 1.4) \times 10^{17}$
	15 K	4.36 ± 0.08	2.0028 ± 0.0001	$(6.6 \pm 2.6) \times 10^{17}$
RTA	*RT*	7.94 ± 0.09	2.0030 ± 0.0001	$(1.4 \pm 0.5) \times 10^{18}$
	15 K	11.30 ± 0.09	2.0026 ± 0.0001	$(8.6 \pm 2.2) \times 10^{18}$

[a]Obtained by the numerical integration of the ESR spectra in Fig. 6.

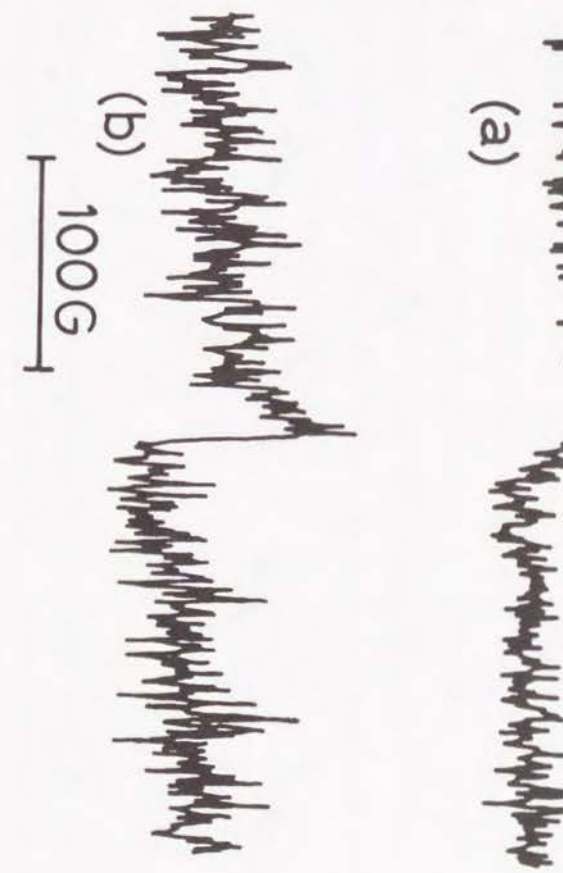

Fig. 5. $\Delta m_s = \pm 2$ signal observed at 15 K for (a) RBA and (b) RTA.

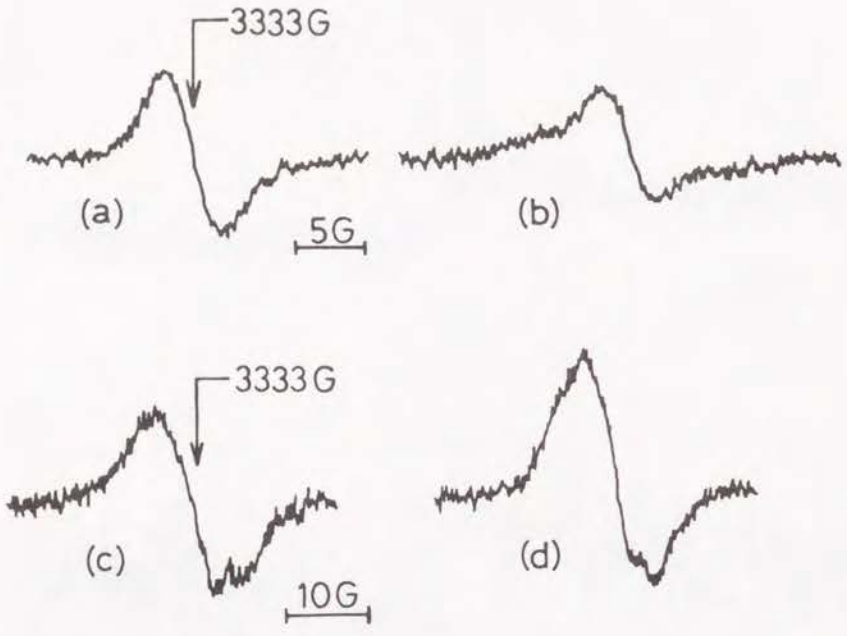

Fig. 6. $\Delta m_s = \pm 1$ signals observed for RBA at (a) room temperature and (b) 15 K and for RTA at (c) room temperature and (d) 15 K.

therefore, be difficult to detect.[18] On the other hand, it is noticed that the $\Delta m_s = \pm 2$ transitions are observable even in randomly oriented molecules because the resonant fields were relatively independent of the orientation of the molecules.[19,20] Thus the observed $\Delta m_s = \pm 1$ signals are mainly due to the isolated radical spins, and neither fine nor hyperfine splitting is observed accordingly.

Comparison of the ΔH_{pp} and g-value of AAPs with those of typical electrically conducting polymers such as poly(3-methylthiophene) [ΔH_{pp} = 6.53 G, g = 2.0024 (Ref. 21)] or *trans*-polyacetylene [ΔH_{pp} = 1.43 G, g = 2.0026 (Ref. 22)] suggests the nature of the spins in the present AAP samples to be of π type. A slight increase in ΔH_{pp} observed in both samples at low temperature could be explained by suppression of the motional narrowing characteristic of π type spins.

Conclusion

We have analyzed magnetic properties of the simplest AAP samples. The spin state and chemical structure of these have also been discussed on the basis of the ^{13}C NMR measurement. It is concluded for the present simplest AAP samples that the spin concentration is small and, furthermore, that macroscopic spin alignment to yield ferromagnetism does not occur. On the other hand, there is an obvious ferromagnetic coupling among a few spins such as triphenylmethyl radicals to form the triplet or higher spin multiplet state. The spin clusters each of which forms such multiplet state in spite of very small spin concentration is peculiar and these spin clusters are considered to be diluted into the whole bulk of the AAP. The interaction between these spin clusters themselves might be weakly antiferromagnetic as is suggested by the Weiss constant.

In this sense, appearance of superparamagnetism due to the existence of spin clusters would be possible in AAPs, although their population ought to strongly depend on the process of the preparation and/or of the heat treatment.

It will be, therefore, of importance to enhance the formation of these clusters and to reduce the total antiferromagnetic interaction for the appearance of ferromagnetism in the AAP members.

References

1. A. A. Ovchinnikov, *Theor. Chim. Acta(Berl.)*, **47**, 297(1978).
2. N. Tyutyulkov, O. E. Polansky, P. Schuster, S. Karabunarliev, and C. I Ivanov, *Theor. Chim. Acta(Berl.)*, **67**, 211(1985).
3. J. S. Miller, A. J. Epstein, and W. M. Reiff, *Acc. Chem. Res.*, **21**, 114(1988).
4. H. Iwamura and A. Izuoka, *J. Chem. Soc. Jpn.*, **1987**, 595, and references therein.
5. J. B. Torrance, S. Oostra, and A. Nazzal, *Synth. Met.*, **19**, 709(1987).
6. J. B. Torrance, P. S. Bagus, I. Johannsen, A. I. Nazzal, S. S. P. Parkin, and P. Batail, *J. Appl. Phys.*, **63**, 2962(1988).
7. A. A. Ovchinnikov and V. N. Spector, *Synth. Met.*, **27**, B615(1988).
8. M. Ota and S. Otani, *Chem. Lett.*, **1989**, 1179.
9. M. Ota, S. Otani, and K. Kobayashi, *Chem. Lett.*, **1989**, 1183.
10. M. Ota, S. Otani, K. Kobayashi, and M. Igarashi, *Mol. Cryst. Liq. Cryst.*, **176**, 99(1989).
11. T. A. Aleksandrova, A. M. Vaserman, A. Yu. D'yakonov, A. M. Shapiro, and A. L. Buchachenko, *Doklady Phys. Chem.*, **302**, 945(1989).
12. K. Tanaka, T. Koike, T. Yamabe, J. Yamauchi, Y. Deguchi, and S. Yata, *Phys. Rev.*, B**35**, 8368(1987).
13. K. Tanaka, S. Yamashita, T. Yamabe, J. Yamauchi, and Y. Deguchi, *Solid State Commun.*, **71**, 627(1989).
14. K. Tanaka, K. Yoshizawa, A. Takata, T. Yamabe, and J. Yamauchi, *Synth Met.*, **39**, 103(1990).
15. See, for example, W. Kemp, *NMR in Chemistry* , Macmillan Publishers Ltd., London, 1986.
16. I. C. Lewis and L. S. Singer, Carbon, **7**, 93(1969).
17. N. Mataga, Theor. *Chim. Acta(Berl.)*, **10**, 372(1968).
18. M. Iwasaki, T. Ichikawa, and T. Ohmori, *J. Chem. Phys.*, **50**, 1984, 1991(1969).

19. J. H. van der Waals and M. S. de Groot, *Mol. Phys.*, **2**, 333(1959).
20. M. S. de Groot and J. H. van der Waals, *Mol. Phys.*, **3**, 190(1960).
21. K. Tanaka, T. Shichiri, K. Yoshizawa, T. Yamabe, S. Hotta, W. Shimotsuma, J. Yamauchi, and Y. Deguchi, *Solid State Commun.*, **51**, 565(1984).
21. I. B. Goldberg, H. R. Crowe, P. R. Newman, A. J. Heeger, and A. G. MacDiarmid, *J. Chem. Phys.*, **70**, 1132(1979).

Chapter 2

Synthesis of Poly(*m*-aniline) by Dehydrohalogenation of *m*-Chloroaniline

In the field of synthetic metals, which are defined as organic compounds showing metallic properties, much work concerning their electrical, optical, and magnetic properties have been reported. Recent reports[1-6] on the success in organic ferromagnets have attracted a great deal of attention. Torrance et al.[1] have synthesized poly(1, 3, 5-triaminobenzene) whose iodine complex shows ferromagnetism up to 400°C, near which the polymer is decomposed. On the other hand, Ovchinnikov et al.[3] have reported that what is called poly-BIPO has saturation magnetization of 0.02 G/g. On the basis of the reports of the two groups, free radicals located on nitrogen or oxygen in π-conjugated systems might be relatively stable at room temperature.

In the present paper, we report the synthesis of poly(*m*-aniline) which could be an extended version of a maternal structure of ferromagnetic polymer proposed by Mataga.[7] For instance, the spin alignment in the dehydrogenated structure of poly(*m*-aniline) is expected to be similar to that of poly(*m*-phenylcarbene), the oligomer of which has been examined by Iwamura et al.[8] The synthetic method is based on the dehydrohalogenation between amine and halide,[9] namely ammonolysis.

In the presence of copper or copper(I) chloride, *m*-chloroaniline polymerizes to form a reddish-orange precipitate under reflux at 220-230°C. A typical polymerization was carried out as follows: 25g. (0.20 mol) of freshly distilled *m*-chloroaniline and 0.5 g. of copper(I) chloride were put into a flask under a high-purity nitrogen flow. After approximately 4 h at the reflux temperature, orange polymer started to appear, and it had been further

refluxed for 2h. After cooling, tetrahydrofuran (THF) was poured into the flask to dissolve the lower molecular weight species, and the polymer was collected by filtration, washed with THF repeatedly, and dried under vacuum at room temperature to yield 7.5 g. (30%) of brown powder. The polymer thus obtained is in the form of amine salt. In order to obtain free amine, **1** and remove the catalyst, the polymer was washed five times with 5%-ammonia ethanolic aqueous solution. The salt form, **2** of the polymer was prepared by treating a part of **1** with 2 mol/l-HCl ethanolic aqueous solution.

The results of the elemental analysis for **1** and **2** of the polymer are listed in Table 1. Clorine contained in **1** is considered due to an unreacted terminal one. This interpretation is supported by the observation of the IR spectrum as follows. An absorption band at 890 cm^{-1} due to the C-Cl stretching, which is observed in the monomer, is much weakened in the polymeric products as shown in Fig. 1. Moreover, the three C-H out-of-plane deformation modes at 840, 770, and 685 cm^{-1} are characteristic of *meta*-linkage of benzene rings,[10] which is in striking contrast with the IR spectrum for usual polyaniline, precisely poly(*p*-aniline).[11] The other vibrational bands observed in the present polymer can be similarly explained according to the analysis for poly(*p*-aniline): the band centered at 3400 cm^{-1} is assigned to the N-H stretching, the four bands at 1630, 1590, 1530, and 1480 cm^{-1} to the benzene and quinone skeletons, the 1380 and 1310 cm^{-1} bands to the C-N stretchings, and the five bands at 1210, 1160, 1100, 1075, and 990 cm^{-1} to the C-H in-plane deformation modes. All of them have a great resemblance to those observed in poly(*p*-aniline) except for the pattern of the C-H out-of-plane deformation modes.

Considering the results given above, the reddish-orange polymer has a poly(*m*-aniline) structure, and we can propose a reaction mechanism as shown in Fig. 2. A side reaction such as an elimination of ammonia could take place in the presence of acid[2] produced by ammonolysis, and the chain length is therefore considered not so long. Judging from the [N]/[C] and the [Cl]/[C] atomic ratios, $n = 7$ or so would be anticipated.

A theoretical work[12] based on the tight-binding crystal orbital method

Table I. Elemental analysis for the neutral form, **1** and the salt form, **2** of the polymer.

Sample	C(wt%)	H(wt%)	N(wt%)	Cl(wt%)	Total(wt%)	Composition
1	72.40	4.79	11.84	8.60	97.63	$C_6H_{4.76}N_{0.84}Cl_{0.24}$
2	65.12	4.55	10.71	16.15	96.53	$C_6H_{5.03}N_{0.85}Cl_{0.50}$

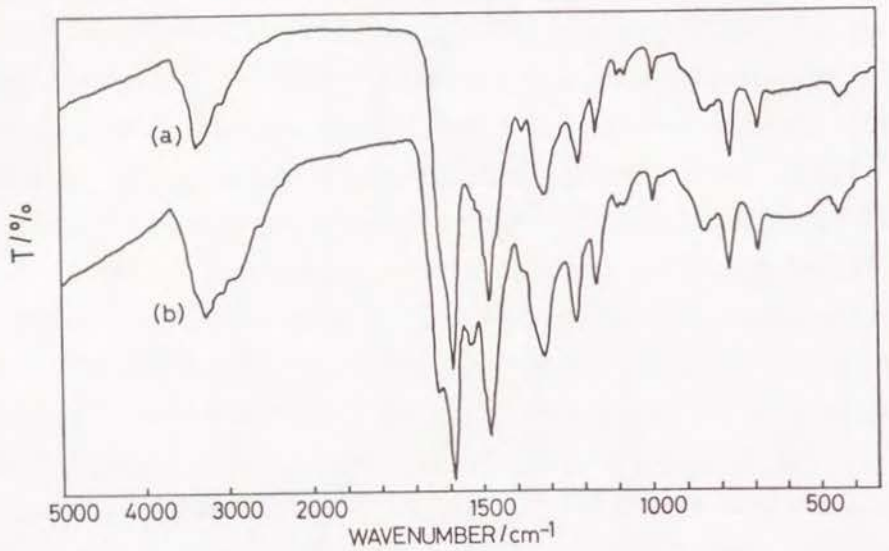

Fig. 1. IR spectra for (a) the neutral form, **1** and (b) the salt form, **2** of the polymer.

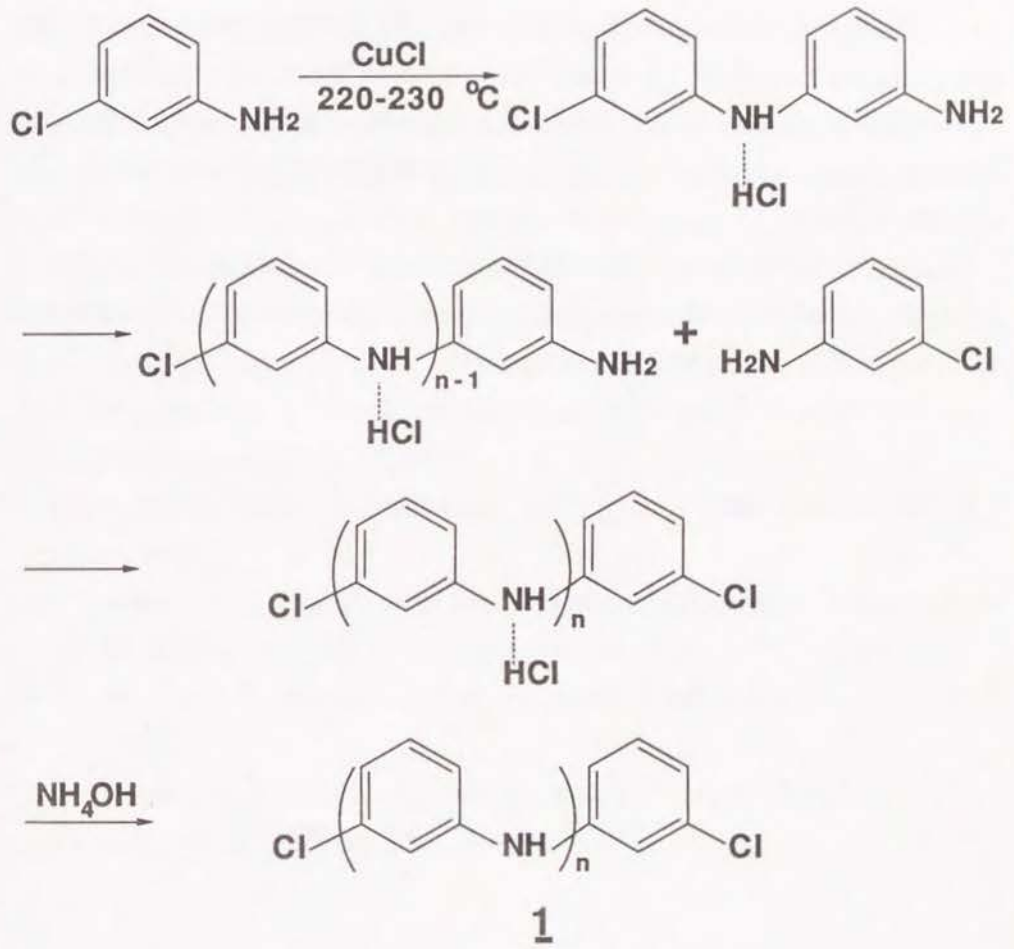

1

Fig. 2. Reaction outline toward poly(*m*-aniline).

shows that the dehydrogenated and the cationic states of poly(*m*-aniline), in which a hydrogen atom and an electron are extracted per each unit cell, respectively, exhibit ferromagnetism when considering a single chain and have similar band structure each other. The spin distribution patterns for the two states are almost all the same. It is also clarified that the spins of these states of poly(*m*-aniline) are delocalized both on the nitrogen atoms and on the benzene rings in contrast to those of poly(*p*-aniline) being localized on the nitrogen atoms.

In conclusion, we have reported the synthetic method for the polymer with a poly(*m*-aniline) structure whose magnetic properties will be of our interest as anticipated by the theoretical calculations.

References

1. J. B. Torrance, S. Oostra, and A. Nazzal, *Synth. Met.*, **19**, 709(1987).
2. J. Johannsen, J. B. Torrance, and A. Nazzal, *Macromolecules*, **22**, 566(1989).
3. Y. V. Korshak, T. V. Medvedeva, A. A. Ovchinnikov, and V. N. Spector, *Nature*, **326**, 370(1987).
4. A. A. Ovchinnikov and V. N. Spector, *Synth. Met.*, **27**, B615(1988).
5. M. Ota and S. Otani, *Chem. Lett.*, **1989**, 1179.
6. M. Ota, S. Otani, and M. Igarashi, *Chem. Lett.*, **1989**, 1183.
7. N. Mataga, *Theor. Chim. Acta(Berl.)*, **10,** 372(1968).
8. H. Iwamura and A. Izuoka, *Nippon Kagaku Kaishi*, **1987**, 595 and references therein.
9. For example, M. A. Stahmann and A. C. Cope, *J. Am. Chem. Soc.*, **68**, 2494(1946).
10. K. Nakanishi, P. H. Solomon, and N. Furutachi, *Infrared Absorption Spectroscopy*, 24th Ed, Nankoudou, Tokyo(1989).
11. M. Inoue, R. E. Navarro, and M. B. Inoue, *Synth. Met.*, **30**, 199(1989).
12. K. Tanaka, A. Takata, K. Yoshizawa, and T. Yamabe, *Polym. Prep*(Japan), **39**, 525(1990).

Chapter 3

Synthesis and ESR Measurements of Polymeric Product of *m*-Chloroaniline as an Approach to Magnetic Polymers

Introduction

A large amount of work has been directed toward the synthesis of organic ferromagnets on the basis of the early theoretical investigations performed by McConnell,[1] Mataga,[2] and Ovchinnikov.[3] Torrance et al.[4] have synthesized poly(1,3,5-triaminobenzene) with three-fold symmetry, some of which have been reported to show ferromagnetism up to 400 °C Considering that the free radicals located on hetero atoms in π-conjugated systems are rather stable like a diphenylpicrylhydrazyl (DPPH) radical, these radicals should be thoroughly investigated.

Poly(*m*-aniline)[5] is an interesting material in relation to an approach to magnetic polymers. In particular, its cationic and dehydrogenated forms are considered to have free radicals interacting ferromagnetically owing to the topological backbone of the polymer, as illustrated in Fig. 1. In this paper, we firstly refer to the electronic and the magnetic properties of the cationic and the dehydrogenated forms of poly(*m*-aniline) based on the one-dimensional tight-binding crystal orbital (CO) method. Secondly, we describe the synthesis of poly(*m*-aniline) and its ESR analysis.

NEUTRAL FORM

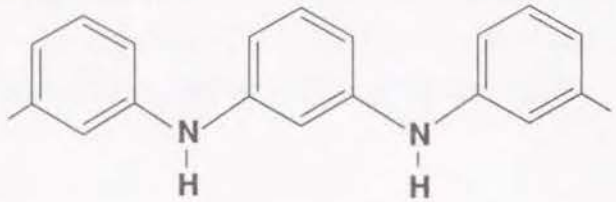

SALT FORM

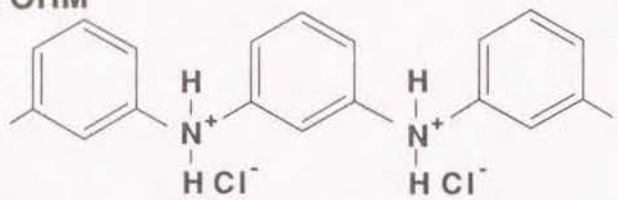

CATIONIC FORM

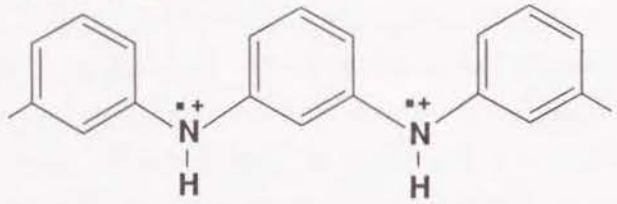

DEHYDROGENATED FORM

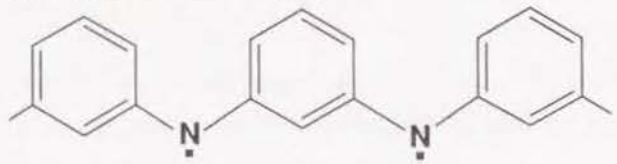

Fig. 1. Idealized structures for the four derivatives of poly(*m*-aniline). The cationic and the dehydrogenated forms have free radicals interacting ferromagnetically.

Theoretical background

The band levels of the cationic and the dehydrogenated forms were calculated using the unrestricted Hartree-Fock (UHF) CO method under the CNDO/2 approximation. The two forms give similar band structures; the bands for both the forms are very flat, and the electrons are therefore localized spatially. Furthermore, the band gap for neutral poly(*m*-aniline) calculated using the restricted HF (RHF) CO method is larger than that of usual polyaniline, i.e., poly(*p*-aniline).[6] As a result, we consider that the electrical conductivity of poly(*m*-aniline) is lower than that of usual polyaniline.

Figure 2 shows the spin densities for the two forms, values of which are close each other. The positive and negative spin densities appear alternately, as usually seen in organic systems; nevertheless, there is totally one spin in each cell. These spins would consequently form a very high spin multiplicity in the long chain.

Synthesis of poly(*m*-aniline)

Leaving aside the theoretical aspect, let us now look at the experimental results. In the presence of copper or copper (I) chloride, *m*-chloroaniline polymerizes to form a reddish-orange precipitate under reflux at 220-230 °C. This reaction is considered to proceed by dehydrochlorination between an amino group and chlorine in the monomer. The method employed for synthesizing this polymer was based on procedures described in a previous paper.[5] IR spectrum and elemental analysis indicate that the poly(*m*-aniline) structure with polymerization degree of 7 to 10 predominates in the polymeric product.

The obtained polymer was washed ten times with 5 %-ammonia aqueous solution to obtain a neutral form and to remove the catalyst. The salt form of the polymer was prepared by treating the neutral form with 2N-HCl aqueous solution; the cationic form was obtained by doping the neutral form with

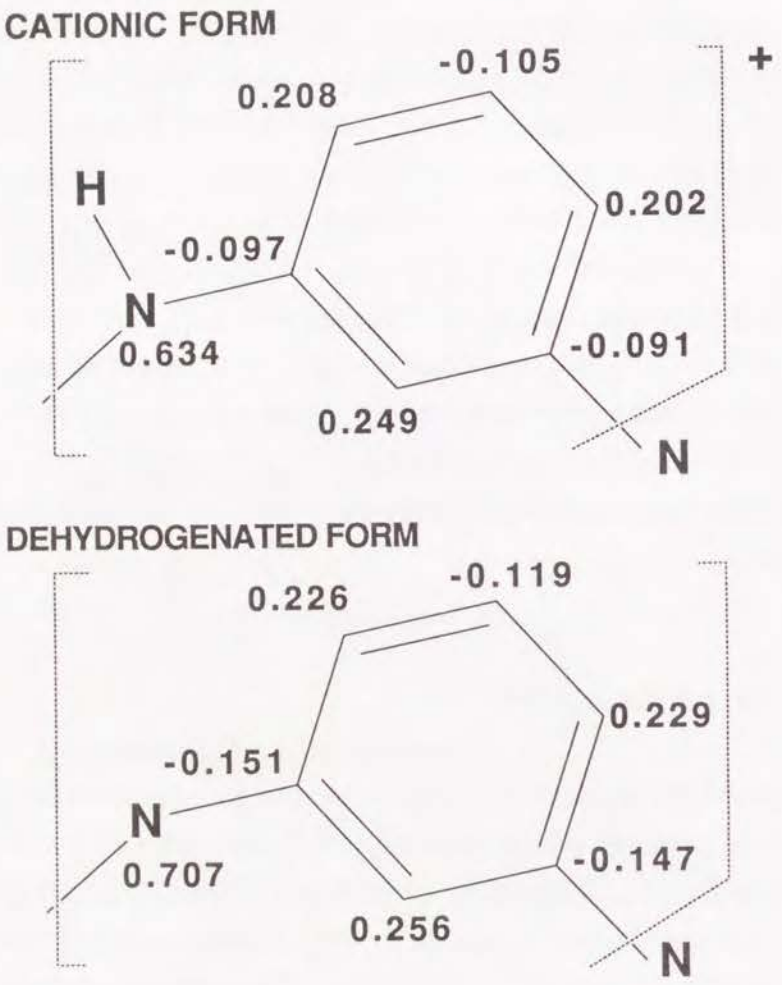

Fig. 2. Spin density distributions for the cationic and the dehydrogenated forms of poly(*m*-aniline).

iodine vapor; the dehydogenated form was prepared by treating the neutral form with 0.5M *p*-benzoquinone ethanolic solution. Idealized structures for these are illustrated in Fig. 1.

ESR measurements

ESR spectra were recorded on a JEOL JES-PE-2X ESR spectrometer at X band with 100 kHz field modulation at room temperature and liquid nitrogen temperature. Mn^{2+}/MgO and $CuSO_4 \cdot 5H_2O$ were used as the references for measuring *g*-values and spin concentrations, respectively.

The *g*-value, the peak-to-peak linewidth (ΔH_{pp}), the peak-to-peak height (ΔI_{pp}) and spin concentration (N_s) obtained from the $\Delta m_s = 1$ signal for the four derivatives of poly(*m*-aniline) are listed in Table I. The *g*-values of the cationic and the dehydrogenated forms are clearly larger than those of the neutral and the salt forms, which suggests that free radicals are actually created on the N sites of the cationic and the dehydrogenated forms of poly(*m*-aniline). However, the increase is small compared with that in usual polyaniline.[7] The spin concentrations are estimated to be in the order of 10^{18}-10^{19} spins$\cdot g^{-1}$. Because of the small spin concentration, the spins are too far to interact one another; consequently, this polymer is paramagnetic. In order to introduce a considerable number of spins into the polymer, a strong electron-acceptor or oxidizing agent is needed.

Conclusion

We have calculated the electronic and the magnetic states of the cationic and the dehydrogenated forms of poly(*m*-aniline) using the UHF CO method. According to this result, the cationic and the dehydrogenated forms of this polymer will make an organic ferromagnet with very high spin multiplicity.

Moreover, we have synthesized a polymeric product with a poly(*m*-

Table I. Results of the ESR measurements of the four derivatives of poly(m-aniline). g-value, peak-to-peak linewidth (ΔH_{pp} in G) and peak-to-peak height (ΔI_{pp} in arbitrary unit).

Form	Observed Temp. (K)	g-value	ΔH_{pp}	ΔI_{pp}
Neutral	298	2.0031	9.20	1.00
Salt	298	2.0029	8.15	2.97
Cationic	298	2.0042	11.93	2.60
Dehydrogenated	298	2.0049	6.42	20.60
Neutral	77	2.0028	10.32	1.81
Salt	77	2.0025	8.75	3.83
Cationic	77	2.0038	12.37	4.93
Dehydrogenated	77	2.0044	6.78	49.08

aniline) structure using dehydrochlorination of *m*-chloroaniline, and derived the salt, the cationic, and the dehydrogenated forms of this polymer. The ESR spectra show that free radicals, considered to be ferromagnetic electrons, are actually generated on the N sites of the polymer. Although this polymer exhibits no cooperative phenomenon at present because of the small spin concentration, this polymer is interesting as a basic skeleton of organic ferromagnets.

References
1. H. M. McConnell, *J. Chem. Phys.*, **39**, 1910(1963).
2. N. Mataga, *Theor. Chim. Acta(Berl.)*, **10**, 372(1968).
3. A. A. Ovchinnikov, *Theor. Chim. Acta(Berl.)*, **47**, 297(1978).
4. J. B. Torrance, P. S. Bagus, I. Johannsen, A. I. Nazzal, S. S. P. Parkin, and P. Batail, *J. Appl. Phys.*, **68**, 2962(1988).
5. K. Yoshizawa, K. Tanaka, and T. Yamabe, *Chem. Lett.*, **1990**, 1311.
6. K. Tanaka, A. Takata, K. Yoshizawa, and T. Yamabe, *Polym. Prep. (Japan)*, **39**, 525(1990).
7. A. G. MacDiarmid, J. C. Chiang, A. F. Richter, and A. J. Epstein, *Synth. Met.*, **39**, 285(1987).

Chapter 4

Polymerization of *m*-Bromoaniline to Poly(*m*-aniline) by the Use of Ullmann Reaction

Introduction

In the field of conducting polymers,[1] which commonly consist of π-conjugated systems, numerous papers concerning the electrical, optical, and magnetic properties have been reported for the last decade. Organic ferromagnetism is one of the most challenging themes in this area. In order to synthesize ferromagnets from C, H, N, and O with only 2*p*-orbitals, we have to consider the topology of molecular structures,[2] because *p*-orbitals have at most three-fold degeneracy in contrast with *d*- and *f*-orbitals having five- and seven-fold degeneracies, respectively. Therefore, a class of polymers and oligomers having degenerate orbitals, or non-bonding molecular orbitals (NBMO) due to the topology of molecular systems has been actively investigated. For instance, Iwamura and coworkers[3,4] have succeeded in the demonstration of a ferromagnetic spin order in *m*-phenylcarbene oligomers by magnetic-susceptibility and ESR measurements. Furthermore, intermolecular interaction between two diphenylcarbenes has been confirmed to be ferromagnetic in a certain stacking orientation by ESR spectroscopy[5] as has been theoretically suggested by McConnell.[6]

On the other hand, Torrance et al.[7-9] have synthesized poly(1,3,5-triaminobenzene) with three-fold symmetry, some of which has been reported to show ferromagnetism up to 400°C. However, they have not been able to reproduce the ferromagnetism as they have claimed that only the "great batch"

of the polymer shows a hysteresis loop. Although there are rather subtle problems concerning the origin of the unpaired electronic spins, we consider that these spins located on nitrogen should be thoroughly investigated as a spin supplier for organic ferromagnets because the unpaired electrons on hetero atoms in π-conjugated systems are very stable in air even at room temperature, e.g, 1,1'-diphenyl-2-picrylhydrazyl (DPPH) and tetraphenyl-pyrrole radicals.[10]

We have performed molecular design of poly(*m*-aniline)[11-13] which is an interesting material in relation to ferromagnetic interactions between the spins located on the chain. In particular, its cationic and dehydrogenated forms are considered to have free radicals interacting ferromagnetically in their chains owing to the topological structure of backbone of the polymer.[12,13]

In our preliminary report,[11] we have described the first synthetic method for preparing poly(*m*-aniline) from *m*-chloroaniline on the basis of the Ullmann reaction. Judging from the [N]/[C] and [Cl]/[C] atomic ratios, however, the average polymerization degree has been estimated to be 7 or so in that method. Moreover, we have shown preliminary results of the ESR measurement[12] and spin density distributions obtained on the basis of the one-dimensional crystal orbital method.[12,13] The present paper describes a detailed prescription of our synthetic method for obtaining the polymer having poly(*m*-aniline) structure with higher polymerization degree. We also refer to the existence of ferromagnetic interaction in this polymer from ESR and magnetization measurements at low temperatures.

Experimental Section

Materials

Reagent-grade *m*-bromoaniline (Aldrich Chemical Company, Inc.) was distilled at 2 mmHg before use. Copper (I) iodide and potassium carbonate (Wako Pure Chemical Industries, Ltd. 99.5 %) were used without further purification. Nitrobenzene (Wako) was distilled under nitrogen atmosphere.

Procedure of polymerization

10 ml. of *m*-bromoaniline (0.092 mole), 9.52 g. of potassium carbonate (0.069 mole), 0.5 g. of copper (I) iodide (3 m mole) and ceramic boiling stones were placed in a 50 ml. flask equipped with a nitrogen-gas inlet, thermometer and a reflux condenser. 10 ml. of nitrobenzene was used as a solvent in Expt. 1 and not in Expt. 2. The reaction mixture was heated to 210 °C during 8 h. and 240 °C during 4 h. in Expt. 1 and Expt. 2, respectively. After cooling the mixture down to room temperature, methanol was added to the flask to dissolve the oligomers and unreacted materials, and a black polymer was collected by filtration and washed with methanol repeatedly. In order to remove the catalyst and the neutralizing agent, the polymer was washed ten times with 50 ml. of 6 M HCl at 80 °C. After that the free amine was obtained by treating the salt with 50 ml. of 10 % ammonia aqueous solution. It was dried under dynamic vacuum for 24 h. Chemical analysis found: C, 74.44 %; H, 4.32 %; N, 14.30 %; Br, 3.57 % for Expt. 1 and C, 76.85 %; H, 4.58 %; N, 14.66 %; Br, 0.55 % for Expt. 2. Molecular formulas are $C_6H_{4.15}N_{0.99}Br_{0.04}$ for Expt. 1 and $C_6H_{4.26}N_{0.98}Br_{0.007}$ for Expt. 2. Molecular weight for these polymers cannot be estimated because the obtained powders are insoluble in common organic solvents such as tetrahydrofuran, dimethylsulfoxide and dimethylformamide. As a result of ICP (inductively coupled plasma) analysis, these materials were observed to contain 163 ppm of copper coming from catalytic system. If we assume that such Cu are all in the form of $(3d)^9$ state (Cu(II)), these spins contribute to 3 % of the total spins. Ferromagnetic impurities such as Fe, Co, and Ni were confirmed to be less than the lowest limit of detection (5 ppm).

The HCl-doping was carried out by immersing the polymer in 6M HCl aqueous solution for several hours, and after that the polymer was dried under dynamic vacuum for 24 h. The iodine-doping was carried out by exposing the pristine polymer to iodine vapor at 40°C for 48 h. The molar contents of HCl and I_3 in the polymer were determined to be 0.25 and 0.21 per benzene unit by elemental analysis and weight uptake, respectively.

Spectroscopic measurements

IR spectra were recorded on a Nicolet 20 DXB FT-IR spectrometer. UV-vis spectrum was recorded on a Shimadzu UV 365 spectrophotometer. The ESCA measurements were performed with a VG ESCALAB MK II utilizing Mg K_α radiation (100W, 10kV, 10mA). ESR spectra were measured at the X-band with a Varian E-112 spectrometer equipped with an Oxford Instruments' liquid-helium-flow cryostat.

Results and Discussion

Reaction mechanism

Many synthetic methods and catalytic systems have been developed for obtaining polymers having π-conjugated bonds such as polyphenylenes.[14-18] The reaction of aryl halides with arylamines is catalyzed to form N-arylarylamines by copper or copper compounds as developed by Ullmann. The Ullmann reaction[19,20] is basically considered to proceed by the coupling of free-radicals generated at relatively high temperature. The reaction outlined in Fig. 1 is mainly based on dehydrobromination, through which the degree of polymerization is very sensitive to the neutralizing agent. It is considered that a complex process including free-radicals is associated with this type of reaction because it proceeds at relatively high temperatures. Without the neutralizing agent, a red oligomer having a polymerization degree of 7 or so is obtained.[11] On the other hand, a high-molecular-weight (M_W = 13000) polymer, which is estimated from the residual bromine on the assumption that the polymer has a linear structure, was formed by using copper (I) iodide and potassium carbonate. As reported in the earlier study,[19] a good yield was obtained without a solvent in this type of reaction. Considering the reaction mechanism, triphenylamine could be formed but in a small amount because of the steric hindrance among the phenyl rings.

Moreover, from the elemental analysis of the polymer, it seems that some dehydrogenation is also involved in this reaction. It is likely that the

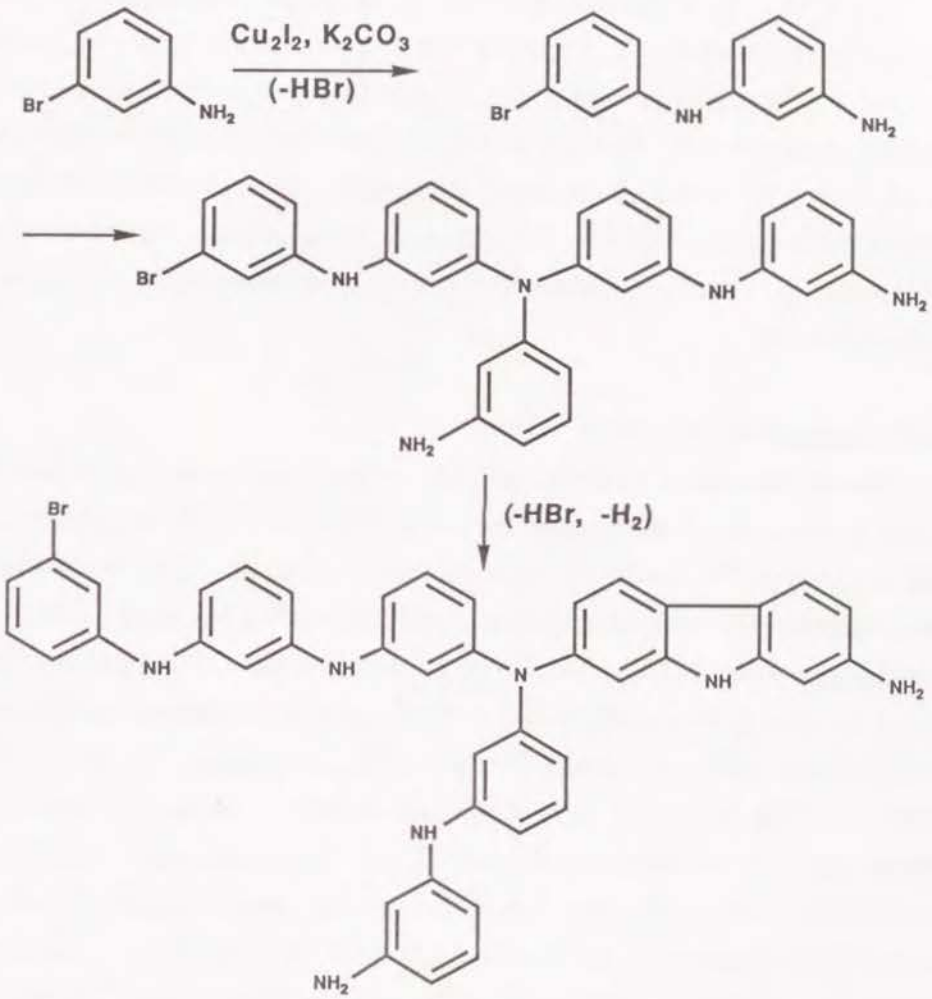

Fig. 1. Outline of the polymerization of *m*-bromoaniline in the presence of copper (I) iodide and potassium carbonate.

dehydrogenation leads to the formation of a carbazole structure to lessen a relatively large steric hindrance between the hydrogens at the sites concerned. We deduce from the elemental analysis and the polymerization mechanism that the overall structure shown in Fig. 2 is produced in this reaction. If this polymer has free radicals, which can be introduced either by doping it with electron acceptors or by abstracting the hydrogen attached to the nitrogen, on the nitrogen sites with high density, it is expected that these electronic spins interact ferromagnetically.[12,13] The structure of the polymer thus obtained is of interest as a basic skeleton for possible manifestation of organic ferromagnetism.

Infrared and ultraviolet-visible spectra

Fourier transform infrared (FT-IR) spectra shown in Fig. 3 can be basically explained on the basis of the vibrational modes of usual polyaniline, that is, poly(*p*-aniline)[21] except for the region of C-H out-of-plane deformations. A weak band observed at 3372 cm^{-1} is assigned to the N-H stretching; a weak band at 3058 cm^{-1} to the aromatic C-H stretching; two strong bands at 1586 and 1486 cm^{-1} with shoulders to the benzene skeleton; a broad band at 1278 cm^{-1} to the C-N stretching; three bands at 1219, 1161, and 998 cm^{-1} to the C-H in-plane-deformation modes. In the C-C stretching region, note that the intensity of the 1586 cm^{-1} band is stronger than that of the 1486 cm^{-1} one in contrast with the case of poly(*p*-aniline),[22] which reveals that poly(*m*-aniline) contains few quinoneimine parts. The three modes observed at 844, 769 and 698 cm^{-1} are assigned to the C-H out-of-plane deformations due to *meta*-substituted benzene rings, although they are generally more complex than that of *para*-substituted ones.[23] This assignment was also supported by Ishida and Iwamura.[24] The FT-IR spectrum of the oligomer is completely consistent with that of the oligomer obtained from *m*-chloroaniline previously reported.[11]

The solution electronic absorption spectrum for the soluble fraction of poly(*m*-aniline) in dimethylformamide is shown in Fig. 4. In contrast with the spectrum of the emeraldine form of poly(*p*-aniline),[25] the intensity of the

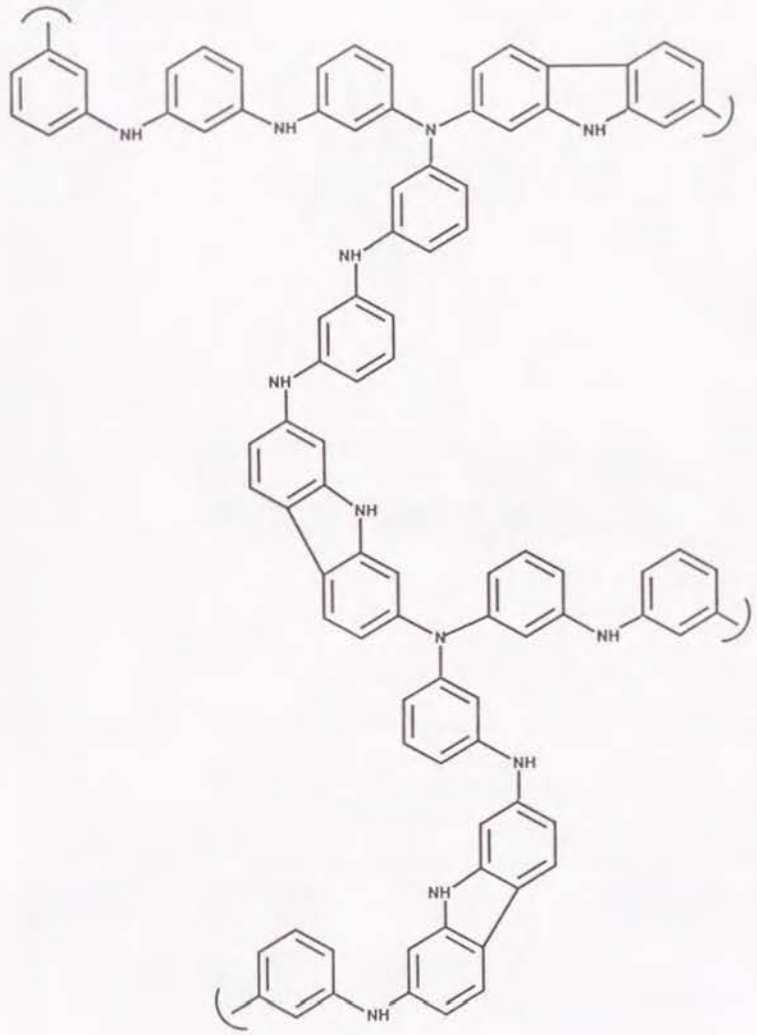

Fig. 2. Plausible structure of the polymer from *m*-bromoaniline. Elemental composition shown here is $C_{90}H_{64}N_{15}$.

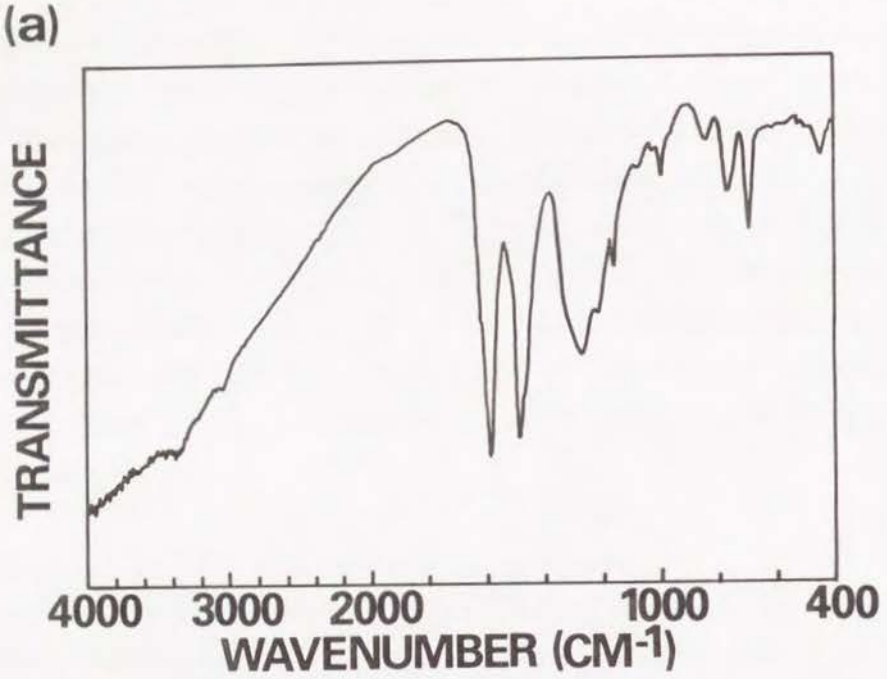

Fig. 3. FT-IR transmission spectra of (a) the polymer and (b) the oligomer.

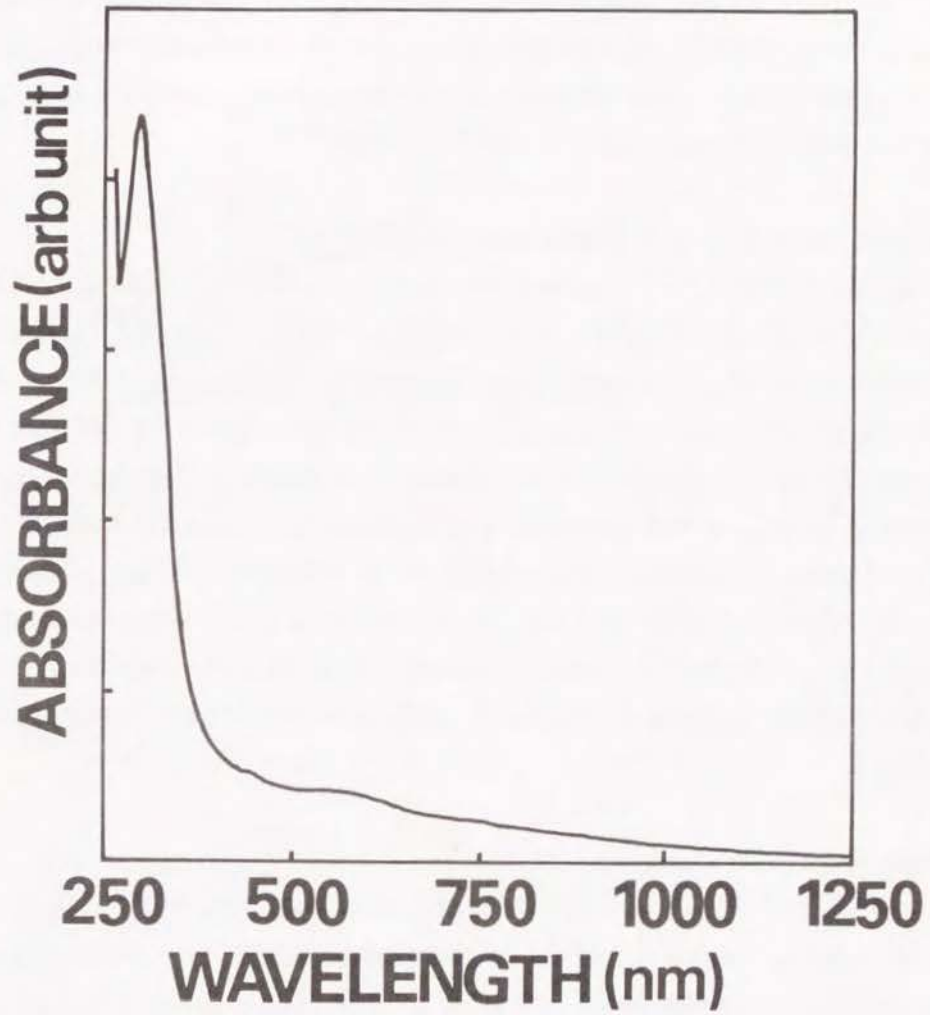

Fig. 4. Electronic absorption spectrum for the soluble fraction of poly(*m*-aniline) in dimethylformamide.

630 nm band is very low in this spectrum; it is rather similar to that of the leucoemeraldine form of poly(*p*-aniline). From the suggestion by Wudl et al.,[22] we consider that there is no quinoneimine moiety in poly(*m*-aniline). This is consistent with the structure of the present material shown in Fig. 2 because the quinoneimine structure in poly(*m*-aniline), generating spins on benzene rings, is considered to be rather unstable.[13]

Electron spectroscopy for chemical analysis (ESCA)

Figure 5 shows ESCA spectra for the polymer and the oligomer. The signals due to Br_{3d5} and Br_{3d3} (72 eV), and Br_{3p1} and Br_{3p3} (190 eV) observed in the oligomer clearly come from unreacted terminal bromine. In contrast, these signals were not observed in the spectrum of the polymer in accordance with the elemental analysis mentioned above. Here let us see an asymmetric C_{1s} narrow spectrum and its simulation, carried out using a mixed Gaussian-Lorentzian peak model and an iterative algorithm, shown in Fig. 6. This peak is divided into two components whose intensity-ratio is exactly 2:1. The two components correspond to the carbon bound only to carbon and that to nitrogen, which reflects the structure of the polymer shown in Fig. 2.

Magnetic-property measurements

The half-field-resonance spectra indicating $\Delta m_s = \pm 2$ transition corresponding to $g \approx 4$ signals of the pristine, HCl-, and iodine-doped polymers have been observed by ESR at 15 K.[26] The *g*-values, the peak-to-peak linewidth (ΔH_{pp}), and the spin concentration of these materials are listed in Table I. From the *g*-values of the pristine polymer and the oligomer, it is seen that these spins are located on nitrogen rather than on carbon. Moreover, from the field dependence of magnetization, a complete saturation (Ms = 0.30 emu•G•g^{-1}) was observed in the iodine-doped polymer at low temperatures.[26] The magnetization was observed to obey the theoretical Brillouin function fitting with $S = 1$. Therefore, these preliminary results demonstrate that the spins created by iodine-doping interact ferromagnetically

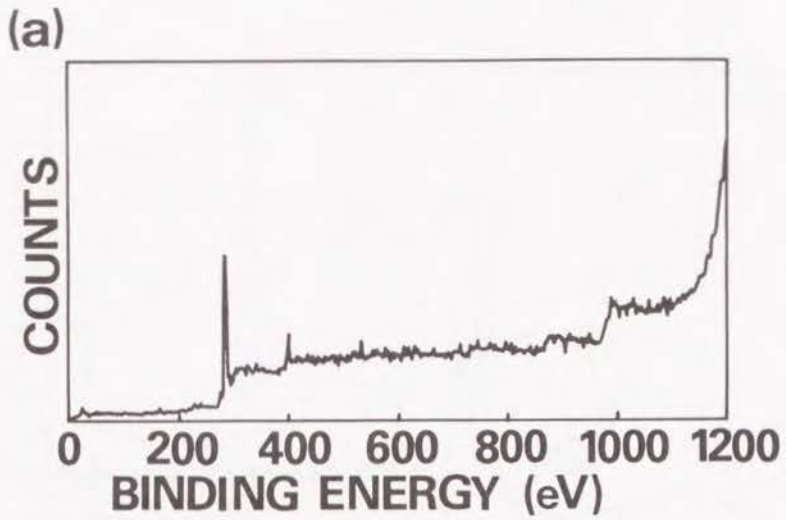

Fig. 5. ESCA wide spectra of (a) the polymer and (b) the oligomer.

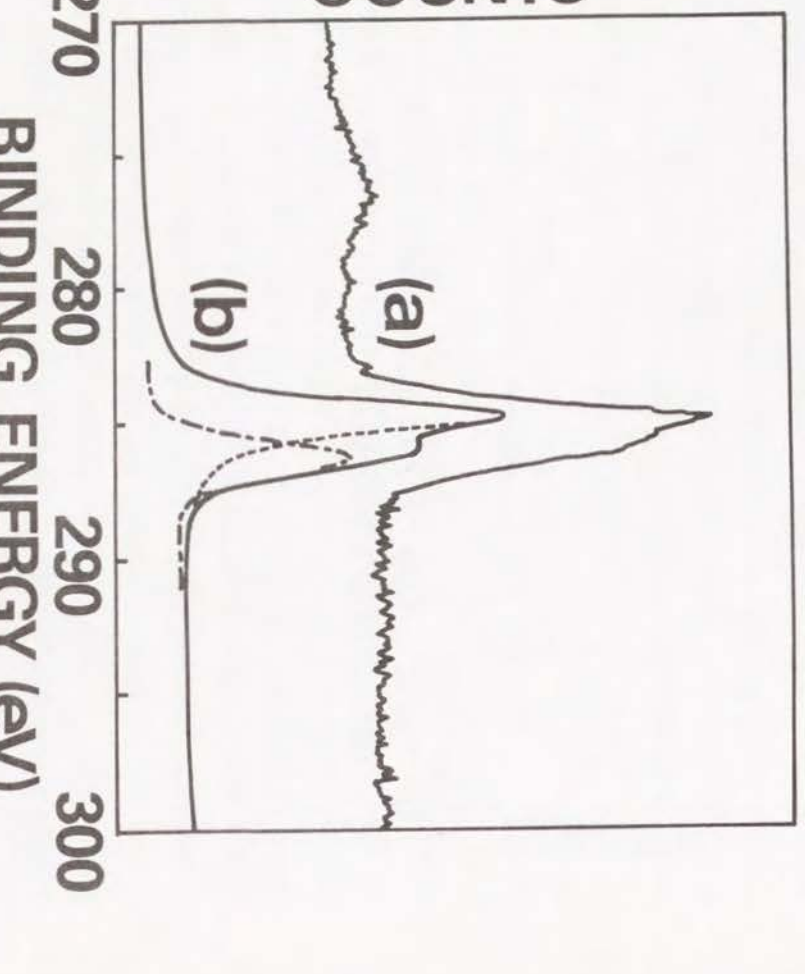

Fig. 6. ESCA C_{1s} narrow spectra of (a) the polymer and (b) its simulation.

Table I. The g-value, the peak-to-peak linewidth (ΔH_{pp}), and the spin concentration (N_s) measured at room temperature of the pristine, HCl-, and iodine-doped polymer and the pristine oligomer.

Sample	g-value	ΔH_{pp} (G)	$Ns \times 10^{19}$ (spins•(g-polymer)$^{-1}$)
Pristine polymer	2.0032 ± 0.0001	9.94 ± 0.1	$(4.5 \pm 0.5) \times 10^{19}$
HCl-doped polymer	2.0029 ± 0.0001	8.27 ± 0.1	$(5.7 \pm 0.5) \times 10^{19}$
Iodine-doped polymer	2.0051 ± 0.0001	13.79 ± 0.1	$(1.0 \pm 0.1) \times 10^{20}$
Pristine oligomer	2.0031 ± 0.0001	7.91 ± 0.1	$(3.6 \pm 0.4) \times 10^{17}$

forming triplet or higher multiplet spin clusters as has been found in alkylene-aromatic polymers.[27]

Conclusion

We have described a synthetic method for preparing a polymer having poly(*m*-aniline) structure from *m*-bromoaniline by the use of the catalytic system of copper (I) iodide and potassium carbonate on the basis of the Ullmann reaction. Although this type of reaction proceeds by a complex free-radical mechanism, the results of the IR and UV-vis spectra are consistent with the *meta*-linked structure. We have shown evidence of ferromagnetic interaction working in the polymer skeleton from the preliminary ESR and magnetization measurements. Further detailed magnetic properties of this polymer clearly need to be examined; these will be reported elsewhere.

References

1. See for example, T. A. Skotheim, *Handbook of Conducting Polymers*; Marcel Dekker, New York, 1986, Vols. 1 and 2.
2. N. Mataga, *Theor. Chim. Acta(Berl.)*, **10**, 372(1968).
3. T. Sugawara, S. Bandow, K. Kimura, H. Iwamura, and K. Itoh, *J. Am. Chem. Soc.*, **108**, 368(1986).
4. Y. Teki, T. Takui, K. Itoh, H. Iwamura, and K. Kobayashi, *J. Am. Chem Soc.*, **108**, 2147(1986).
5. A.Izuoka, S. Murata, T. Sugawara, and H. Iwamura, *J. Am. Chem. Soc.*, **105**, 2631(1987).
6. H. M. McConnell, *J. Chem. Phys.*, **39**, 1910(1963).
7. J. B. Torrance, S. Oostra, and A. Nazzal, *Synth. Met.*, **19**, 709(1987).
8. J. B. Torrance, P. S. Bagus, I. Johannsen, A. I. Nazzal, S. S. P. Parkin, and P. Batail, *J. Appl. Phys.*, **63**, 2962(1988).
9. J. Johannsen, J. B. Torrance, and A. Nazzal, *Macromolecules*, **22**, 566(1989).
10. S. H. Pine, *Organic Chemistry*; 5th. Ed., McGraw-Hill, New-York, 1987.
11. K. Yoshizawa, K. Tanaka, and T. Yamabe, *Chem. Lett.*, **1990**, 1331.
12. K. Tanaka, K. Yoshizawa, A. Takata, T. Yamabe, and J. Yamauchi, *Synth. Met.*, **43**, 3297(1991); paper presented at the International Conference on Science and Technology of Synthetic Metals, Tübingen, Germany, September 1990.
13. K. Yoshizawa, A. Takata, K. Tanaka, and T. Yamabe, to be published.
14. P. Kovacic and C. Wu, *J. Polym. Sci.*, **47**, 45(1960).
15. P. Kovacic and A. Kyriakis, A. *J. Am. Chem. Soc.*, **85**, 454(1963).
16. Y. M. Paushkin, L. S. Polak, O. Y. Omarov, and I. I. Patalakh, *J. Polym. Sci.*, **C16**, 2215(1967)..
17. E. Ibuki, S. Ozasa, and K. Murai, K. *Bull. Chem. Soc. Jpn.*, **48**, 1868(1975).
18. T. Yamamoto, Y. Hayashi, and A. Yamamoto, *Bull. Chem. Soc. Jpn.*,

51, 2091(1978).
19. P. E. Weston and H. Adkins, *J. Am. Chem. Soc.*, **50**, 859(1928).
20. M. A. Stahmann and A. C. Cope, *J. Am. Chem. Soc.*, **68**, 2494(1946).
21. M. Inoue, R. E. Navarro, and M. B. Inoue, *Synth. Met.*, **30**, 199(1989).
22. F. Wudl, R. O. Angus, F. L. Lu, P. M. Allemand, D. J. Vachon, M. Nowak, Z. X. Liu, and A. J. Heeger, *J. Am. Chem. Soc.*, **109**, 3677(1987).
23. K. Nakanishi, P. H. Solomon, and N. Furutachi, *Infrared Absorption Spectroscopy* (in Japanese), 24 th. Ed., Nankoudou, Tokyo, 1989.
24. T. Ishida and H. Iwamura, *Chem. Lett.* **1991**, 317.
25. M. Ohira, T. Sakai, M. Takeuchi, Y. Kobayashi, and M. Tsuji, *Synth. Met.*, **18**, 347(1987).
26. K. Yoshizawa, K. Tanaka, T. Yamabe, and J. Yamauchi, to be published.
27. K. Tanaka, K. Yoshizawa, A. Takata, T. Yamabe, and J. Yamauchi, *J. Chem. Phys.*, **94**, 6868(1991).

Chapter 5

Ferromagnetic Interaction in Poly(*m*-aniline): Electron Spin Resonance and Magnetic Susceptibility

Introduction

Molecular design and synthesis of organic ferromagnets is one of the most challenging themes in synthetic metals. For instance, Iwamura and coworkers[1,2] have succeeded in obtaining a ferromagnetic spin order in *m*-phenylcarbene oligomers confirmed by magnetic-susceptibility and electron spin resonance (ESR) measurements. Furthermore, intermolecular interaction between two diphenylcarbenes has been found ferromagnetic in a certain stacking orientation[3] as has been theoretically suggested by McConnell.[4] Ferromagnetic intermolecular interaction in galvinoxyl radicals has been also extensively investigated.[5-8] Moreover, bulk high spin state based on charge transfer molecular complexes has been reported.[9]

Torrance et al.[10,11] have synthesized poly(1,3,5-triaminobenzene) with three-fold symmetry, an iodine complex of which has been reported to show ferromagnetic behavior up to 400°C. They have concluded that the ferromagnetism is associated with the unpaired electronic spins in the organic polymer, because the magnetic moment disappeared after heat treatment. However, such ferromagnetism has not been able to be reproduced since then. Although there are rather subtle problems concerning the origin of the unpaired spins, we consider that this kind of spin located on nitrogen in π-conjugated systems should be thoroughly investigated as a spin supplier in organic ferromagnets in view of the chemical stability.

We have performed molecular design of poly(*m*-aniline)[12-15] whose structure is interesting in relation to possible ferromagnetic interaction among the spins. In our previous papers,[12,15] we have described the synthetic method for preparing poly(*m*-aniline) from *m*-chloroaniline or *m*-bromoaniline on the basis of the Ullmann reaction. We have paid much attention to its cationic and dehydrogenated forms as ferromagnetic polymers, because the spins in both these forms are considered to interact ferromagnetically owing to the topology of the skeleton.[13,14] In fact, our theoretical calculation based on the one-dimensional tight-binding crystal orbital (CO) method has shown that a ferromagnetic (ferrimagnetic) state is more stable than a nonmagnetic one in both the cationic and dehydrogenated forms.[14] Furthermore, we have preliminarily found from ESR measurements that unpaired spins are actually created on the nitrogens by HCl- or iodine-doping of this material.[13] The present paper describes detailed analyses of the ESR and magnetic susceptibility measurements of the pristine and doped poly(*m*-aniline). In particular, we stress here the ferromagnetic interaction observed in the iodine-doped state of this polymer.

Experiment

Poly(*m*-aniline) was synthesized from *m*-bromoaniline using copper (I) iodide and potassium carbonate on the basis of the Ullmann reaction. Without using the neutralizing agent, its oligomer having a polymerization degree of 7 or so was obtained. The products were washed ten times with 6M HCl at 80 °C in order to remove the catalyst and the neutralizing agent. The synthesis of poly(*m*-aniline) and the doping method have been completely described in our previous papers.[12,15]

ESR spectra at X-band were recorded on a Varian E-112 spectrometer equipped with an Oxford Instruments' liquid-helium-flow cryostat at 15 to 260 K and on a JEOL JES-PE-2X ESR spectrometer at room temperature. An ESR sample tube containing 10 mg of sample powder was evacuated down to less than 10^{-4} Torr for 2 h and then charged with high purity helium gas (99.9999%) as a heat medium up to 10 Torr before sealing. A Mn^{2+}/MgO solid solution was used as a reference for the *g*-values and magnetic field calibration. The spin concentration was determined using $CuSO_4 \cdot 5H_2O$ as a standard. The 100 kHz field-modulation width was kept less than 25% of the peak-to-peak linewidth (ΔH_{pp}). For the experiment of *in situ* iodine-doping, 10 mg of pressed pellet of the pristine polymer was sealed in another evacuated ESR tube and joined via a breakable seal to another evacuated tube (10^{-4} Torr at 77 K) containing iodine-crystals.

Magnetic susceptibility and magnetization were measured using an Oxford Instruments' Faraday-type magnetic balance. A quartz cell was stuffed with 50 mg of the materials, and then 80 mg of liquid paraffin was added to fix the powder. The magnetization curve for the iodine-doped polymer was recorded at 2.0 and 4.4 K up to the magnetic field of 50 kG. The correction of the diamagnetism of the quartz cell and liquid paraffin was performed as usual. The magnetic susceptibility was measured in the temperature range 2-260 K under the magnetic field of 10 kG.

The content of transition metal impurities were measured with a Jobin Yvon Model JY48 ICP (inductively coupled plasma) emission spectrometer. Ferromagnetic impurities such as Fe, Co, and Ni were confirmed to be less than the lowest limit of detection (< 5ppm). On the other hand, 163 ppm of Cu coming from the catalytic system was detected. If we assume that such Cu are all in the form of $(3d)^9$ state (Cu (II)), these spins contribute to 3% of the total spins (97% organic spins). Broad signals due to these spins were observed in the ESR spectra at 15 K only when we measured these materials under the condition employing large amplitude and modulation width of 20 G.

Results and discussion

ESR measurements

The spin concentrations of the pristine polymer and oligomer are found to be 4.5×10^{19} and 3.6×10^{17} spins•(g-polymer)$^{-1}$ at room temperature, respectively, from a comparison between the double integral of the observed $\Delta m_s = \pm 1$ signals and that of the $CuSO_4 \cdot 5H_2O$ standard. It is indicated that on an average, one spin exists per 150 and 20000 aniline units for the pristine polymer and oligomer, respectively. The *g*-values of the pristine polymer (2.0032) and the HCl-doped polymer (2.0029) are clearly larger than those originated from carbons in typical conducting polymers such as *trans*-polyacetylene (2.00263),[16] polypyrrole (2.0025),[17] and polyacenic materials (2.0022-2.0027).[18] Note that the spins of polypyrrole are not centered at nitrogen but at carbon forming a π-conjugated chain judging from its *g*-value.[17] On the other hand, the *g*-value of the HCl-doped poly(*m*-aniline) is slightly smaller than that of the corresponding polyaniline, or poly(*p*-aniline), (2.0032)[19] and Würster's Blue cation radicals (2.00325).[20] From the *g*-value analysis, the spins of the present materials were found to be mainly located on nitrogens although they are in some degree delocalized on phenyl rings. Doping of the polymer with iodine increases the spin concentration up to 10^{20} spins•(g-polymer)$^{-1}$, being very large in organic polymers. The *g*-value, the ΔH_{pp}, and the spin concentration of the pristine, HCl-, and iodine-doped polymers and the pristine oligomer measured at room temperature are listed in Table I.

Here let us look at the result of the *in situ* iodine-doping carried out for the polymer at room temperature. Throughout the doping process, the peak height of the ESR signal (the first derivative) kept almost constant, but the lineshape of the signal was broadened with the doping time. Figure 1 shows a change in the *g*-value and the ΔH_{pp} of the polymer as a function of the doping time. Both of them increase with the doping time, and they are saturated at about 40 h. Broadening of ESR signals is inherent in the iodine-doped organic materials.[18,20,21]

Table I. The *g*-value, the peak-to-peak linewidth (ΔH_{pp}), and the spin concentration (N_S) measured at room temperature of the pristine, HCl-, and iodine-doped polymer and the pristine oligomer. The values in parentheses of N_S was obtained assuming $S = 1$.

Sample	*g*-value	ΔH_{pp} (G)	N_S (spins•(g-polymer)$^{-1}$)
Pristine polymer	2.0032 ± 0.0001	9.94 ± 0.1	4.5(± 0.5) × 10^{19} (1.7×10^{19})
HCl-doped polymer	2.0029 ± 0.0001	8.27 ± 0.1	5.7(± 0.5) × 10^{19} (2.1×10^{19})
Iodine-doped polymer	2.0051 ± 0.0001	13.79 ± 0.1	1.0(± 0.1) × 10^{20} (3.8×10^{19})
Pristine oligomer	2.0031 ± 0.0001	7.91 ± 0.1	3.6(± 0.4) × 10^{17}

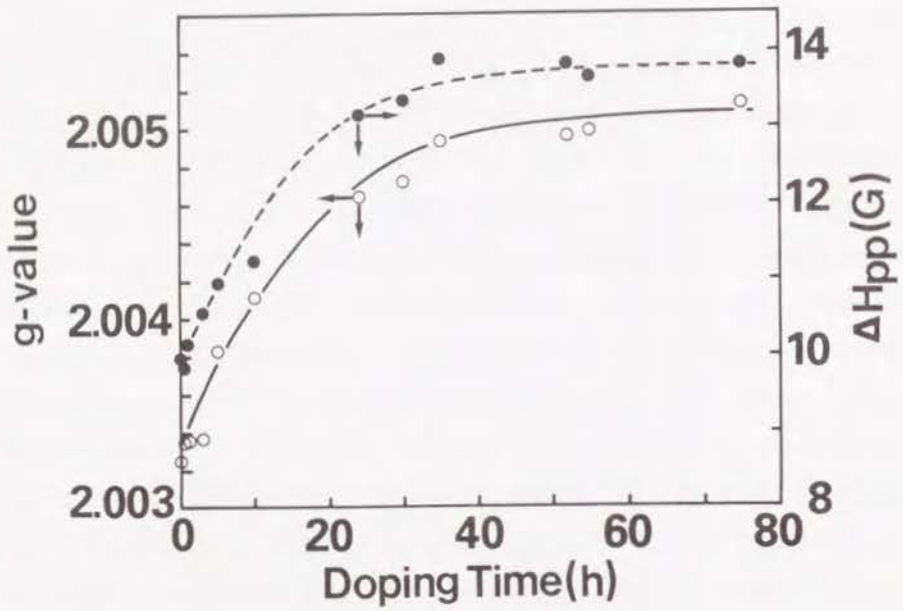

Fig. 1. Change in g-value and peak-to-peak linewidth (ΔH_{pp}) of poly(*m*-aniline) induced by iodine-doping as a function of doping time.

Associated with the increase in the g-value and the ΔH_{pp}, the spin concentration also increases as shown in Fig. 2. At an early stage of the doping process, a very slight decrease in the spin concentration was observed in the present material as typically found in conducting polymers.[21] For example, the ESR signal intensity of *trans*-polyacetylene has been observed to decrease down to 50 % by iodine-doping.[22] In poly(*m*-aniline), however, the extent of this decrease was much smaller. This result signifies that the spins are at a relatively deep level in the band gap and they are rather stable compared with the spins located on pure carbon skeletons such as polyacetylene. As the doping proceeds, iodine molecules would accept electrons from the lone pair of the nitrogen to make I_3^- or I_5^- anions as has been observed in the Raman spectrum of iodine-doped β-carotene and *trans*-polyacetylene.[23] As a result, positively charged polarons, or cation radicals, are actually generated in the polymer skeleton; that is, on an average, one spin per 60 aniline units was observed in the iodine-doped state. This result thus demonstrates that the spin concentration becomes extremely large with an increase in the dopant concentration if the electron-accepting ability of the dopant is strong enough. In the present paper, this type of spin is of our special interest in relation to the molecular design of a ferromagnetic polymer.

Let us now look at the temperature dependence of the ESR signals. The temperature dependence of the ΔH_{pp} of all the samples is plotted in Fig. 3. The lineshapes were found to be Lorentzian in all the cases within the whole temperature range from the ratio of $\Delta H_{1/2}/\Delta H_{pp}$, where $\Delta H_{1/2}$ stands for the outside half-height-linewidth as defined in our previous paper.[18] Lorentzian lineshapes are characteristic of the spins located in relatively long π-conjugated systems. We hence consider that these spins are delocalized on the nitrogen and the phenyl rings associated with the g-value analysis mentioned above. As shown in Fig. 3, an abrupt increase in the linewidth for the three types of the polymer was observed at 40 K, probably suggesting the occurrence of long-range interaction between the spins.[24,25] Together with the observation of the temperature dependence of the ΔH_{pp}, the g-values are also dependent on temperature; the g-values of these materials decrease as

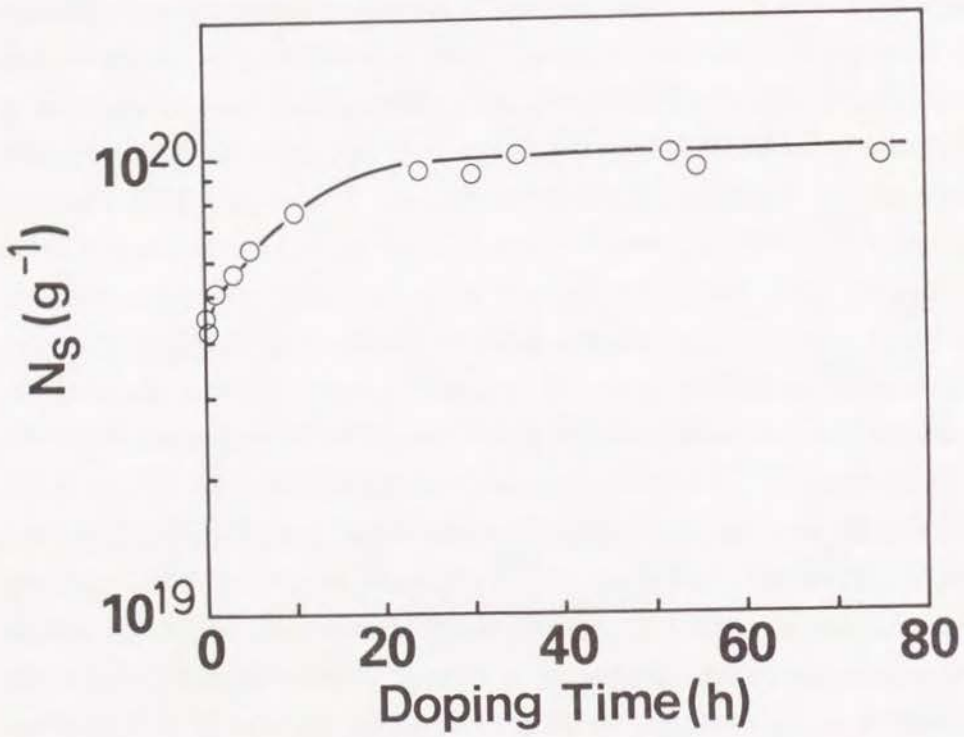

Fig. 2. Increase in spin concentration (N_S) of poly(*m*-aniline) induced by iodine-doping as a function of doping time.

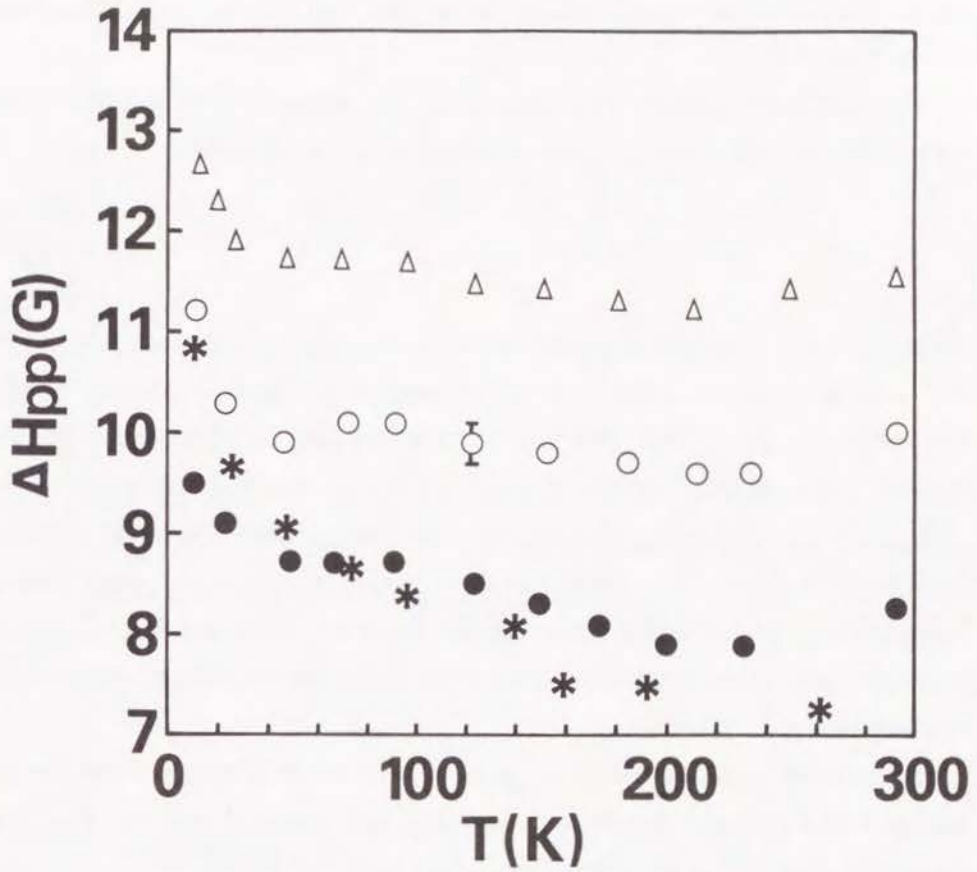

Fig. 3. Temperature dependence of peak-to-peak linewidth (ΔH_{pp}) for poly(*m*-aniline). ○: pristine polymer, ●: HCl-doped polymer, Δ: iodine-doped polymer, and ∗: pristine oligomer.

temperature decreases. The temperature dependence of the ΔH_{pp} and the g-values would be attributed to magnetic short- and long-range orderings, which implies the presence of both the intrachain and interchain interactions.[24,25]

Magnetic susceptibility (χ) is proportional to an intensity of an ESR signal; therefore, when the lineshapes are unchanged, χ is expressed as

$$\chi = c\Delta H_{pp}{}^2 I_{pp}, \tag{1}$$

where I_{pp} is a full height of a differential curve and c a constant depending on the measurement conditions such as sensitivity and amplitude of the apparatus.[26] Reciprocal χ is plotted as a function of temperature for the pristine, HCl-, and iodine-doped polymer in Fig. 4. The intercepts of the horizontal axis for these materials at low temperatures give positive values in contrast with those at high temperatures giving negative values. This is characteristic of ferrimagnetism, as has been expected for ferromagnetic polymers from theoretical consideration based on the one-dimensional tight-binding method.[13,14,27]

Figures 5(a) and 5(b) show χT plots as a function of temperature for the iodine-doped polymer and the pristine oligomer, respectively. In Fig. 5(a) theoretical fittings based on the Curie-Weiss law,

$$\chi = C/(T - \theta), \tag{2}$$

and the one-dimensional Ising model,[28]

$$\chi = (g^2\mu_B{}^2/k_BT)\exp(2J_{ex}/k_BT), \tag{3}$$

are also shown. Here C is the Curie constant; θ, the Weiss constant; μ_B, the Bohr magneton; and J_{ex}, exchange energy.

In the iodine-doped polymer, χT increases as the temperature decreases, which implies the existence of ferromagnetic interaction between the spins

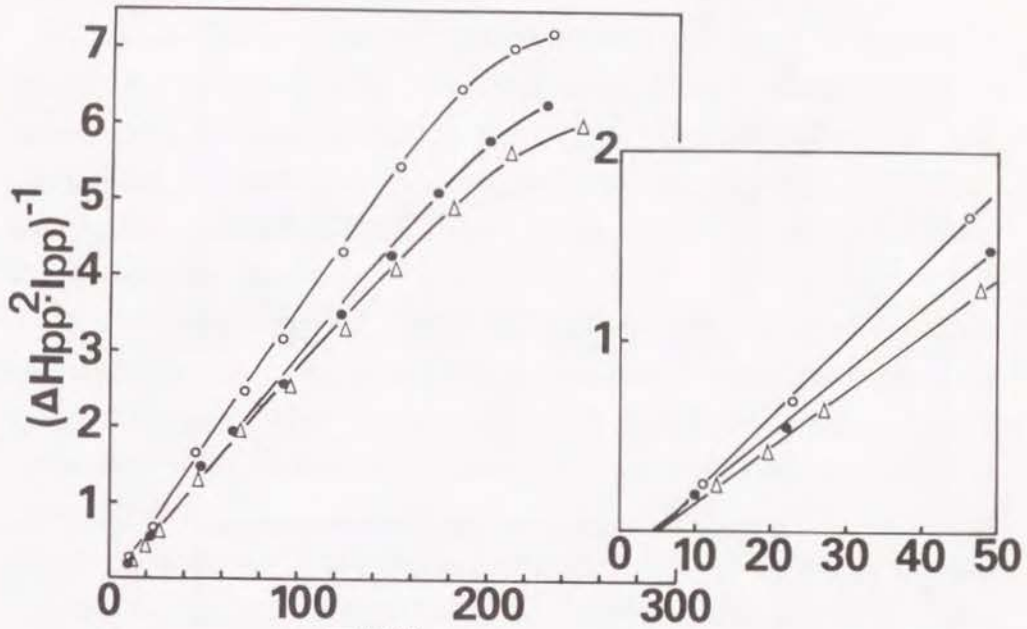

Fig. 4. Reciprocal χ ($\Delta H_{pp}{}^2 I_{pp}$) plot for poly(m-aniline) as a function of temperature. The vertical axis is drawn in an arbitrary unit. ○: pristine polymer, ●: HCl-doped polymer, and △: iodine-doped polymer.

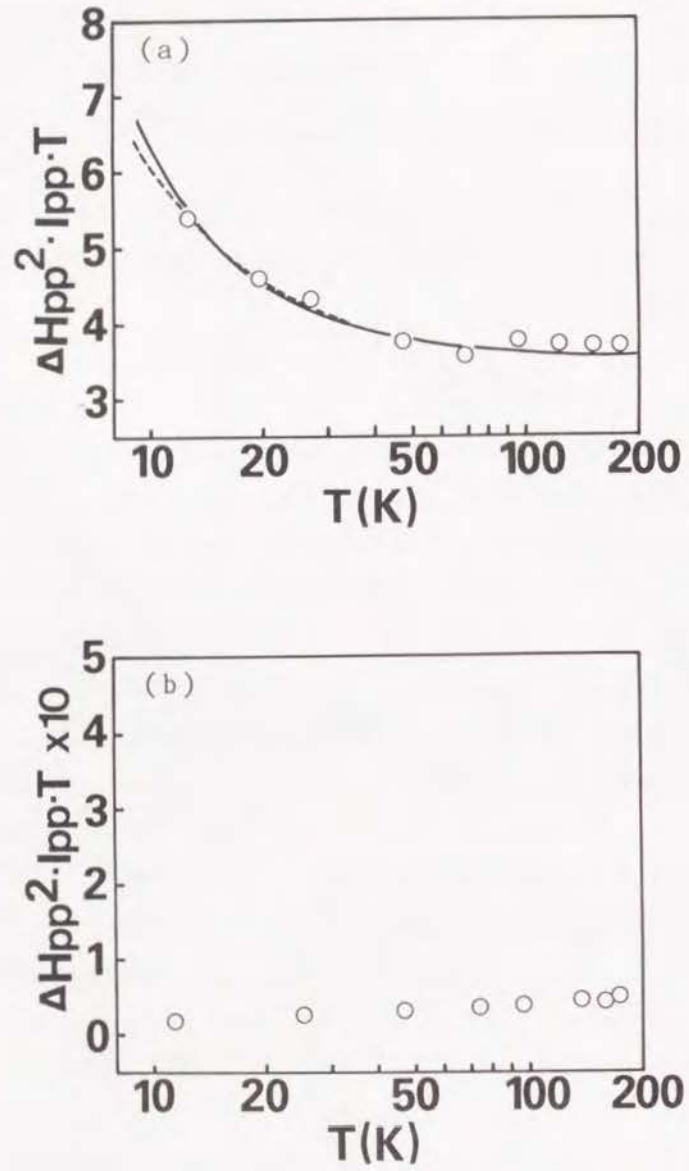

Fig. 5. χT versus T plot for (a) the iodine-doped polymer and (b) the pristine oligomer. Solid and broken lines in (a) are theoretical fittings based on the Curie-Weiss law ($\theta = 4.5$ K) and the one-dimensional Ising model ($J_{ex} = 0.25$ meV), respectively. In the oligomer, χT is almost independent of temperature.

within the temperature range examined here. In these simulations, θ and J_{ex} take positive values in the Eqs. (2) and (3), respectively, although they are very small ($\theta = 4.5$ K, $J_{ex} = 0.25$ meV).

On the other hand, χT is almost independent of temperature (Curie law) in the oligomer as shown in Fig. 5(b). Notice that the vertical axis shown here is ten times as large as that in Fig. 5(a). This is because the spin concentration of the oligomer is quite small compared with that of the iodine-doped polymer, and actually no interaction operates among the dilute spins in the oligomer accordingly.

The observation of half-field-resonance, or $\Delta m_s = \pm 2$ signals corresponding to $g \approx 4$ is a clear evidence of magnetic interaction between the spins. The signals have been detected in a triplet or higher multiplet state of molecules[5-8,29] and polymers.[30] Figure 6 illustrates the $\Delta m_s = \pm 2$ signals of the pristine, HCl-, and iodine-doped polymers observed at 15 K. A similar signal was observed in the iodine-doped polymer at 77 K, but its strength was weaker than that observed at 15 K. Furthermore, in the HCl-doped polymer, the spectrum shows hyperfine structure probably due to the nitrogen nucleus. On the other hand, the fine structure of the $\Delta m_s = \pm 1$ spectra originated from paired spins have not been observed even at low temperatures as in the case of alkylene-aromatic polymers.[31] In usual polymers pairwise spins are considered not to have specific distance because of the randomness of their structure as has been mentioned in the previous papers[30,31]; hence, the $\Delta m_s = \pm 1$ spectra based on the multiplet state have not been observed in the present study. Therefore, the fine structure of the $\Delta m_s = \pm 1$ spectrum characteristic of pairwise spins is probably smeared out owing to the wide distribution of spin-spin distance.

Magnetization and magnetic susceptibility

We are now in the position to describe the magnetic properties measured on a Faraday-type balance. The magnetization (M) of the iodine-doped polymer at 4.4 and 2.0 K is shown as a function of the applied magnetic field (H)/temperature (T) in Fig. 7. The saturation of magnetization was observed

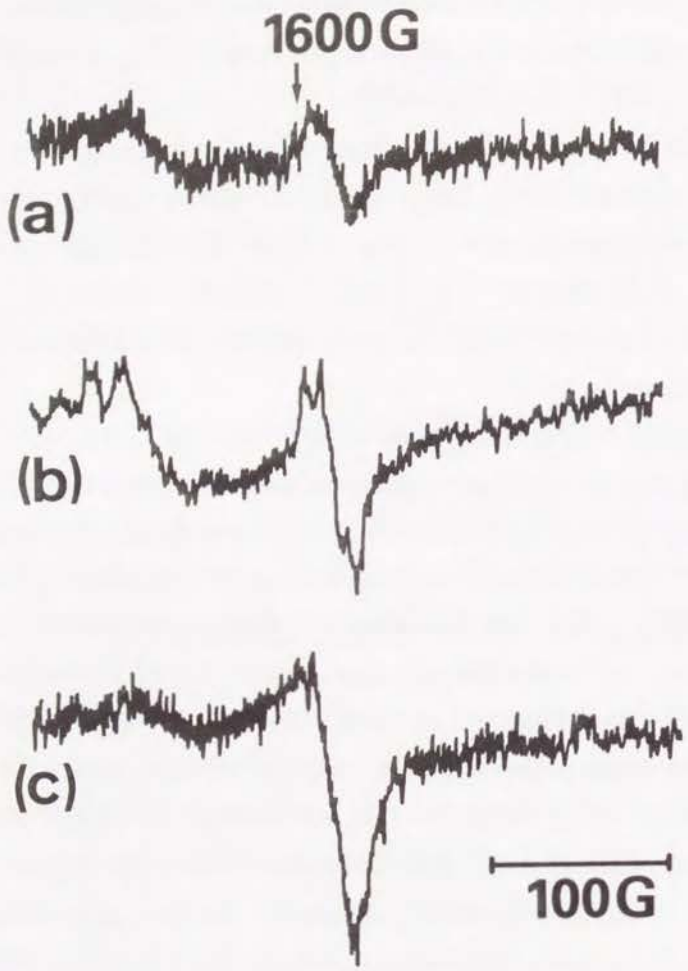

Fig. 6. Forbidden $\Delta m_s = \pm 2$ signals observed in the (a) pristine, (b) HCl-, and (c) iodine-doped polymers at 15 K. A similar signal to (c) has also been observed at 77 K.

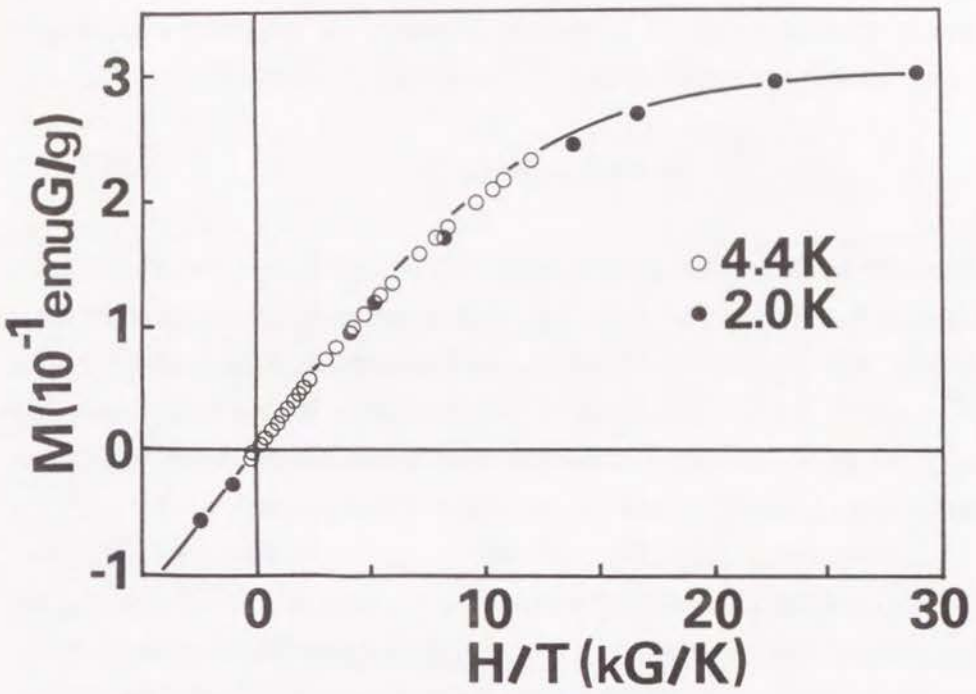

Fig. 7. Magnetization curve of the iodine-doped polymer as a function of H/T. A solid line is a theoretical curve of the Brillouin function employing $S = 1$.

to appear in high magnetic field and at low temperatures although the magnetization curve did not show the hysteresis. This value is about 30 times as large as that of the Torrance's polymer,[10,11] reflecting a larger spin concentration. The magnetization is theoretically analyzed as

$$M(H, T) = M_S B_J(Jg\mu_B H / k_B T), \tag{4}$$

where M_S is saturation magnetization (0.30 emuG•g^{-1}) and $B_J(x)$ is the Brillouin function. The total angular momentum quantum number, J, is assumed to be equal to the total spin quantum number, S, as usual in organic materials.[32] To find an average S, the simulation is also demonstrated in Fig. 7, where one can see that there is clear ferromagnetic interaction (on an average $S = 1$) among the spins in the iodine-doped polymer.

The temperature dependence of magnetic susceptibilities for the pristine, the HCl-, and the iodine-doped polymers is shown in Fig. 8. Analyzing the experimental data into a sum of a temperature-independent diamagnetic term, χ_{dia}, and a temperature-dependent term obeying the Curie-Weiss law, that is,

$$\chi = \chi_{dia} + C /(T - \theta), \tag{5}$$

we obtain the magnetic data of these materials listed in Table II. Here χ_{dia} was determined from the gradient at higher temperatures of the χT vs T plot. C and θ were determined from the gradient and the intercept of the $1/(\chi - \chi_{dia})$ vs T plot, respectively. The Weiss constants are almost zero within an experimental error. The gram Curie constant of the iodine-doped polymer was smaller than that of the HCl-doped one owing to the heavy atomic weight of iodine in spite of the spin concentration of the iodine-doped form being larger. The Curie-type spin concentration (N_C) was determined from the following formula,

$$C = N_C g^2 \mu_B^2 S(S + 1)/3k_B , \tag{6}$$

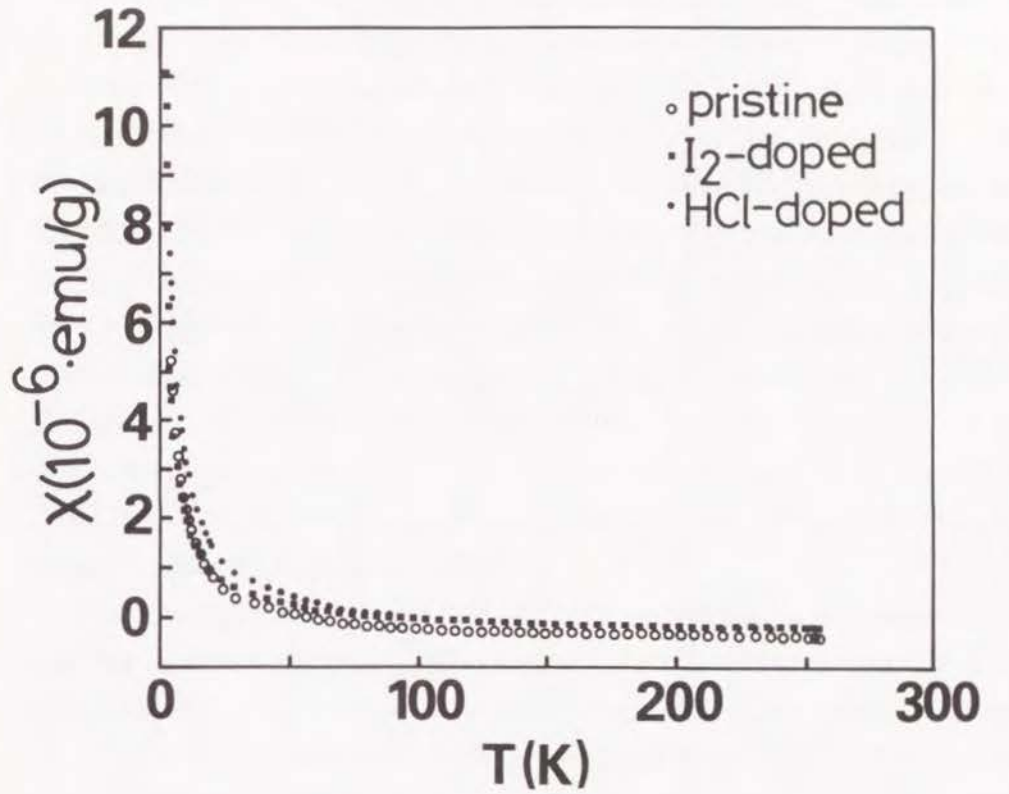

Fig. 8. Temperature dependence of the magnetic susceptibility of the pristine, HCl-, and iodine-doped polymer.

Table II. Diamagnetic susceptibility (χ_{dia}), Curie constant (C), Weiss constant (θ), and Curie-type spin concentration (N_C) obtained from the temperature dependence of magnetic susceptibility. The values in parentheses of θ was obtained from the extrapolation at temperatures higher than 40 K.

Sample	χ_{dia} (emu•g^{-1})	C(emu•K•g^{-1})	θ(K)	N_C(spins•g^{-1})
Pristine-polymer	-5.0(± 0.1) × 10^{-7}	2.8(± 0.1) × 10^{-5}	0 ± 1 (4.4)	1.7(± 0.1) × 10^{19}
HCl-doped polymer	-3.5(± 0.1) × 10^{-7}	4.0(± 0.1) × 10^{-5}	0 ± 1 (4.2)	2.4(± 0.1) × 10^{19}
Iodine-doped polymer	-2.2(± 0.1) × 10^{-7}	2.7(± 0.1) × 10^{-5}	0 ± 1 (4.5)	1.6(± 0.1) × 10^{19}

where S is assumed to be unity on the basis of the analysis of the magnetization described above. The results obtained here are consistent with those of the ESR measurements, which ensures that the Cu impurities from the catalyst does not affect the present magnetic-susceptibility measurements.

From $1/(\chi - \chi_{dia})$ vs T plot of the iodine-doped polymer shown in Fig. 9, we can observe some ferromagnetic interaction to operate among these spins in a certain temperature range. In fact, the straight line at temperatures higher than 40 K gives a positive intercept (θ = 4.5 K); on the other hand, the line below 40 K passes through the origin of the coordinate axes. This suggests that antiferromagnetic interaction sets in below 40 K possibly owing to interchain interaction as is also suggested by the temperature dependence of the ΔH_{pp}. This kind of magnetic behavior has also been claimed in phenylcarbene oligomer.[1] In contrast with the results of the ESR measurements, ferrimagnetic characteristics were not observed in the magnetic susceptibility measurements.

The present results obtained from the ESR and the magnetic susceptibility measurements are interesting associated with the molecular design of organic ferromagnets. From our theoretical calculations, it has been clarified that the spins located at the nitrogen sites are ferromagnetically coupled through the π-conjugation over the phenyl rings with antiferromagnetic array.[13,14] Note that the valence bond (VB) and the CO methods, the latter being based on the mean-field approximation, give an identical result concerning the spin order. Moreover, the band width around the Fermi level is extremely narrow compared with that of poly(*p*-aniline) because of the nature of nonbonding molecular orbital, coming from the topology of the basic skeleton of poly(*m*-aniline).[13,14] The polarons in poly(*m*-aniline) are therefore considered less mobile than those of poly(*p*-aniline); in fact, the electrical conductivity of the iodine-doped poly(*m*-aniline) is considerably low (10^{-7} S•cm^{-1})[33] in contrast with the HCl-doped poly(*p*-aniline) (5 S•cm^{-1}).[34]

Indirect spin-interaction through itinerant π-electrons of "Fermi sea" has been observed for phthalocyanine containing copper ions.[35] This mechanism is in a sense similar to the Ruderman-Kittel-Kasuya-Yoshida

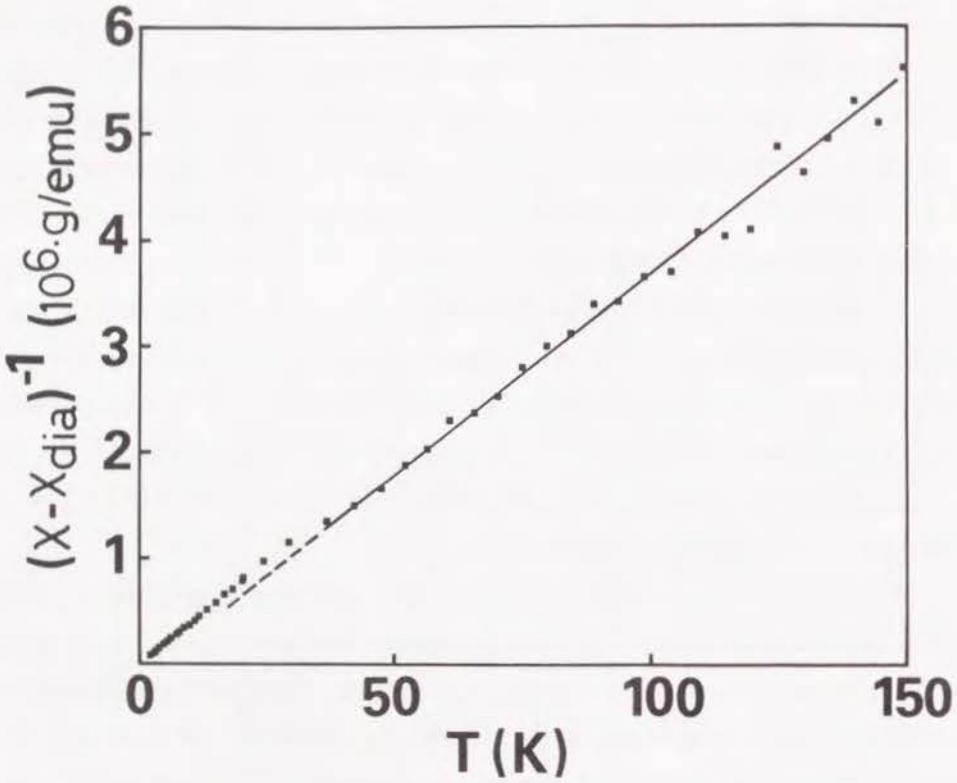

Fig. 9. $1/(\chi - \chi_{dia})$ plot of the iodine-doped polymer as a function of temperature.

(RKKY) interaction[36] for local moments coupled through conduction electrons. In the present case, on the other hand, the magnetic interaction would be determined by the topology of the polymer skeleton rather than by the interspin distance because the nearest neighboring interaction in organic compounds are known to be strongly antiferromagnetic. Since odd number of atoms are inserted between the main spin sites of poly(*m*-aniline), these spins are indirectly but ferromagnetically coupled. This situation is schematically shown in a structure of poly(*m*-aniline) (Fig. 10), where the spins located at more distant sites could be coupled through the spin-polarization of the phenyl rings, because the two spin-density-waves (SDW) originating from these parallel spins would constructively interfere to stabilize a ferromagnetic spin-coupling. When the spin of poly(*m*-aniline) is transferred to the phenyl rings in the sense of the VB picture in Fig. 11, which is probable from the *g*-value analysis in the above, the ferromagnetic interaction would also be able to operate. Roughly speaking, this type of polarization due to through-bond-interaction is estimated to extend further than 10 Å from a spin center on the basis of the mean-field approximation.[37] Therefore, ferromagnetic interaction with the aid of the spin-polarization can occur up to the separation of 20 Å between two spins if the topology of a polymer skeleton is relevant to a ferromagnetic spin-coupling.

In contrast with the case in poly(*m*-aniline) , the polarons in poly(*p*-aniline) are mobile in the light of the large band width[14] to contribute to the high electrical conductivity of this polymer, but cannot be paired ferromagnetically because of the *para*-linked topology of this polymer.[38]

Conclusion

We have shown the existence of weak ferromagnetic interaction acting between the spins in the poly(*m*-aniline) skeleton on the basis of the temperature dependence of the ESR signal intensity, the observation of the forbidden $\Delta m_s = \pm 2$ signals, saturation magnetization, and the Brillouin

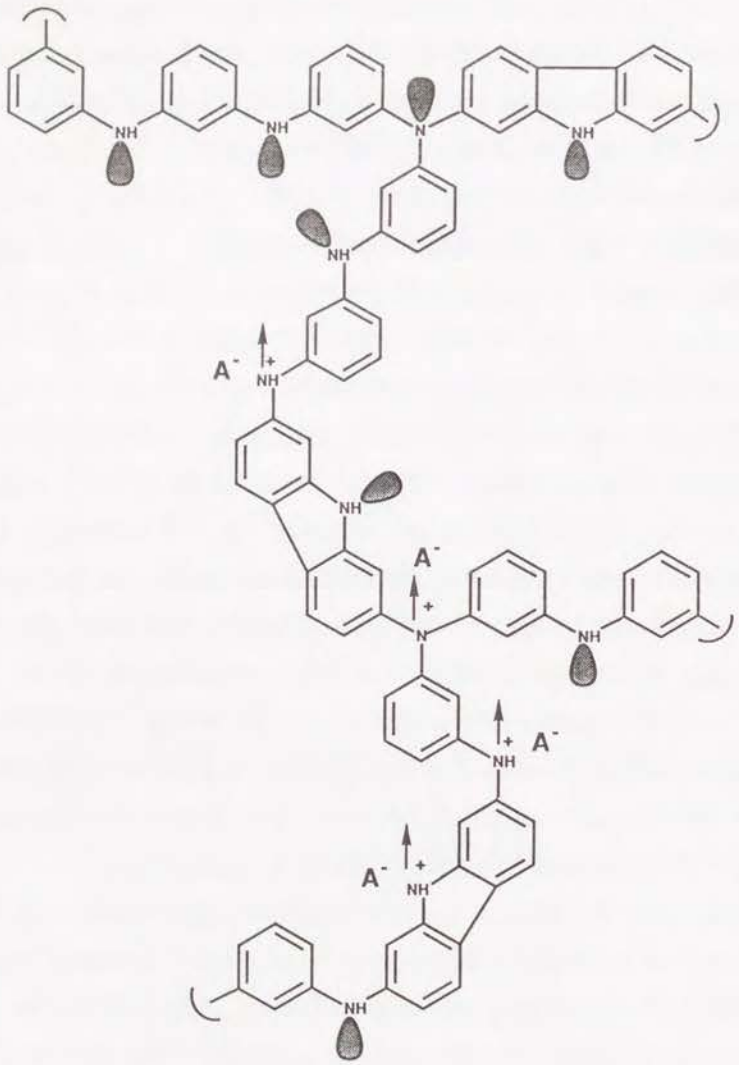

Fig. 10. Schematic representation of poly(*m*-aniline) doped with electron-acceptors (A^-). Arrows stand for electronic spins. Note that the spins are ferromagnetically coupled because of the *meta*-linked topology of the polymer skeleton.

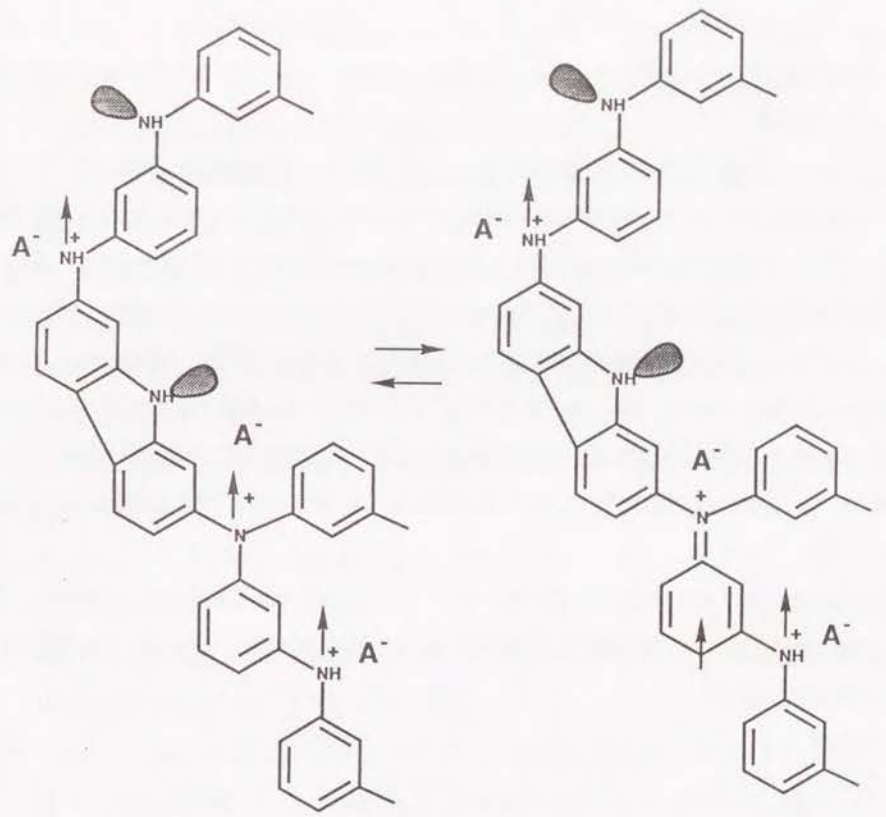

Fig. 11. Resonance forms of the polymer doped with electron-acceptors. In this form, ferromagnetic interaction also acts between the spins.

function fitting. Doping of this polymer with iodine has been observed to increase the spin concentration up to 10^{20} spins•(g-polymer)$^{-1}$ from the *in situ* ESR measurements of the doping process. Furthermore, we have observed saturation magnetization of 0.30 emu•G•g^{-1} and spin clusters of $S = 1$ in the iodine-doped poly(*m*-aniline) from the temperature- and field-dependence of the magnetization.

In particular, the cation radicals induced by electron-acceptors is of our interest because the spin concentration can be controlled in some extent by the strength of the electron-accepting ability and the content of dopants. Such spins at the nitrogen sites of poly(*m*-aniline) created by doping are not mobile, but are coupled through the spin-polarization of the phenyl rings at low temperatures due to the *meta*-linked topology of the polymer skeleton rather than the through-space coupling. The through-bond-interaction is considered to operate among rather distant spins with the aid of the induced SDWs.

The magnetic properties of the spins located on nitrogen are clearly important, and further investigation is desirable toward the realization of organic ferromagnets.

References

1. T. Sugawara, S. Bandow, K. Kimura, H. Iwamura, and K. Itoh, *J. Am. Chem., Soc.*, **108**, 368(1986).
2. Y. Teki, T. Takui, K. Itoh, H. Iwamura, and K. Kobayashi, *J. Am. Chem. Soc.*, **108**, 2147(1986).
3. A. Izuoka, S. Murata, T. Sugawara, and H. Iwamura, *J. Am. Chem. Soc.*, **109**, 2631(1987).
4. H. M. McConnell, *J. Chem. Phys.*, **39**, 1910(1963).
5. K. Mukai and A. Sogabe, *J. Chem. Phys.*, **72**, 598(1980).
6. K. Mukai, K. Ueda, K. Ishizu, and Y. Deguchi, *J. Chem. Phys.*, **77**, 1606(1982).
7. K. Awaga, T. Sugano, and M. Kinoshita, *Chem. Phys. Lett.*, **128**, 587(1986).
8. K. Awaga, T. Sugano, and M. Kinoshita, *J. Chem. Phys.*, **85**, 2211 (1986).
9. L. Y. Chiang, R. B. Upasani, D. P. Goshorn, and P. Tindall, *Mat. Res. Soc. Symp. Proc.*, **173**, 15(1990).
10. J. B. Torrance, S. Oostra, and A. Nazzal, *Synth. Met.*, **19**, 709(1987).
11. J. B. Torrance, P. S. Bagus, I. Johannsen, A. I. Nazzal, S. S. P. Parkin, and P. Batail, *J. Appl. Phys.*, **63**, 2962(1988).
12. K. Yoshizawa, K. Tanaka, and T. Yamabe, *Chem. Lett.*, **1990**, 1331.
13. K. Tanaka, K. Yoshizawa, A. Takata, T. Yamabe, and J. Yamauchi, *Synth. Met.*, **43**, 3297(1991); paper presented at the International Conference on Science and Technology of Synthetic Metals, Tübingen, Germany, September, 1990.
14. K. Yoshizawa, A. Takata, K. Tanaka, and T. Yamabe, to be published.
15. K. Yoshizawa, K. Tanaka, T. Yamabe, and J. Yamauchi, to be published.
16. I. B. Goldberg, H. R. Crowe, P. R. Newman, A. J. Heeger, and A. G. MacDiarmid, *J. Chem. Phys.*, **70**, 1132(1979).
17. J. C. Scott, P. Pfluger, M. T. Krounbi, and G. B. Street, *Phys. Rev.*,

B**28**, 2140(1983).
18. K. Tanaka, T. Koike, T. Yamabe, J. Yamauchi, Y. Deguchi, and S. Yata, *Phys Rev.*, B**35**, 8368(1987).
19. H. H. S. Javadi, R. Laversanne, A. J. Epstein, R. K. Kohli, E. M. Scherr, and A. G. MacDiarmid, *Synth. Met.*, **29**, E439(1989).
20. J. Yamauchi, H. Fujita, and Y. Deguchi, *Bull. Chem. Soc. Jpn.*, **52**, 2819(1979).
21. See, for example, P. Bernier, in *Handbook of Conducting Polymers*, T. A. Skotheim, Ed., Marcel Dekker, New York, 1986, p. 1099.
22. J. M. Pochan, H. W. Gibson, and J. Harbour, *Polymer*, **23**, 439(1982).
23. I. Harada, Y. Furukawa, M. Tasumi, H. Shirakawa, and S. Ikeda, *J. Chem Phys.*, **73**, 4746(1980).
24. N. Azuma, J. Yamauchi, K. Mukai, H. Ohya-Nishiguchi, and Y. Deguchi, *Bull Chem. Soc. Jpn.*, **46**, 2728(1973).
25. J. Yamauchi and Y. Deguchi, *Bull. Chem. Soc. Jpn.*, **50**, 2803(1977).
26. The Chemical Society of Japan Ed., *Jikken Kagaku Koza (Chemical Experiment Lecture)*, vol. 13, Maruzen, Tokyo, 1967.
27. N. Tyutyulkov, O. E. Polansky, P. Schuster, S. Karabunarliev, and C. I. Ivanov, *Theoret. Chim. Acta (Berl.)*, **67**, 211(1985).
28. See, for example, C. Domb, *Advances in Phys.*, **9**, 149(1960).
29. M. Iwasaki, T. Ichikawa, and T. Ohmori, *J. Chem. Phys.*, **50**, 1991(1969).
30. M. Iwasaki, T. Ichikawa, and T. Ohmori, *J. Chem. Phys.*, **50**, 1984(1969).
31. K. Tanaka, K. Yoshizawa, A. Takata, T. Yamabe, and J. Yamauchi, *J. Chem. Phys.*, **94**, 6868(1991).
32. H. Iwamura and A. Izuoka, *J. Chem. Soc. Jpn.*, **1987**, 595.
33. K. Yoshizawa, K. Tanaka, and T. Yamabe, unpublished results.
34. A. G. MacDiarmid, J. C. Chiang, A. F. Richter, and A. J. Epstein, *Synth. Met.*, **18**, 285(1987).
35. M. Y. Ogawa, S. M. Palmer, K. Liou, G. Quirion, J. A. Thompson, M. Poirier, and B. M. Hoffman, *Phys. Rev.* B**39**, 10682(1989).

36. See, for example, J. M. Ziman, *Principles of the Theory of Solids*, 2nd Ed., Cambridge University Press, 1972.
37. K. Tanaka, K. Yoshizawa, and T. Yamabe, to be published.
38. A. J. Epstein, J. M. Ginder, F. Zuo, R. W. Bigelow, H. -S. Woo, D. B. Tanner, A. F. Richter, W. -S. Huang, and A. G. MacDiarmid, *Synth. Met.*, **18**, 303(1987).

GENERAL CONCLUSION

In this thesis the electronic structure of midgap levels appearing in photoexcited π-conjugated polymers, the instability problems accompanied by one-dimensional electron systems, and the molecular design and construction toward ferromagnetic polymers, which are parts of the central subjects in the field of solid state chemistry, have been studied. The past 10 years have seen considerable advances in our understanding of the novel organic solid-state properties such as electrical conductivity, superconductivity, magnetism, and nonlinear optics. A principal goal of this field is to achieve close cooperation between theoretical understanding and experimental work, and consequently to predict such solid-state properties of molecular assemblies and polymers on the basis of the molecular theories.

It is important to recognize through recent investigations in this field that molecular- and polymer-based materials with large π-electron systems exhibit extremely large nonlinear responses, in many cases much larger than those of inorganic materials. Of particular importance for the nonlinear optics of the conjugated systems is the fact that the origin of the nonlinear effects is the polarization of the π-electron cloud. The midgap levels appearing in photoexcited conjugated polymers, which have been discussed in Chapters 1 and 2 of Part I, seems to be the key to understanding the nonlinear optical properties of this type of polymers, although the author at that time was not fully conscious of the significant relationship between the midgap levels and the nonlinear optical properties. In the light of the nonlinear optical process of the π-conjugated polymers, the author would like to develop the idea of the molecular orbital interaction that is used for describing the midgap levels. It seems possible to discuss this problem on the basis of the idea presented here, together with the treatment of dynamical motion of nuclei.

The most difficult, but the most important problem in one-dimensional solids is the prediction of cooperative effects that are the result of intermolecular and interchain interactions through the bulk, since there is always some interaction between adjacent molecules or chains in actual one-

dimensional solids. A phase of crystals or an alignment of polymer chains definitely affects superconducting phenomena, magnetic properties, and nonlinear optical process of these solids. Therefore, the study of the forces acting between molecules or polymers and the influence of molecular shapes on the solid-state properties is extremely important. In recent years, remarkable success has been achieved in molecular dynamics owing to the extensive use of supercomputers. In the field of solid state chemistry and physics, however, the molecular dynamics has not yet been applied to the prediction of soid-state properties to the author's present knowledge.

To achieve organic superconductivity one must overcome the Fermi-surface instabilities, or the CDW and SDW states that are insulating phases at low temperature in one-dimensional solids. The origin of both the states is the electron-hole correlation due to the nesting of the Fermi surface (Chapter 4 of Part I). Thermal excitation of electrons across the energy gap at finite temperature causes a decrease in the CDW and SDW amplitude. These states can be, however, suppressed by the existence of finite interchain coupling, which gives a crossover temperature separating a superconductive phase from insulating ones. Below that temperature the Fermi-surface instabilities no longer occur. On the other hand, Peierls transition temperature (T_p) in conducting polymers is estimated to be very high, for example, T_p = 10000 K for $(CH)_x$, below which the insulating phase, i.e., bond-alternating structure, is more stable than the metallic and SDW states as described in Chapter 5 of Part I.

Interchain soliton-hopping has been treated by our colleagues and others in association with electrical conduction mechanism between chains. In this thesis the interchain and intermolecular problems have been discussed associated with a simple intersoliton problem on two chains and intermolecular ferro- and antiferromagnetic spin couplings in Chapter 3 of Part I and in Chapter 1 of Part II, respectively. It is against the author's will not to have fully treated the intermolecular or interchain problems in this study. In particular, the study of spin alignment between polymer chains is indispensable for designing ferromagnetic polymers (Chapter 2 of Part II),

because there is no net moment if antiparallel spin alignment occurs between neighboring polymer chains. At present, however, this problem is very difficult to treat, and therefore neither strategies nor theoretical models have been presented so far.

As often stated, bulk magnetic behaviors require ferromagnetic coupling throughout a material, i.e., inter- as well as intramolecular coupling. We have designed polymers, on the basis of the extension of Mataga's models, that could have very high-spin alignment (alkylene-aromatic polymer and poly(*m*-aniline)) in Part III. Ferromagnetic interaction has been observed to act in spin clusters located in these polymers not through the bulk. Apart from the interchain problem, there is another difficulty for the development of organic ferromagnets along this strategy. Namely, as the molecule becomes larger, the orbital levels form bands and gap between bonding and antibonding bands becomes smaller. If this gap becomes comparable to kT, ferromagnetic spin alignment is no longer possible as a result of thermal activation of electrons.

Another molecular design for organic ferromagnets is clearly based on molecular crystals composed of molecules with doublet, triplet, or higher multiplet spin configuration. Also in this method, quantitative spin control throughout the bulk becomes of central interest. Dougherty's suggestion concerning this point is very interesting. That is, a very high-spin structure is divided into two building blocks. The first is simply a structure that contains a permanent magnetic moment, i.e., a free radical, triplet biradical, radical ion, and so on; the second fragment is a ferromagnetic coupling unit. This is a skillful use of indirect exchange coupling. Such an analysis is not new in intramolecular spin coupling, for example, ferromagnetic interaction in phenylcarbene oligomer offers strong evidence for this approach. It seems important to use this approach for the design of intermolecular magnetic coupling. This approach may succeed because the nearest neighbor magnetic interaction is often antiferromagnetic rather than ferromagnetic. Along this strategy, we have recently started a program to construct organic ferromagnets based on molecular crystals (*Chem. Lett.*, submitted).

The recent discovery of superconductivity and soft ferromagnetism in doped fullerene (C_{60}) is very encouraging for the future of novel organic materials in which π-electrons play an essential role in such solid-state properties. The author believes that a large number of organic functional materials will be developed in the near future and that our understanding of solid state chemistry will be greatly expanded by these materials.